Cross-Bridge Mechanisms of Skeletal Muscle Fatigue: Effects of Hydrogen Ion, Inorganic Phosphate, and Age

Cassandra Rae Nelson
Marquette University

CROSS-BRIDGE MECHANISMS OF SKELETAL MUSCLE FATIGUE: EFFECTS OF HYDROGEN ION, INORGANIC PHOSPHATE, AND AGE

By

Cassandra R. Nelson, B.S., M.S.

A Dissertation submitted to the Faculty of the Graduate School,
Marquette University,
in Partial Fulfillment of the Requirements for
the Degree of Doctor of Philosophy.

Milwaukee, Wisconsin

August 2014

ABSTRACT
CROSS-BRIDGE MECHANISMS OF SKELETAL MUSCLE FATIGUE: EFFECTS OF HYDROGEN ION, INORGANIC PHOSPHATE, AND AGE

Cassandra R. Nelson, B.S., M.S.

Marquette University, 2014

Intense muscle contraction induces high rates of glycolysis and ATP hydrolysis with resulting increases in inorganic phosphate (P_i) and H^+, factors thought to induce fatigue by interfering with steps in the cross-bridge cycle. Force inhibition is less at physiological temperatures; thus the role of low pH in fatigue has been questioned. Effects of pH 6.2 and collective effects with 30 mM P_i on the pCa-force relationship were assessed in skinned fast and slow rat skeletal muscle fibers at low (15℃) and near-physi ological temperatures (30℃). At Ca^{2+} levels characteristic of fatigue, low pH significantly depressed force at both temperatures and in combination with P_i, depressed myofibrillar Ca^{2+} sensitivity and peak force to a greater extent than either metabolite alone.

Individual effects of elevating H^+ or P_i on velocity and power have been well characterized but collective effects less studied. Thus, the effects of simultaneously elevating H^+ and P_i on velocity, power, stiffness, and rate of force development (k_{tr}) were measured. H^+ and P_i significantly depressed peak fiber power to a greater extent than either ion alone. Force-stiffness ratios significantly decreased with pH 6.2 + 30 mM P_i in both fiber types, suggesting these ions decreased the number and/or force of the high-force state of the cross-bridge. Taken with the finding that low cell pH prolongs the time in the AM·ADP state, thereby depressing velocity, the evidence suggests that H^+ and P_i are significant mediators of skeletal muscle fatigue.

The loss of muscle mass and function with age, or sarcopenia, is a significant public health problem. Sarcopenia is characterized by a loss of power with age, but mechanisms of such decrements or sex-specific effects are unknown. Peak force, k_{tr}, and myofibrillar ATPase (among other parameters) were measured in muscle fibers from the vastus lateralis of young (20-30 yr) and old (>70 yr) men and women. The results demonstrate a sex-specific age effect characterized by less absolute peak force, slower cross-bridge kinetics (i.e. reduced k_{tr}), and reduced economy in type I fibers from older women. Thus, age-related changes in cross-bridge function represent a potential mechanism for sarcopenia in older women.

ACKNOWLEDGMENTS

Cassandra R. Nelson, B.S., M.S.

I would like to thank my advisor, Dr. Robert Fitts, for his guidance, time, understanding, and support over the last 5 years. Surely this Ph.D. would not have happened without his commitment to my goal. Not only was Dr. Fitts a terrific mentor, but he was a fun, enthusiastic advisor who sought to give me as many opportunities as possible in my time here. Dr. Fitts always gave great advice on science but even better advice on life, emphasizing that positively impacting others' lives is what will live with you through the years as an educator.

I would also like to thank my committee members, Dr. Edward Blumenthal, Dr. James Buchanan, Dr. Sandra Hunter, Dr. Alexander Ng, and Dr. Danny Riley for their support and thoughtful input throughout the Ph.D. process. I truly appreciate the time and energy all of my committee members put into this journey.

I had the wonderful opportunity of teaching, mentoring, and working with many undergraduates in the Fitts lab in my time here and truly enjoyed the friendships I developed with all of them, especially Cathryn Krier, Laura Mark, and Joe Rehfus.

Thank you to the wonderful staff of the Biological Sciences department, especially Patti Colloton, Deb Weaver, Kirsten Boeh, Dan Holbus, Janell Romatowski, and Tom Dunk. Without any one of these people, this Ph.D. would

not have happened. I am sincerely grateful for all of the work these people did on my behalf and on behalf of the Fitts lab.

A special thanks to the Department of Biological Sciences at Marquette University as a whole. The atmosphere in this department embodies Marquette's mission of "being the difference." The department continuously offered me opportunities for service and mentoring outside of my little bubble of research, and I feel this helped me grow as an educator and as a scientist. There are many wonderful people in this department (too many to list), and it has been a privilege to work alongside those individuals.

Finally, I would like to thank my family. Thanks to my parents, my siblings, my husband, Mike, and my daughter, Brooke for the love and support throughout the years. You are only as strong as your support network, and I have been absolutely blessed with the most wonderfully supportive, loving family.

TABLE OF CONTENTS

LIST OF TABLES

CHAPTER 5

CHAPTER 6

LIST OF FIGURES

CHAPTER 1

CHAPTER 2

CHAPTER 3

ABBREVIATIONS

ADP	adenosine diphosphate
AM	actomyosin
AT	activation threshold
ATP	adenosine triphosphate
Ca^{2+}	calcium
EGTA	ethylene glycol tetraacetic acid
fl	fiber lengths
FV	force velocity
IEF	isoelectric focusing
k_{tr}	rate of force development
Mg^{2+}	magnesium
MHC	myosin heavy chain
MLC	myosin light chain
MLC_2	myosin light chain 2
MLC_2-P	myosin light chain 2-phosphorylated
ns	not significant
OM	Older Men
OW	Older Women
pCa	concentration of calcium (log scale)
P_i	inorganic phosphate
P_o	peak force

SEM	standard error of the mean
SR	sarcoplasmic reticulum
VL	vastus lateralis
V_{max}	loaded shortening velocity
V_o	unloaded shortening velocity
YM	Young Men
YW	Young Women

CHAPTER 1

REVIEW OF LITERATURE

Introduction

Skeletal muscle contraction occurs when myosin projects toward filamentous actin and repetitively binds to actin subunits to generate force and net movement (Huxley 1957; 1969; Zeng *et al.* 2004). A process dependent on ATP and calcium, the cross-bridge theory proposes that the myosin head binds to the actin filament in an initial conformation and then undergoes a change of state which moves the actin filament past the myosin filament (Holmes & Geeves 2000). First proposed over 50 years ago (Huxley 1957), the cross-bridge theory is well supported by structural, physiological, and biochemical data (Holmes & Geeves 2000). Figure 1.1 is a schematic of the cross-bridge cycle, beginning with the rigor state A (no bound ATP or substrates) at the top and center of the figure. Following ATP binding to the myosin head, actin and myosin disassociate to an unbound state, B. Hydrolysis of ATP and Ca^{2+} binding to troponin C (not pictured) free the myosin binding site on the actin, and actin and myosin weakly interact to form state C, $AM{\cdot}ADP{\cdot}P_i$. By an unknown mechanism, the weakly bound bridge transitions to a strongly bound bridge (step 3) and forms state D, $AM{\cdot}ADP{\cdot}P_i$*. P_i dissociation and the power stroke follow (step 4), and completion of the myosin tail swing and ADP release (steps 5 and 6) complete the cross-bridge cycle (Geeves *et al.* 2005; Fitts 2008).

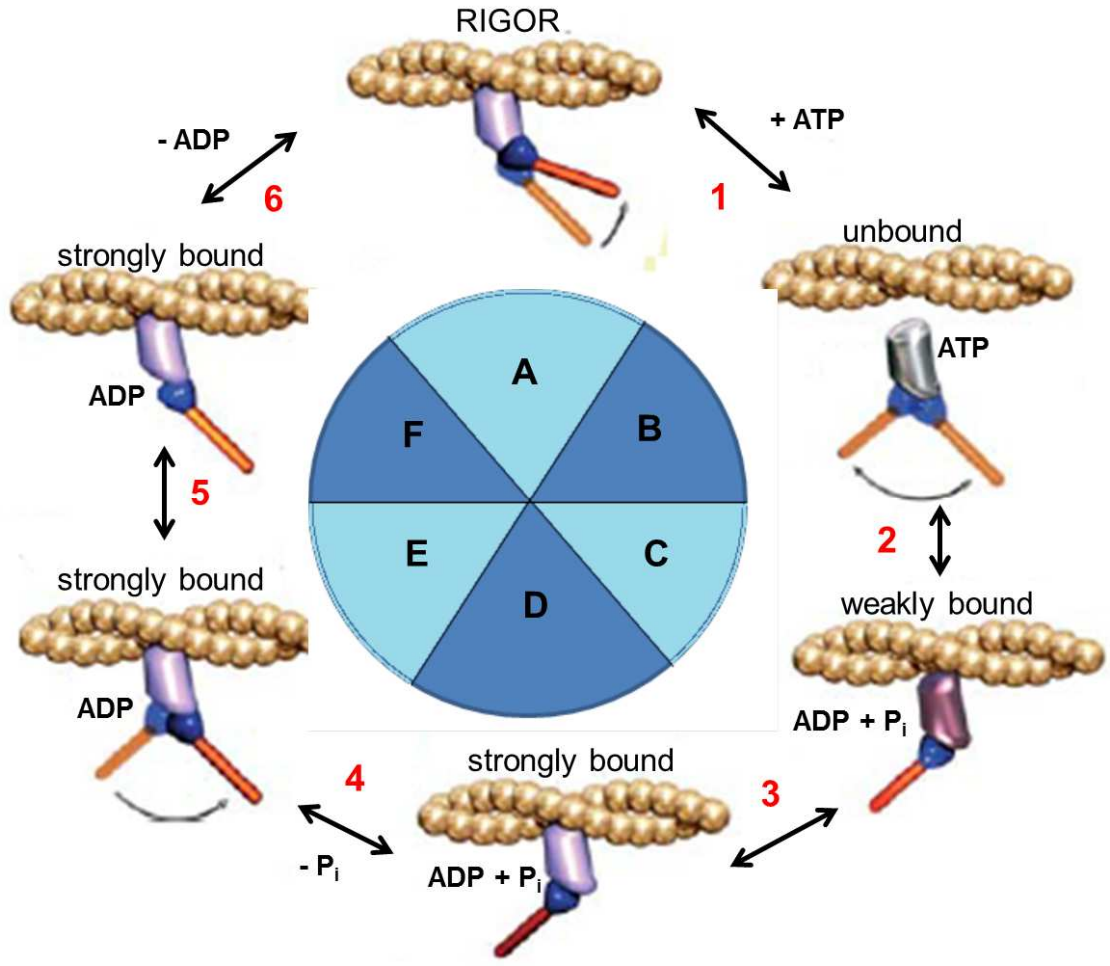

Figure 1.1: Schematic of the cross-bridge cycle

Modified from Geeves *et al*. (2005) and Fitts (2008), with permission from the American Journal of Physiology. Actin is the beaded protein on top in state A (rigor) while myosin is bound below. States D-F represent strongly bound cross-bridges.

Muscle fatigue is defined as a loss of power that results from declines in both force and velocity and is implicated in clinical situations such as respiratory or cardiac failure (Fitts 1994; 2008; Kent-Braun *et al.* 2012). Fatigue can be examined from the perspective of single molecules (Debold 2012) to intact

organisms (Kent-Braun *et al.* 2012). While fatigue can be experienced in the CNS, in highly motivated athletes, it is believed that up to 90% of fatigue experienced is peripheral muscle fatigue, or fatigue at the level of the single skeletal muscle cell (Fitts 1994). Studies utilizing single fibers (living, chemically skinned, mechanically peeled) have provided insights on how actin and myosin interact to generate force, velocity and power and how this may be compromised in fatigue (Kent-Braun *et al.* 2012).

High rates of ATP hydrolysis and glycolysis during a fatiguing task result in a buildup of metabolites, specifically hydrogen ion (H^+) and inorganic phosphate (P_i) (Fitts 2008). These metabolites exert negative effects on excitation-contraction coupling and the actomyosin cross-bridge cycle and combine to depress peak power and ultimately depress performance (Fitts 1994; 2008; Allen *et al.* 2008). While our understanding of muscle fatigue has advanced, a mechanistic understanding of how fatigue occurs at the level of the cross-bridge cycle is still evolving.

The major source of acid (H^+) in skeletal muscle is anaerobic production of lactic acid (lactate + free H^+ in solution) from glucose and glycogen, and the increase in lactate is highly correlated to the fall in muscle pH (Fitts 1994). Reaching levels as low as pH 6.2 in frog and human muscle, free H^+, not lactate, has been shown to be a primary force-depressing agent (Chase & Kushmerick 1988; Wilson *et al.* 1988; Thompson *et al.* 1992; Fitts 1994; Knuth *et al.* 2006). Acidosis is believed to depress force by inhibiting the forward rate constant of step 3 (Figure 1.1) and to depress velocity by inhibiting fiber ATPase and/or

slowing the ADP-release step (Figure 1, steps 2 and 6, respectively) (Cooke *et al.* 1988; Fitts 2008; Debold 2012). P_i is hypothesized to depress force by accelerating the reverse rate constant of step 3 (Figure 1.1). Though it has no effect on velocity, levels of P_i observed with fatigue (up to 30 mM) depress power (Cady *et al.* 1989; Debold *et al.* 2004).

Early studies on the effects of elevating H^+ and P_i in skinned fibers were performed at temperatures <20℃ because of experime ntal limitations (Cooke *et al.* 1988; Metzger & Moss 1990b). Fibers could not maintain sarcomeric integrity with contractions at physiological temperatures. Since the mid-1990's, temperature jump-plate technology has allowed for experiments in skinned fibers to be conducted at near-physiological temperatures (30℃) (Pate *et al.* 1995; Nelson & Fitts 2014). Elevating temperature accelerates the forward rate constant of force generation (Figure 1.1, step 3) and speeds the entire cross-bridge cycle (Fitts 2008). Experiments in this dissertation were conducted primarily at 15℃ (to compare to previous studies) and also at 30℃. The advantage of manipulating temperature is that it is a fatigue-independent mechanism of altering cross-bridge kinetics. Clinically, 30℃ measurements are of greater interest since this is near the temperature where muscle operates *in vivo*.

Any discussion of muscle fatigue requires consideration of the different fiber types in skeletal muscle. Here, slow type I fibers, fast oxidative type IIa fibers and fast glycolytic IIx fibers were studied. Fast fiber types are characterized by high sarcoplasmic reticulum (SR) and myofibrillar ATPase

activities and possess high maximal shortening velocities (V_o) whereas slow fibers have low SR and myofibrillar ATPase activity and slower V_o's (Fitts 1994). The velocities of the fiber types differ because they contain different isoforms of the myosin heavy chain (MHC) located in the globular head of the myosin, with fiber type specific ATPase activities (type IIx > type IIa > type I) (Bottinelli *et al.* 1991). The head portion of the MHC contains the actin and ATP binding sites (Geeves & Holmes 1999). It is well known that fast muscles fatigue more rapidly and to a greater extent than slow muscles, in part due to their greater dependence on anaerobic metabolism (glycolysis and high energy phosphate metabolism) and the resulting increased production of H^+ and P_i (Fitts 1994).

The effects of elevating H^+ and P_i on single fiber mechanical properties at 30℃ are summarized in table 1.1 (Debold *et al.* 2004; 2006; Knuth *et al.* 2006; Fitts 2008; Nelson & Fitts 2014). The table contains published effects of elevating H^+ alone, P_i alone, and both H^+ and P_i (the pH 6.2 + 30 mM P_i condition), prior to the work in this dissertation, on force, calcium sensitivity (quantified by pCa_{50}, or the concentration of Ca^{2+} required to elicit half-maximal force), velocity, and power at 30℃ in skinned fibe rs. The question marks indicate unknown effects that were the primary focus of this thesis (Chapters 3 and 4). In particular, these studies were designed to elucidate the combined effects of low pH plus high P_i and establish the cellular mechanisms by which these ions reduce force, velocity, and power.

	Fiber type	pH 6.2	30 mM Pi	pH 6.2 + 30 mM Pi
Peak Force (P_o)	Type I	↓ 12%	↓ 19%	?
	Type II	ns	ns	↓ 52%
Calcium Sensitivity (pCa_{50})	Type I	?	↓ 10%	?
	Type II	?	↓ 10%	?
Maximal Velocity (V_{max})	Type I	↓ 16%	ns	?
	Type II	↓ 16%	ns	↓ 18%
Peak Power (W/l)	Type I	↓ 34%	↓ 26%	?
	Type II	↓ 18%	↓ 18%	?

Table 1.1: Summary of the effects of H^+ and P_i in type I and II fibers at 30℃.

Values are percent change from control conditions (pH 7, no added P_i), taken from references Debold *et al.* (2004, 2006), Knuth *et al.* (2006), Karatzaferi *et al.* (2008) in rat or rabbit skinned fibers. Question marks are unknown values addressed in this dissertation. ns = not significant.

Effects of H^+ and P_i on force, calcium sensitivity and stiffness

Experiments performed on skinned fibers at temperatures <20℃ demonstrated that low cell pH (6.2) and elevated P_i (30 mM) had a significant depressive effect on force at saturating calcium (Metzger & Moss 1987a; Chase & Kushmerick 1988; Pate *et al.* 1995; Debold *et al.* 2004; Knuth *et al.* 2006). However, when the temperature was raised to near-physiological (≥30℃), the depressive effects of H^+ or P_i on peak force were significantly attenuated (Pate *et al.* 1995; Coupland *et al.* 2001; Debold *et al.* 2004; Knuth *et al.* 2006), leading some to question the validity of either metabolite as an important fatiguing agent (Table 1.1) (Allen *et al.* 2008).

Conventionally, skinned fiber experiments utilize pCa 4.5 (~32 µM) as a supramaximal Ca^{2+} concentration. However, in a fatiguing event, myoplasmic free Ca^{2+} is not maximal, as SR Ca^{2+} release is depressed in part due to Mg^{2+} inhibition of the ryanodine receptor and precipitation of Ca^{2+} with P_i in the sarcoplasmic reticulum (Westerblad & Allen 1991; 1992; Allen & Westerblad 2001; Allen *et al.* 2008). During fatigue, the amplitude of the myoplasmic Ca^{2+} transient is depressed and may reach levels < pCa 6.0 (1 µM) (Allen & Westerblad 2001). Thus, evaluating the depressive effects of low cell pH or elevated P_i on force must be studied at submaximal Ca^{2+} concentrations to accurately mimic fatigue. This is most commonly done by assessing the force-calcium or pCa-force relationship.

Like the studies done at peak Ca^{2+} concentrations, early studies investigating the role of low cell pH or elevated P_i at submaximal Ca^{2+} concentrations in skinned fibers were conducted at room temperature or lower (Hermansen & Osnes 1972; Fabiato & Fabiato 1978; Metzger & Moss 1990a). At room temperature, Hermansen and Osnes (1972) showed no significant effect of pH in rabbit soleus fibers on the pCa-force curve at pH 6.5 vs. pH 7.0 conditions while Fabiato and Fabiato (1978) reported pH 6.2 to significantly shift the pCa_{50} 0.35 units (~1 µM) compared to pH 7.0 in frog semitendinosus. Metzger and Moss (1990a) reported a ~1 µM pCa_{50} shift from pH 7 to pH 6.2 at 15℃ in rat soleus fibers. Prior to the work prese nted in chapter 3, it was unknown how pH 6.2 affected the pCa-force relationship at near-physiological temperatures.

Several investigators have shown that high P_i depressed calcium sensitivity in muscle fibers (Millar & Homsher 1990; Martyn & Gordon 1992) and recently, this was shown to be not only true, but twofold higher at 30℃ (Debold *et al.* 2006).

While it is important to study the effects of elevations in H^+ and P_i in isolation, in an *in vivo* situation, the metabolites rise concomitantly. Thus, fatigue is most accurately mimicked by studying the collective effects of elevating H^+ and P_i. Early studies conducted at low temperatures (10-15℃) found that collectively elevating H^+ and P_i resulted in a 50-85% decline in peak force (P_o), varying based on fiber type, pH (6.0-6.2) and/or P_i concentration (15-30 mM) (Cooke *et al.* 1988; Chase & Kushmerick 1988; Potma *et al.* 1995). More recently, Karatzaferi *et al*. (2008) described an 80% and 50% decline in P_o at 10 and 30℃, respectively, in rabbit psoas fibers at pH 6. 2 + 30 mM P_i conditions. Collective effects of elevating H^+ and P_i on the pCa-force relationship at low or high temperatures were unknown prior to this work and are discussed in detail in Chapter 3.

Low pH and high P_i may inhibit force by reducing the number of bridges and/or the force per cross-bridge. One way to distinguish between these is to measure fiber stiffness, which is known to be dependent on the number of bound actomyosin cross-bridges. Stiffness is determined by applying small (approximately 0.05% of fiber length), 2 kHz sinusoidal length changes (dl) to the fiber and measuring the resulting force oscillations (dP) (Nocella *et al.* 2011). To maximize the number of attached bridges, the length oscillations are of high

frequency (faster than cross-bridge cycle rate) and low amplitude so that actomyosin bridges do not break. Stiffness is calculated as a ratio of change in tension (normalized for cross-sectional area of the fiber) per change in length. The force-stiffness ratio (peak isometric force/stiffness) provides information on the force produced per actomyosin cross-bridge. For example, when the temperature is raised, stiffness remains unchanged while peak force increases. This increases the force-stiffness ratio, implying that raising temperature increases the amount of force produced per individual cross-bridge (Figure 1.2) (Galler & Hilber 1998).

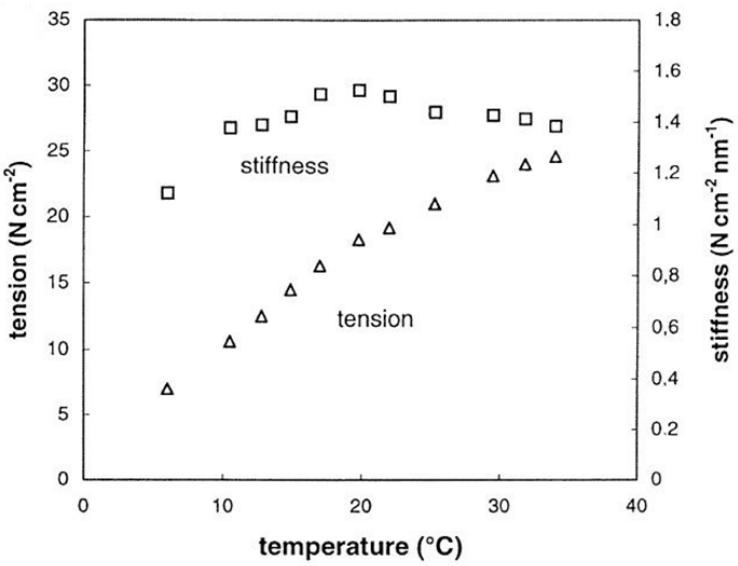

Figure 1.2: Temperature dependence of peak force and stiffness.

Data from a maximally Ca^{2+} activated rat vastus lateralis skinned fiber, from Galler & Hilber (1998), with permission from John Wiley & Sons, Inc. and *Acta Physiologica*.

Methods of measuring stiffness vary and therefore conclusions about the effects of H^+ and/or P_i on stiffness are controversial. Metzger and Moss (1990a) reported a fiber-type dependent effect of low pH (6.2) on stiffness, in that stiffness was reduced at pH 6.2 in fast but not slow fibers at 15℃, suggesting a decreased number of actomyosin cross-bridge attachments in fast but not slow fibers. The published effects of elevated P_i on stiffness vary and are on fast fibers exclusively. One recent study described that force and stiffness were depressed equally in the presence of 25 mM P_i, leaving the force-stiffness ratio unchanged (Caremani *et al.* 2008) while other studies have reported a decrease in the force-stiffness ratio with elevated P_i (Brozovich *et al.* 1988; Dantzig *et al.* 1992). To our knowledge, the collective effects of elevated H^+ and P_i on fiber stiffness prior to the work presented here (Chapter 4) were unknown.

Effects of H^+ and P_i on velocity and power

The extent of muscle fatigue is perhaps best related to changes in peak power, which is obtained at intermediate velocities and forces (Fitts 1994). Since power is a function of both force and velocity, it is considerably higher in fast fibers and greatly affected by temperature (Debold *et al.* 2004; Knuth *et al.* 2006). Elevated levels of H^+, but not P_i, depress velocity (Debold *et al.* 2004; Knuth *et al.* 2006). Maximal velocity can be determined in two ways: (1) a slack test where maximal velocity (V_o) is determined from a series of unloaded shortening steps, or (2) from extrapolation of a series of loaded contractions to zero load

(V_{max}), first described by A.V. Hill (1938) (See Chapter 2*, Methods)*. V_o is typically higher than V_{max}, especially at higher temperatures, due to sarcomere non-uniformity that occurs with loaded contractions (Widrick *et al.* 1996). It has been shown in skinned fibers that at both low (15℃) and high (30℃) temperatures, pH 6.2 has a significant depressive effect (~16%) on V_{max} in both type I and II fibers at 30℃ (Table 1.1) (Pate *et al.* 1995; Knuth *et al.* 2006). It has been suggested that H^+ mediates declines in velocity by slowing ADP release, otherwise described as prolonging t_{on} (the duration of the strongly bound state following the power stroke) (Figure 1.1, state F) and/or slowing the ATPase rate of myosin (Figure 1.1, transition 2) (Cooke *et al.* 1988; Debold *et al.* 2008). At 30℃, Karatzaferi *et al.* (2008) described an 18% reduction in V_{max} in pH 6.2 + 30 mM P_i conditions in fast rabbit psoas fibers. In combination with elevated H^+, it appears that P_i has no additional effect on the depression of velocity; thus it can be assumed that any depression in V_{max} when the ions are collectively elevated is due to H^+. Chapter 4 investigates collective effects of H^+ and P_i on velocity in slow as well as fast fibers.

Though high P_i does not change velocity, power is depressed with 30 mM P_i in type I and II fibers at both low and high temperatures (Table 1.1) (Debold *et al.* 2004). Elevated H^+ also depresses power; in fact, in type II fibers at 30℃, the ions individually depress power by 18% each (Table 1.1) (Debold *et al.* 2004; Knuth *et al.* 2006). The collective effects of pH 6.2 + 30 mM P_i on peak power are relatively unstudied. One study on fast fibers at 30℃ did not report any power values, instead showing a figure of power curves at various fatigue-like

conditions (Figure 1.3) (Karatzaferi *et al.* 2008). This study found that phosphorylating myosin light chain 2 (MLC_2-P) exacerbated the pH+P_i reduction in power at 30℃ (Figure 1.3, gray vs. bl ack short dashed lines), an effect briefly discussed in Appendix 2 of this document. However, regardless of phosphorylation status of the fibers, collectively elevating the ions resulted in a synergistic depressive effect on power, a finding that we also observe (Chapter 4).

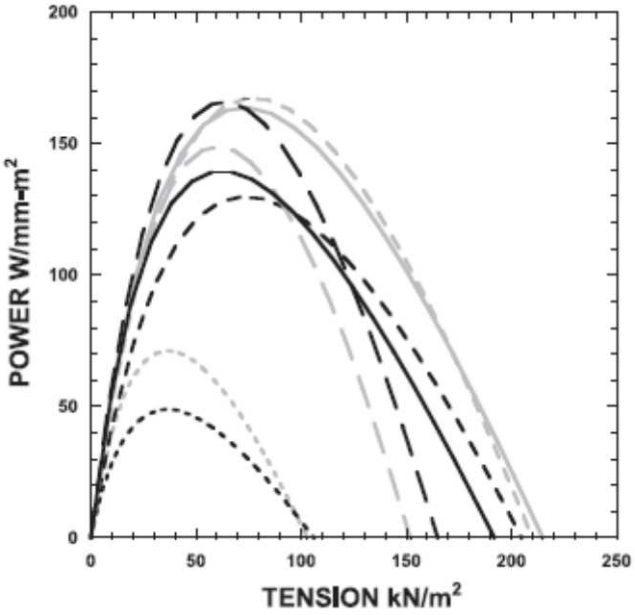

Figure 1.3: Power produced under 8 conditions at 30℃.

Data from a rabbit psoas fiber, shown as a function of load (peak force). Curves for control fibers are gray and experimentally phosphorylated black. Conditions indicated by solid lines (pH 7, 5 mM P_i), long dashes (pH 7, 30 mM P_i), medium dashes (pH 6.2, 5 mM P_i) and short dashes (pH 6.2, 30 mM P_i), from Karatzaferi *et al*. (2008), with permission from the American Journal of Physiology.

Effects of H^+ and P_i on k_{tr} and ATPase

An important property of muscle is the rate of tension development (dp/dt or k_{tr}). This is particularly true of phasic contractions where contraction durations (and thus time for force development) are short (Fitts 1994). The k_{tr} is thought to be limited by the forward rate constant of the transition from a low-force cross-bridge (Figure 1.1, state C) to the high-force cross-bridge (Figure 1.1, state D) and not SR Ca^{2+} release rate, Ca^{2+} diffusion, or binding to troponin-C (Brenner 1987; Metzger *et al.* 1989; Fitts 1994). The sum of the forward and reverse rate constants (Figure 1.1, step 3) determines the rate of force redevelopment (k_{tr}) of a fully active fiber following a slack-unslack procedure (Fitts 2008). The k_{tr} is calcium, fiber type, and highly temperature sensitive (Metzger & Moss 1987a; 1990b; 1990c). At saturating levels of Ca^{2+}, elevating P_i accelerates k_{tr}, and lowering pH does not change k_{tr} at 15℃ (Metzger & Moss 1990b; Tesi *et al.* 2000). Collective effects of low pH plus high P_i on k_{tr} at 15 or 30℃ had not been studied until the work presented here in chapter 4.

Maximal shortening velocity is proportional to the myofibrillar ATPase activity (Barany 1967). The myofibrillar ATPase activity assesses the rate of ATP hydrolysis in the cross-bridge cycle (Figure 1.1, step 2), which is thought to at least in part limit the speed of the overall cycle (Cooke *et al.* 1988). ATPase can be measured by coupling ADP formation to the oxidation of reduced nicotinamide adenine dinucleotide (NADH to NAD^+) using the glycolytic enzymes pyruvate kinase (PK) and lactate dehydrogenase (LDH) (Schluter & Fitts 1994). It is

reasonable to hypothesize that if something has a depressive effect on shortening velocity, it may also depress myofibrillar ATPase activity.

At 10℃, Cooke *et al*. (1988) found a small depressive effect of 20 mM P_i on ATPase (15-20%) and a larger 25-30% reduction in ATPase at pH 6.0 (no added P_i). Another study investigated the individual and collective effects of pH 6.0 + 30 mM P_i on ATPase activity and fiber economy at 15℃ in ty pe I and II fibers (Potma *et al.* 1995). Fiber economy is described by the force-ATPase ratio and corresponds to how much force is produced per molecule of ATP hydrolyzed. According to Potma and colleagues (1995), the fatigue condition of pH 6.0 + 30 mM P_i depressed myosin ATPase activity in type II fibers and compromised fiber economy in both fiber types. Type II fiber economy was depressed the most by pH 6.0 + 30 mM P_i because force dropped even more than ATPase activity (Potma *et al.* 1995). In Chapter 5, we investigate ATPase activity in human fibers at temperatures closer to physiological (both 23 and 30℃) and evaluate the individual and collective ef fects of elevating H^+ and P_i.

Aging and fiber function

The loss of muscle mass and function with age, known as sarcopenia, is a significant scientific and public health problem, estimated to cost the United States healthcare system over $20 billion annually (Janssen *et al.* 2004; Frontera *et al.* 2012). Sarcopenia is characterized by muscle weakness, a decrease in muscle power, and a reduction in an individual's ability to function (Frontera *et al.*

2012). The first experiments on human single fibers date back to 1975 but the effects of aging and sarcopenia on the single fiber level in humans have only been studied since 1997 (Wood *et al.* 1975; Larsson *et al.* 1997). It is important to characterize age-related changes at the single fiber level because it offers investigators the ability to isolate a physiological system and examine the performance of the actin-myosin cross-bridges in the absence of nervous system or endocrine input (Frontera *et al.* 2012).

One caution when reviewing studies in human physiology is that there is a historical and current bias in studying proportionately more males than females and a presumption that sex differences do not exist (Kim *et al.* 2010; Hunter 2014). It is clear, however, that in regards to muscle fatigue, sex differences do exist and need to be further explored (Hunter 2014).

On the single fiber level, it is controversial as to whether peak force normalized for cross-sectional area (kN/m^2) or maximal shortening velocity decline with age, as some investigators report no change (Trappe *et al.* 2003) and others a reduction with age (Larsson *et al.* 1997; Frontera *et al.* 2000; Krivickas *et al.* 2001). It has been established that whole muscle power output decreases with age (Lanza *et al.* 2003) but on the single cell level, it is not clear whether or not peak fiber power declines (Trappe *et al.* 2003; Krivickas *et al.* 2006). Trappe *et al.* (2003) showed that, when normalized for cell size, there were no sex or age differences in peak fiber power.

All of the single fiber experiments ever performed on human fibers have been at temperatures between 15-25℃, far from wher e muscle operates *in vivo*.

As shown with the rat single fiber data, there is a temperature effect on elevated H^+ and P_i mediated depressions, and the same may be true in human fibers when observing changes with age. Thus, there is a need to characterize the effects of aging on single fiber function at near-physiological temperatures ($\geq$30℃).

One human fiber study reported a decline in peak force (kN/m^2) with age in male fibers and measured stiffness to investigate the mechanisms of such force depression (Ochala *et al.* 2007). Aging increased instantaneous stiffness per force unit in both type I and IIa fibers, and the authors suggest this could be due to an increased number of low-force cross-bridges with age (Ochala *et al.* 2007). Miller and colleagues (2013) measured stiffness and k_{tr} from young versus older male and female subjects and reported slowed cross-bridge kinetics in older women; that is, older women had lower k_{tr}'s in type I and IIa fibers at 25℃. They also reported a significantly higher stiffness at pCa 4.5 in older women in type I and IIa fibers compared to the other three groups (young men, young women, older men) at 15℃ (Miller *et al.* 2013). Therefore, despite the thought that peak power normalized for cell size may not change with age (Trappe *et al.* 2003), it is clear that some cross-bridge mediated effects on aged single fibers are emerging and warrant further investigation (Ochala *et al.* 2007; Miller *et al.* 2013).

There has been no work done on the effects of fatigue (elevating H^+ and/or P_i) on human fibers and/or how the ions may affect the performance of

fibers from young vs. older adults. The work herein (Chapter 5) begins the investigation of the interface of age and fatigue on the single fiber level.

Summary

The overall aims of this work were as follows:

(1) Characterize collective effects of elevated H^+ and P_i on peak force and the pCa-force relationship at 15 and 30℃ in type I and II rat fibers (Chapter 3).

(2) Characterize collective effects of elevated H^+ and P_i on velocity, power, stiffness, and k_{tr} at 15 and 30℃ in type I and II rat fibers (Chapter 4).

(3) Characterize age or sex differences in force, calcium sensitivity, velocity, power, k_{tr}, stiffness, and ATPase activity at 15 and 30℃ (Chapter 5) in human fibers.

(4) Describe how the fatigue condition (elevating H^+ and P_i) alters the performance and contractile properties of fibers from older versus young adults and determine if any sex differences exist (Chapter 5).

CHAPTER 2

METHODS

Ethical Approval

All experiments and the protocol for animal care and disposal were approved by the Marquette University Institutional Animal Care and Use Committee (IACUC).

Solutions

Compositions of relaxing (pCa 9.0) and maximal activating (pCa 4.5) solutions were derived from a computer program utilizing the stability constants reported by Fabiato and Fabiato (1979; Fabiato 1988), which include adjustments for temperature, pH, and ionic strength. All solutions contained (mM) 20 Imidazole, 7 EGTA, 4 free MgATP and 14.5 creatine phosphate. P_i was added as K_2HPO_4 to yield a total concentration of 30 mM. No P_i was added (0 mM) to the control or pH 6.2 alone condition. Mg^{2+} was added in the form of $MgCl_2$ with a specified free concentration of 1 mM. Ionic strength was adjusted to 180 mM with KCl, and with solution at 15 or 30℃ , the pH was adjusted to 6.2 or 7.0 with KOH. Ca^{2+} was added as $CaCl_2$. Sample relaxing and activating solutions (25 ml total volume) are listed in Table 2.1.

Stock Solution	Relaxing Solution at 15°C	Activating Solution at 15°C	Relaxing Solution at 30°C	Activating Solution at 30°C
Condition	pH 7	pH 7	pH 6.2 + 30 mM P_i	pH 6.2 + 30 mM P_i
1 M KCl	1.98 ml	1.60 ml	0.66 ml	0.53 ml
200 mM Imidazole	2.50 ml	2.50 ml	2.50 ml	2.50 ml
100 mM EGTA	1.75 ml	1.75 ml	1.75 ml	1.75 ml
100 mM $MgCl_2$	1.35 ml	1.32 ml	1.43 ml	1.42 ml
100 mM $CaCl_2$	0.004 ml	1.75 ml	0.00125 ml	1.22 ml
Disodium ATP	72 mg	74 mg	84 mg	85 mg
PC (14.5 mM)	119 mg	119 mg	119 mg	119 mg
K_2HPO_4	--	--	131 mg	131 mg

Table 2.1: Sample relaxing and activating solutions.

Samples illustrated are for 25ml total volume solution. Note that the amount of imidazole, EGTA, and PC does not change as the solution conditions change.

Single Fiber Preparation

All single fiber experiments in this dissertation employ the skinned fiber method. Skinned fibers are experimentally derived by dissecting small muscle bundles from a rat or obtaining bundles from a human subject and subjecting the muscle to a skinning solution (described below) that permeabilizes the muscle cell membrane. From a muscle bundle, a single fiber can be pulled out using fine forceps. Because of the permeabilized nature of the fiber, during experimentation, the extracellular solution then becomes the intracellular milieu of the skinned single fiber.

For animal experiments (Chapters 3 and 4), male and female (Chapter 3) and only male (Chapter 4) rats were anaesthetized with Nembutal (50 mg/kg body weight intraperitoneal) after which the soleus (type I fibers), the deep region of the lateral head of the gastrocnemius and superficial region of the medial head of the gastrocnemius (type II fibers) were removed and placed in a 4℃ relaxing solution. The rats were subsequently killed with a pneumothorax while still heavily anesthetized. Muscles were dissected into small bundles (40-50 fibers) in relaxing solution, tied to glass capillary tubes, and stored in skinning solution composed of 50% relaxing solution and 50% glycerol (vol/vol) at -20℃ for $\leq$ 4 weeks.

For human experiments (Chapter 5), vastus lateralis (VL) needle biopsies 3-4 mm in length were obtained from young (20-30yr) and old (70+ yr) male and female subjects. Biopsies were collected by the Trappe lab at Ball State University (Trappe *et al.* 2003), immediately submerged in a skinning solution, and stored at -20℃. Samples were shipped overnigh t to the Fitts lab on ice. Upon arrival, biopsies were transferred to fresh skinning solution and stored for up to 4 weeks at -20℃.

On the day of experimentation, a single muscle fiber was isolated and suspended between a force transducer (Sensor One Technologies Model AE801) and servomotor (Aurora Scientific High-Speed Length Controller Model 312C) in a set up chamber containing relaxing solution. Fibers were studied using a novel single-fiber microsystem recently developed by the Fitts lab, modified from that first described by Karatzaferi *et al.* (2004). The system

(shown in Figure 2.1) has four individual temperature-controlled Peltier units mounted between a water cooled stainless steel platform and 6x6 mm stainless steel posts that project down within 2 mm of a glass coverslip. The position and force transducers are positioned such that the fiber is suspended in 100 µl of solution between the glass slide and one of the stainless steel posts with an individual post maintained at a temperature between 10 and 30℃. T he first post where the fiber is visualized has a hole drilled through it with the Peltier unit mounted on the side so that sarcomere length can be measured by laser diffraction and clamped at an optimal length during the measurement of k_{tr}. The entire unit is mounted on a ball bearing slide so that the Peltier units can be easily moved to position the fiber at a given post, set at a given temperature.

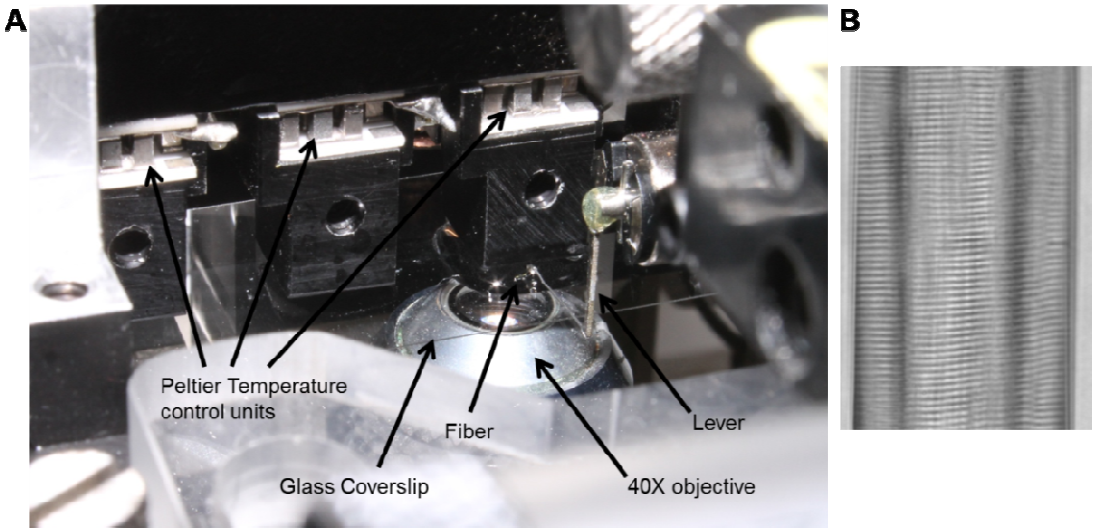

Figure 2.1: Single fiber microsystem.

(A) Experimental set-up. (B) Single fiber visualized at 40X.

Prior to experimentation, the fiber resting in relaxing solution was briefly (30 sec) exposed to a Brij 58 (Sigma) solution to disrupt sarcoplasmic reticulum (SR) membranes still intact after exposure to the skinning solution. The set-up post with relaxing solution in which the fiber was initially suspended was kept at 10℃ while the second post was adjusted to 15 or 30 ℃. Using an inverted microscope, the fiber was viewed at 800x and sarcomere length adjusted to 2.5µm (Stephenson & Williams 1982). Fiber length was determined by measuring the distance between the fixed points of attachment. Fiber diameter was assessed from a digital image of the fiber obtained while it was briefly suspended in air. Three measurements of fiber width were made along the fiber, and the average diameter determined assuming a cylindrical shape (Metzger & Moss 1987b).

Many of the experiments described in this dissertation are performed at the near-physiological temperature of 30℃, a value close to the average body temperature of 37℃. Single skinned fibers are nearly impossible to study at 37℃ due to sarcomere non-uniformity and fiber deterioration, but there is evidence that 30℃ is a strong representation of the temperature observed *in vivo*. Figure 2.2 shows the relationship between temperature and isometric force in slow skinned rabbit fibers (Davis & Epstein 2007). From this figure, it is apparent that isometric force plateaus at a temperature between 26 and 30℃. There is evidence that both maximal shortening velocity and the rate of force development (k_{tr}) increase as temperature increases, up to 35℃, and show no temperature plateau (Ranatunga & Wylie 1983).

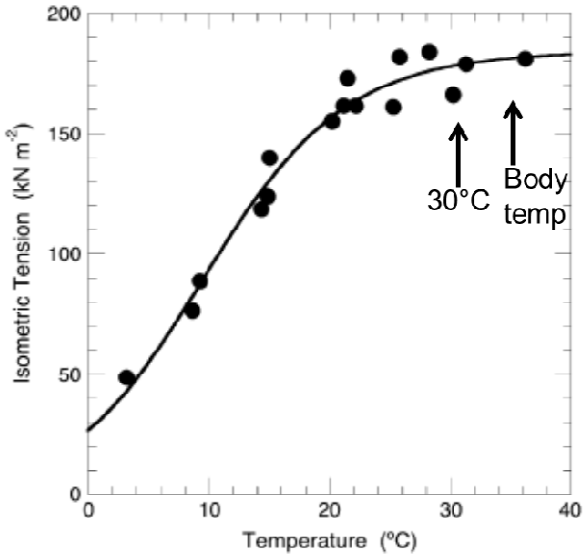

Figure 2.2: Isometric tension vs. temperature.

Data from rabbit soleus fibers, figure modified from Davis & Epstein (2007), with permission from Elsevier and *Biophysical Journal*.

Experimental Design

Single fibers were subject to a number of experiments, described here in the following order:

(1) pCa force relationship

(2) V_o and the force-velocity relationship

(3) stiffness-k_{tr}

(4) ATPase

pCa force relationship (Chapters 3 and 5)

The purpose of the pCa-force relationship is to characterize the force production of the fibers at submaximal levels of Ca^{2+} observed with fatigue.

From the pCa-force curve, calcium sensitivity can be quantified by pCa_{50}, or the concentration of Ca^{2+} at which there is half-maximal force and activation threshold (AT), or the concentration of Ca^{2+} at which force first develops.

The pCa-force relationship was determined by subjecting each fiber to a series of activating solutions ranging from pCa 7.0 to 4.5 at pH 7.0, pH 6.2 or pH 6.2 + 30 mM P_i at 15 or 30℃. For an individual fiber, the pCa-force relationship was analyzed as described in detail elsewhere (Widrick *et al.* 1998). Briefly, force elicited at a given pCa was allowed to plateau and then expressed as a fraction of peak force, i.e., submaximal force/peak force at pCa 4.5 (P_r). Least squares regression lines were fit to data points <50% of peak force and data points >50% peak force. Activation threshold (AT), the pCa at initial force development, was defined as Ca^{2+} concentration where log $[P_r/(1-P_r)] = -2.5$ (Widrick *et al.* 1998) (Figure 2.3). Half-maximal activation (pCa_{50}) was calculated as the mean intercept of least squares regression lines with the line y=0. The slope of the line fit to the data above P_r=0.5 was defined by n_1, and the slope of the line fit to data below P_r=0.5 was indicative of thick filament cooperativity and defined by n_2 (Debold *et al.* 2006) (Figure 2.3). The pCa-force curves in figures 3.4, 3.5, and 5.2C were constructed with GraphPad Prism (San Diego, CA) and fitted with a four-parameter logistic curve.

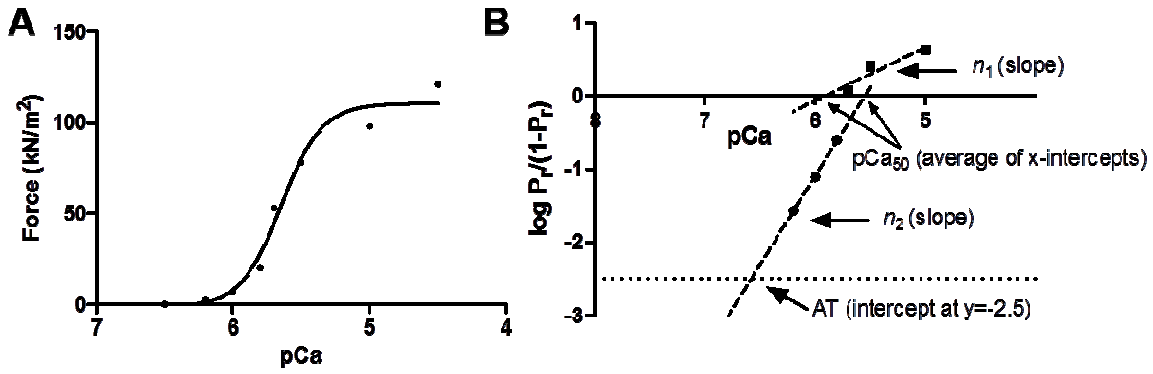

Figure 2.3: Representative pCa-force data from type II human fiber.

(A): pCa-force relationship for this fiber at 15℃. pCa is the –log of Ca^{2+} concentration. (B) Hill plots of data from (A). n_1, n_2, pCa_{50}, and AT determined from this plot as indicated by arrows and described in text. For this fiber, pCa_{50}= 5.73 , AT= 6.59, n_1= 0.73, n_2= 2.42.

Type I or type IIa fibers were taken through control (pH 7 + 0 mM P_i) and experimental (either pH 6.2 + 0 mM P_i, pH 7 + 0 mM P_i, or pH 6.2 + 30 mM P_i) pCa-force curves at both temperatures. Fast type IIx fibers were not stable enough to maintain sarcomere uniformity through more than two pCa-force curve tests. At the onset and conclusion of each pCa-force curve test, peak force (pCa 4.5) at 15℃ was measured. If a fiber's final peak force was <90% of the initial force, that fiber's data was eliminated. Approximately 10% of fibers were eliminated. All fibers were exposed to the given conditions (i.e., pH 7 vs. pH 6.2 condition) in a random order to control for order effects.

V_o and the force-velocity relationship (Chapters 4 and 5)

Unloaded shortening velocity, or V_o, was determined by imposing a series of rapid slack steps (100-400 µm) after the fiber was maximally activated in pCa

4.5 solution, as previously described and shown in Figure 2.4 (Edman 1979; Widrick 2002; Knuth *et al.* 2006). Fiber V_o (fiber lengths/sec) was determined from the slope of the least squares regression line of the plot of slack distance versus the time required for the redevelopment of force. The time from the initial slack (0 ms) to where force first starts to redevelop is designated as the time required for the redevelopment of tension. In Figure 2.4, the 400 µm slack step had a time to redevelop tension of 60 ms.

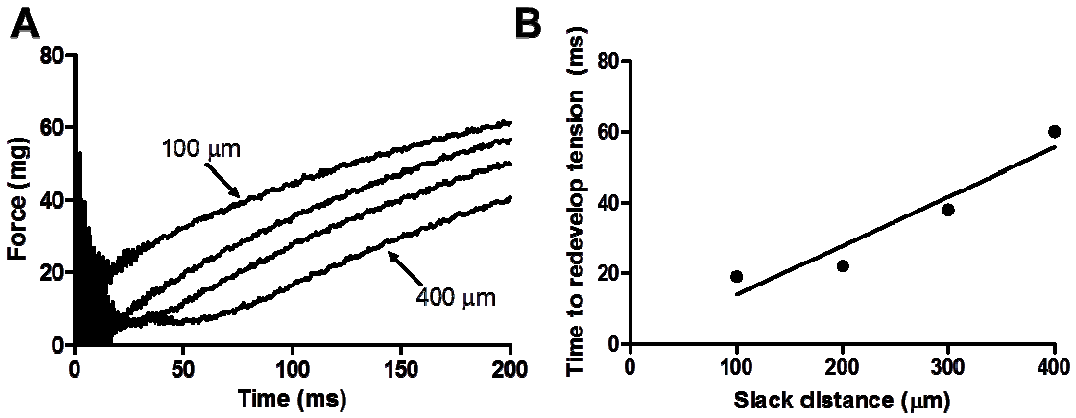

Figure 2.4: Determination of V_o for type I human fiber.

(A) Force records at various slack distances at 15°C. (B) Time to redevelop tension from A vs. slack distance. The time to redevelop tension in the 400 µm slack step was 60 ms. Slope of this plot is V_o and in this example was 1.65 fl/sec.

Single fiber force-velocity parameters were determined by maximally activating the fiber and then stepping it to three submaximal isotonic loads as previously described and shown in Figure 2.5 (Widrick *et al.* 1996; Knuth *et al.*

2006). Each load was maintained for a predetermined time (80-100 ms for slow fibers at 15℃, 30-40 ms for fast fibers at 15℃ an d 20-30 ms for both fiber types at 30℃). Each fiber was contracted 4-6 times; the refore, 12-18 data points were obtained for each force-velocity curve. Force (as a percentage of peak) and corresponding shortening velocities were fit to the Hill equation (Hill 1938) with the use of an iterative non-linear curve-fitting procedure (Marquardt-Levenberg algorithm). V_{max} was determined as the y-intercept of the fitted plot in fl/sec (Figure 2.5C). Peak fiber power was calculated with the fitted parameters of the force-velocity curve and P_o. Composite or average force-velocity and force-power curves were constructed by summating velocities or power values from 0-100% of P_o in increments of 1% (Widrick *et al.* 1996).

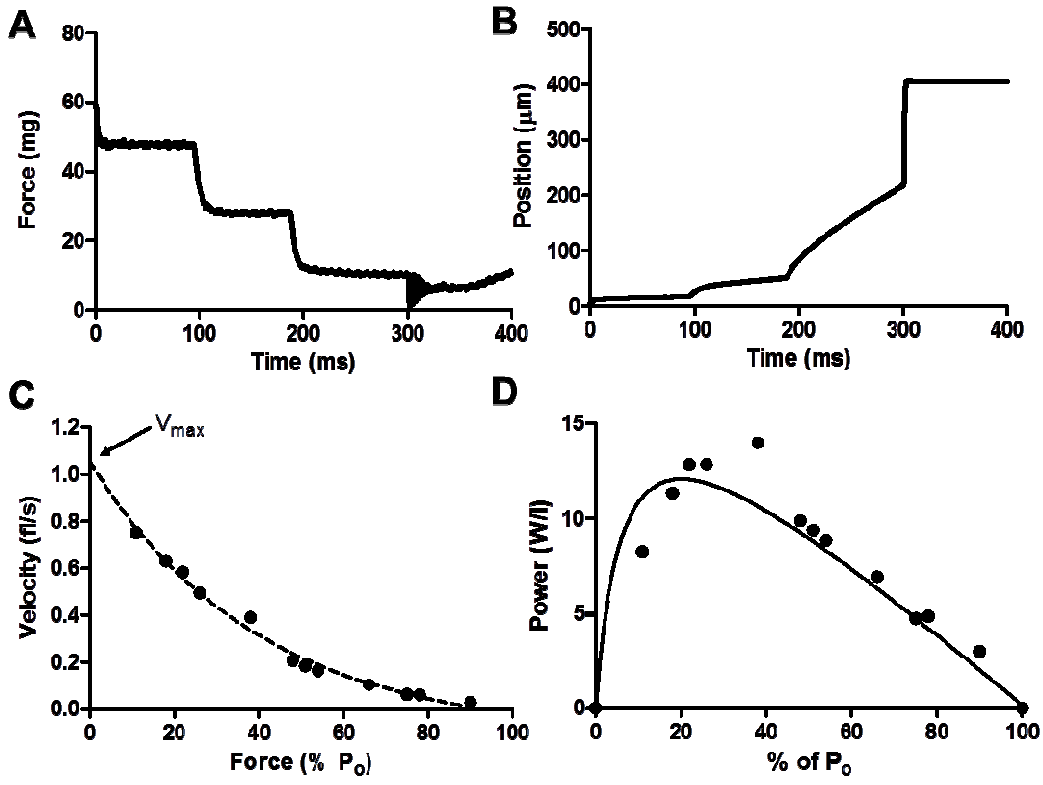

Figure 2.5: Force-velocity data from representative type I human fiber.

(A) and (B) Force and position records, respectively, for 3 consecutive 100 ms isotonic steps at 15℃. Velocities are the slopes of the steps in B. (C) Force-velocity plot for this fiber, points obtained from forces in (A) and velocities in (B) For this example, V_{max}=1.06 fl/s. 3-4 additional contractions run to obtain a range of points. (D) Power curve for this fiber, constructed utilizing the parameters in the force-velocity curve in (C).

For force-velocity experiments, slow and fast fibers were subject to control and experimental conditions, and slow fibers were stable enough to perform experiments at both temperatures (i.e. the fibers maintained $\geq$90% of initial P_o throughout the experiment). Fast fiber experiments were conducted either at 15 or 30℃.

Stiffness-k_{tr} (Chapters 4 and 5)

Stiffness was assessed to give an indication of the number of bound cross-bridges. Stiffness measurements were made using Sarcomere Length Control (SL Control), developed by Dr. Kenneth Campbell (Campbell & Moss 2003). Fibers were vibrated at an amplitude of 0.05% of fiber length (mean fiber length 2.20 mm, mean vibration amplitude 1.1 µm) and a frequency of 2kHz in both relaxing solution and when fully activated. Stiffness was calculated from the equation (Δforce per cross sectional area in activating solution - Δforce per cross sectional area in relaxing solution) / (Δlength) and expressed in N/mm^3.

k_{tr}, defined as the rate of force development, or the rate of tension redevelopment following a slack-unlack procedure, was measured directly following stiffness. A rate constant, k_{tr} gives an indication of how the fiber, under a given condition, proceeds through the low-to high-force transition of the cross-bridge cycle (Figure 1.1, step 3). During maximal activation, the fiber was rapidly slacked (10-20 ms slack) and re-extended to its original sarcomere length, and k_{tr} was determined by fitting the redevelopment of tension to a single exponential equation in SL Control (Figure 2.6). The duration of the slack was 20 ms at 15℃ and 10 ms at 30℃. For rat fast fiber k_{tr} measurements at 15 and 30℃ (Chapter 4), sarcomere length was laser clamped at 2.5 µm to prevent sarcomere non-uniformity during tension redevelopment. Laser clamp works by clamping sarcomere length within 0.5 nm per sarcomere by controlling the position of the first-order line of the laser diffraction pattern from the fiber (Metzger *et al.* 1989). Laser clamp was not employed with slow type I fibers, as k_{tr} values were not

different with and without the clamp (Fitzsimons *et al.* 2001). No k_{tr}'s collected on human fibers utilized the laser clamp (Chapter 5).

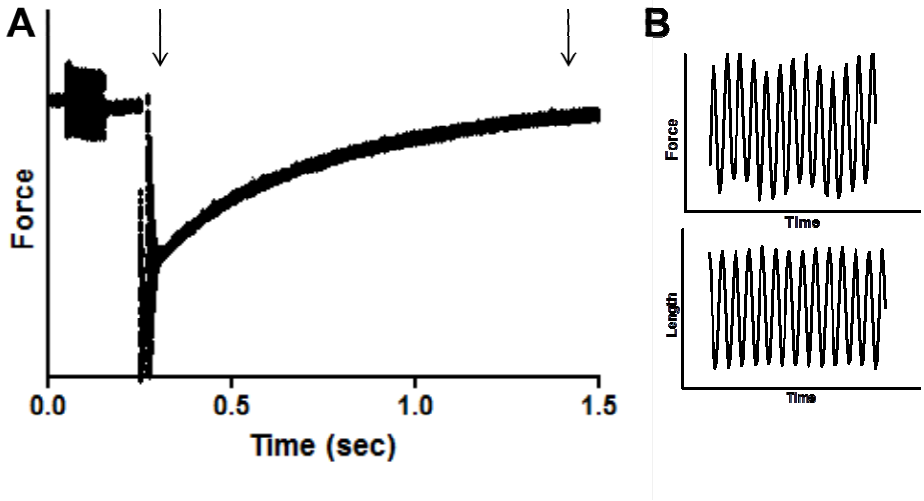

Figure 2.6: Representative stiffness-k_{tr} trace from human type I fiber.

(A) A maximally activated fiber subject to stiffness and slack-re-extension procedure. k_{tr} defined by single exponential fit between arrows. (B) Close-up of force oscillations in (A) (top) with corresponding length oscillations (bottom). Force oscillations averaged between 0.01 and 0.015 mN in fully activated fibers while length oscillations were on average 1.1 µm in amplitude.

To estimate the number of low-force bridges, we modified a technique of Colombini *et al.* (2010). The technique measures stiffness at P_o, different force values (% of P_o), and with rigor. Columbini *et al.* (2010) achieved various levels of P_o by blocking cross-bridge formation with N-benzyl-p-toulene sulphonamide (BTS) at 5℃ , while we reduced force by varying solution pCa between 7.0 and 4.5 at 15℃. The two methods were not compared in this work. Both force and stiffness were measured at 5-6 pCa points for each experimental group. At the

end of each experiment, the fiber was subjected to individual rigor solutions (composition described below) in a balanced order, based on whatever condition was tested with that fiber (pH 7 + 0 mM P_i, pH 6.2 + 0 mM P_i, pH 7 + 30 mM P_i or pH 6.2 + 30 mM P_i). The force and stiffness produced at a given pCa and condition were normalized to the force and stiffness obtained in rigor at the appropriate condition. The rigor solutions were similar to the activating solutions described in Table 2.1 except that ATP and PC were not added and sufficient KCl was added to yield a total ionic strength of 180 mM (Metzger & Moss 1990a).

ATPase (Chapter 5)

ATPase measurements were made by synchronizing two programs: SkinM, a custom made single-fiber force data acquisition system, and NIS Elements, an imaging system that fluorescently measured the oxidation of NADH. Measuring ATPase activity quantifies the rate at which ATP is hydrolyzed by myosin ATPase in the cross bridge cycle (Figure 1.1, step 2).

Solutions differed slightly from the experiments previously described. ATPase solutions contained no creatine phosphate to eliminate the creatine kinase reaction (catalytic reaction combining creatine and ATP to form phosphocreatine and ADP) (Silvestri & Wolfe 2013). Solutions contained the adenylate kinase inhibitor P1,P5-di(adenosine-5') pentaphosphate (100mM) to eliminate ADP removal by the adenyl kinase reaction (ADP + ADP → ATP + AMP), phosphenolpyruvate (10 mM) (substrate), and 250µM NADH, which was added to each solution fresh the day of experimentation (Schluter & Fitts 1994).

Sarcolemma and SR ATPase activity are inhibited by the skinning solution and Brij procedure.

Since the myofibrillar ATPase assay involves coupling ADP formation to the oxidation of reduced nicotinamide adenine dinucleotide (NADH to NAD), the glycolytic enzymes pyruvate kinase (PK, 100 U/ml) and lactate dehydrogenase (LDH, 100 U/ml) were added as solids to the solutions on the day of experimentation to carry out the following reactions: (Schluter & Fitts 1994).

(i) ATP → ADP + P_i (the measure of interest)

(ii) Phosphoenolpyruvate + ADP → pyruvate + ATP (catalyzed by pyruvate kinase)

(iii) Pyruvate + NADH + H^+ → lactate + NAD^+ (catalyzed by lactate dehydrogenase)

The decrease in NADH fluorescence must be linear over a given experimental trial and is what is used to measure ATPase activity (Schluter & Fitts 1994). If the decrease is not linear, more substrate or ATP must be added to the solution.

After a fiber was isolated, tied, and suspended in the microsystem shown in Figure 2.1, fiber length and diameter were determined, and the microsystem was anchored to a microscope with epifluorescent capabilities. Experiments were conducted in the dark due to the light-sensitivity of NADH. A beam of light from a Nikon Inc Xenon 75 Watt Halogen lamp struck a cube contained in the Nikon Eclipse TE 2000-U microscope that through a specific filter emitted a 340 nm beam of light that shone on the fiber (excitation wavelength). The fiber then,

through epifluorescence, emitted a wavelength of 470nm back through the cube, and this fluorescence decline was recorded by a Roper Scientific Photometrics CoolSnap ES Camera and analyzed using NIS-Elements. The rate at which images were collected second collected varied depending on the temperature of the measurements. At 15℃, 2-3 frames/second were collected while at 30℃, 5-6 frames/second were collected. Measurements were made in both relaxing (baseline) and activating solutions. The baseline level of ATPase activity (recorded at each experimental temperature) was very minimal and was subtracted from any subsequent measures in activating solution. ATPase experiments were made at 15, 23 (room temp), and 30℃. A representative ATPase experiment is shown in figure 2.7.

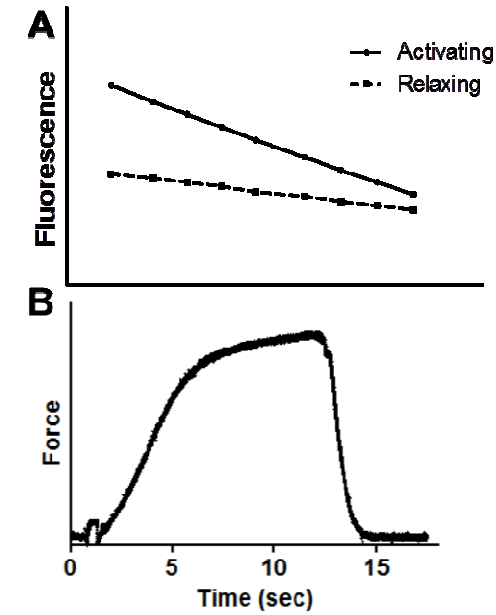

Figure 2.7: Representative ATPase data from human type I fiber.

(A) NADH oxidation at 15℃ in a single fiber in activat ing (solid line) and relaxing (dashed line) solutions, shown as a linear fluorescent decline, plotted versus time (fluorescence in arbitrary units). (B) Simultaneous recording of maximal force vs. time.

Following individual fiber experiments, epifluorescent activity was recorded from a set NADH solutions of standard concentration (230-250 µM) to construct a standard curve, from which ATPase activity could be calculated. ATPase activity was expressed in µmol/sec/g (adjusted for fiber volume), assuming 1 mm fiber = 1 µg of fiber (Schluter & Fitts 1994).

Myosin heavy chain composition and fiber typing

Following contractile measurements, fibers were solubilized in 10µl of 1% SDS sample buffer and stored at -20℃. The myosin heavy chain profile was

obtained by running samples on 7.5% (wt/vol) Tris-HCl pre-cast gels (Bio-Rad) and stained with the Silver Stain Plus kit (Bio-Rad).

Rat fibers were identified as type I, IIa, IIx, or IIb as shown in Figure 2.8. In Chapter 3, fibers were separated into 3 groups for all experiments: type I, IIa, and IIx. In Chapter 4, type IIa and IIx fibers differed in their k_{tr} values at both 15 and 30℃. However, the depression in velocity, power, or stiffness from pH 6.2 + 30 mM P_i was not different between the IIa and IIx fiber types. Thus, the data presented in chapter 4 for all parameters except k_{tr} combined IIa and IIx fibers (no IIb fibers were included in that study) to most accurately compare to previous publications (Debold *et al.* 2004; 2006; Knuth *et al.* 2006).

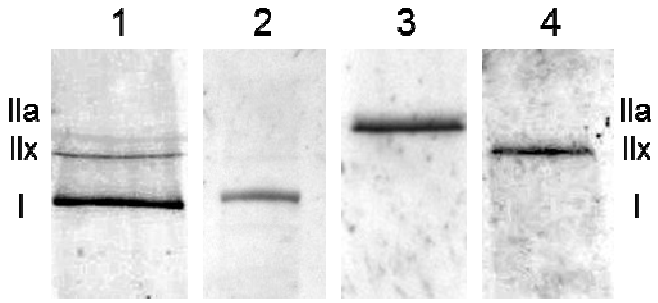

Figure 2.8: Myosin heavy chain gel (7.5%) with rat fibers

Lane 1, fiber with a predominant type I band and minor type IIa and IIx bands. Lanes 2-4, type I, IIa, and IIx fibers, respectively (Figure from Nelson & Fitts, 2014).

Human fibers were run on 12% polyacrylamide gels, and silver stained as described by Guilian *et al*. (1983). Fibers were then identified by their myosin light chain profile (Figure 2.9) and classified as type I or II fibers.

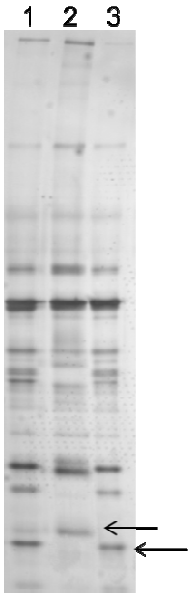

Figure 2.9: Myosin light chain gel (12%) with human fibers

Each lane represents a single fiber. Fibers typed based on myosin light chain 2 band (arrows). Lanes 1 and 3 are type II fibers and lane 2 is a type I fiber.

Statistics

All data were graphed and analyzed with Graph Pad Prism 5 (San Diego, CA).

Chapters 3 and 4 assessed the effects of H^+ and P_i (the pH 6.2 condition in Chapter 3 only and the pH 6.2 + 30 mM P_i condition in both chapters 3 and 4) on various physiological parameters such as calcium sensitivity, velocity, force, and more at two temperatures-- 15 and 30℃. A two- way ANOVA (temperature x condition) was used to detect any overall differences between means. For the dependent variables such as velocity, force, power, k_{tr}, stiffness, pCa_{50}, AT, n_1, and n_2, if the ANOVA detected an overall difference between the means, post-

hoc unpaired t-tests were used to test for significance between individual groups (i.e. pH 7 vs. pH 6.2). The significance level was set to $p<0.05$.

In chapter 5, fibers from the young men, young women, old men, and old women were separated based on age and sex into four groups. Training status was not taken into account when performing statistical analysis in this work but should be considered as this data moves forward. For a given dependent variable (peak force), a two-way ANOVA was used to detect any age and age-by-sex interaction effects. Since nearly all variables had multiple observations within the same individual (i.e peak force, n=6 observations from 1 individual), a linear mixed model was used. For all analyses, if a main or interaction effect was noted, post hoc t-tests were performed to identify pairwise differences and considered significant at $p<0.05$.

CHAPTER 3

EFFECTS OF LOW CELL PH AND ELEVATED INORGANIC PHOSPHATE ON THE PCA-FORCE RELATIONSHIP

Introduction

Experiments in single muscle fibers were initially performed at low temperatures (5-20℃) where low cell pH (pH 6.2) an d elevated P_i (30mM) significantly depressed peak force at saturating (maximal) Ca^{2+} (Metzger & Moss 1987a; Pate & Cooke 1989; Coupland *et al.* 2001). Temperature jump-plate technology allowed for single fiber experiments to be conducted at physiological temperatures (30-35℃), and the depressive effects of low cell pH and elevated P_i on peak force were less pronounced (Pate *et al.* 1995; Coupland *et al.* 2001; Debold *et al.* 2004).

In a fatiguing event, myoplasmic free Ca^{2+} is not maximal, as SR Ca^{2+} release is attenuated and the amplitude of the myoplasmic Ca^{2+} transient is depressed and may reach levels < pCa 6.0 (1 µM) (Allen & Westerblad 2001). At 30℃, 30 mM P_i reduced peak force by 19% in type I and did not significantly reduce force in type II fibers, (Debold *et al.* 2004), while pH 6.2 reduced peak force by 12% in type I and didn't significantly depress force in type II fibers (Knuth *et al.* 2006). Debold *et al.* (2006) showed that elevated P_i (30 mM) depresses force at submaximal Ca^{2+} concentrations at near-physiological

temperatures. The reduction in myofilament Ca^{2+} sensitivity by P_i was more pronounced at 30℃ compared with 15℃. Like P_i, the depressive effects of low cell pH on peak force are reduced at near-physiological temperatures, leading some to question the role of low cell pH in fatigue (Pate *et al.* 1995; Westerblad *et al.* 1997; Stackhouse *et al.* 2001; Allen *et al.* 2008). However, the effects of low cell pH have yet to be evaluated at submaximal Ca^{2+} concentrations that are characteristic of fatigue. Therefore, the first aim of this chapter evaluated the effects of acidosis at submaximal Ca^{2+} at 15 and 30℃.

While it has been shown that both metabolites individually depress myofilament calcium sensitivity at 15℃ (Metzger & Moss 1990a; Martyn & Gordon 1992), the collective effects of low cell pH and elevated P_i on the pCa-force relationship are unknown. Thus, a second aim of this chapter was to assess the combined effects of pH 6.2 and 30 mM P_i on the pCa-force relationship at cold (15℃) and near-physiological (30℃) temperatures.

Results

Representative force traces from slow and fast fibers at various Ca^{2+} concentrations are shown in figures 3.1 and 3.2. The time required for a fiber to reach peak force was shorter at higher temperatures.

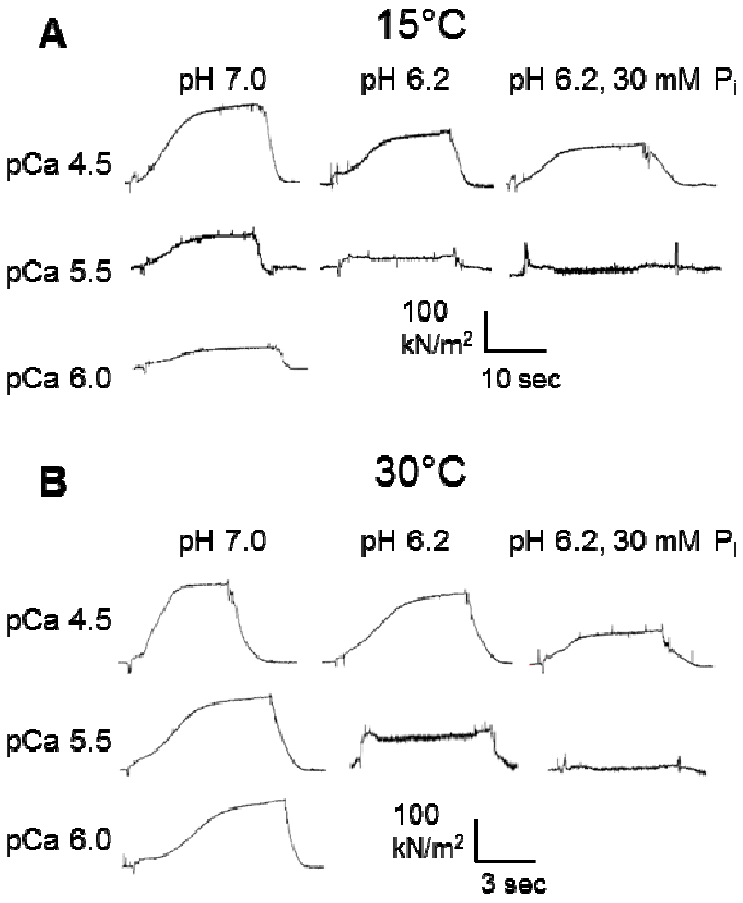

Figure 3.1: **Selected type I force records.**

(A) 15℃ and (B) 30℃. Force records obtained at p H 7, pH 6.2, and pH 6.2 + 30 mM P_i at pCa 4.5, 5.5, and 6.0. No force was observed at pCa 6.0 with pH 6.2 or pH 6.2 + 30 mM P_i conditions for either temperature.

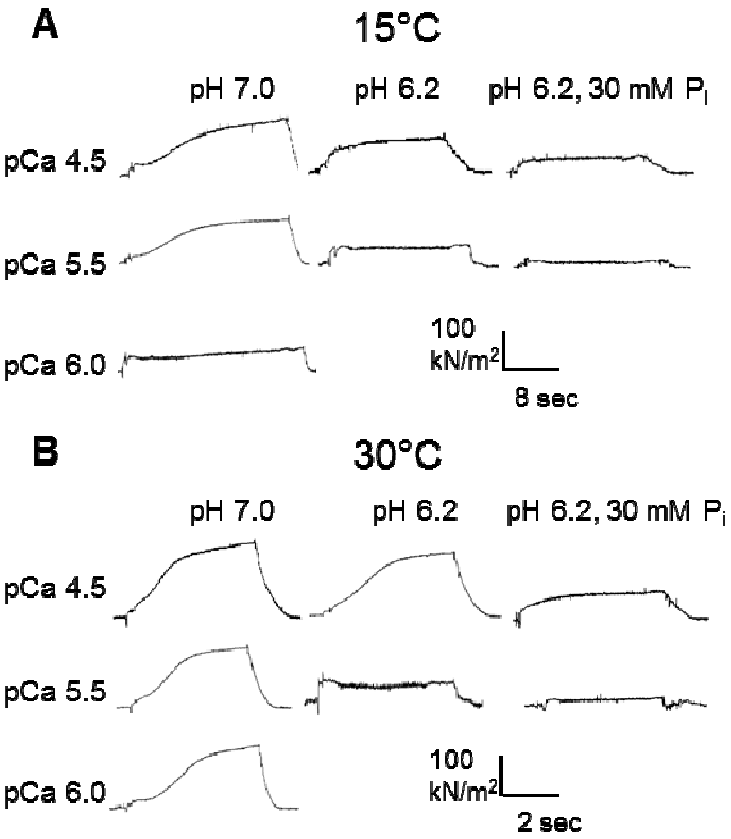

Figure 3.2: **Selected type II force records.**

(A) 15℃ and (B) 30℃. Force records obtained at pH 7, pH 6.2, and pH 6.2 + 30 mM P_i at pCa 4.5, 5.5, and 6.0. No force was observed at pCa 6.0 with pH 6.2 or pH 6.2 + 30 mM P_i conditions for either temperature.

Increasing temperature from 15 to 30℃ increased pe ak force (Figure 3.3) and the slope of the pCa-force relationship below pCa_{50} (quantified by n_2) (Figures 3.4 and 3.5, Tables 3.1-3.3) in all fiber types at control conditions (pH 7, 0 mM P_i). An increased myofibrillar Ca^{2+} sensitivity was observed with increasing temperature in all fiber types, indicated by significant increases in AT and pCa_{50}

(Tables 3.1-3.3). The higher temperature elevated n_2, reflective of increased thick filament cooperativity, in type I and IIa but not IIx fibers in control conditions (Tables 3.1-3.3). More Ca^{2+} was required to initiate force in type IIx versus type I fibers at control conditions as indicated by significant fiber type differences in AT at both 15 and 30℃ ($p<0.01$).

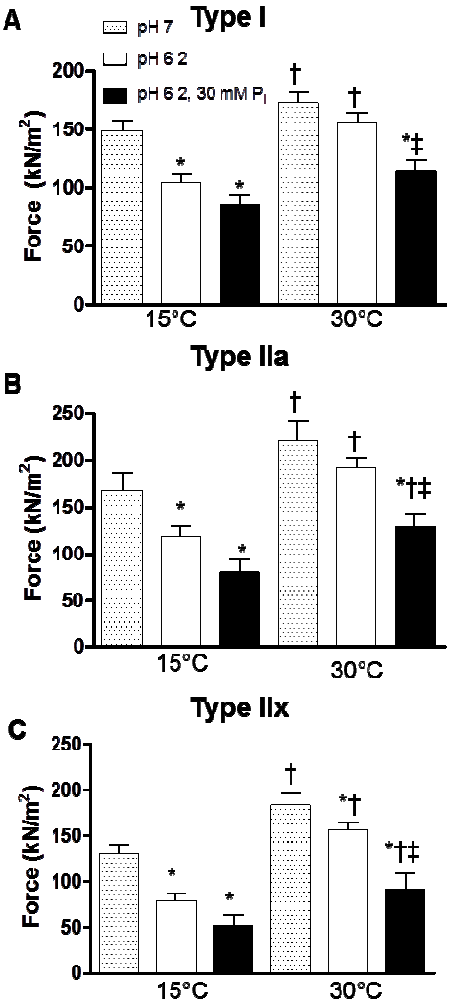

Figure 3.3: **Peak force (P_o) elicited at pCa 4.5.**

Values are means ± SEM for type I (A), type IIa (B), and type IIx (C) fibers. *Significantly different from pH 7 condition at the same temperature, $p<0.05$. †Significantly different from comparable condition at 15℃. ‡Significantly different from pH 6.2 condition at the same temperature, $p<0.05$.

	15°C			30°C		
	pH 7.0	pH 6.2	pH 6.2, 30mM P_i	pH 7.0	pH 6.2	pH 6.2, 30mM P_i
n	*19*	*19*	*10*	*20*	*18*	*10*
pCa_{50}	6.06 ± 0.05	5.40 ± 0.02*	5.18 ± 0.10*‡	6.77 ± 0.02†	5.56 ± 0.02*†	5.16 ± 0.10*‡
AT	6.92 ± 0.04	6.08 ± 0.05*	5.75 ± 0.06*‡	7.33 ± 0.06†	6.09 ± 0.05*	5.85 ± 0.09*‡
n_1	2.15 ± 0.15	1.86 ± 0.29	1.84 ± 0.60	1.84 ± 0.50	2.23 ± 0.29	2.08 ± 0.37
n_2	2.99 ± 0.16	3.51 ± 0.28	3.68 ± 0.91	4.02 ± 0.45†	4.50 ± 0.43†	3.96 ± 1.04

Table 3.1: Type I fiber force characteristics

Values are means ± SEM, obtained from linearized Hill plots of the pCa-force curve. *n,* number of fibers. pCa_{50} and activation threshold (AT) are shown in negative log units. *Significantly different from pH 7.0 condition at same temperature, p<0.05. †Significantly different from comparable condition at 15℃, p<0.05. ‡Significantly different from pH 6.2 condition at same temperature, p<0.05.

	15°C			30°C		
	pH 7.0	pH 6.2	pH 6.2, 30mM P_i	pH 7.0	pH 6.2	pH 6.2, 30mM P_i
n	*17*	*9*	*7*	*7*	*7*	*7*
pCa_{50}	5.96 ± 0.07	5.31 ± 0.04*	4.90 ± 0.10*‡	6.73 ± 0.11†	5.49 ± 0.06*†	5.04 ± 0.13*‡
AT	6.90 ± 0.07	6.11 ± 0.09*	5.77 ± 0.10*‡	7.21 ± 0.13†	5.99 ± 0.10*	5.61 ± 0.07*‡
n_1	2.00 ± 0.23	1.69 ± 0.18	2.44 ± 0.63	1.27 ± 0.34	3.32 ± 0.71*†	2.26 ± 0.42
n_2	2.85 ± 0.26	3.59 ± 0.63	3.22 ± 0.72	5.03 ± 0.75†	5.40 ± 1.08†	4.59 ± 0.99

Table 3.2: Type IIa fiber force characteristics

Values are means ± SEM, obtained from linearized Hill plots of the pCa-force curve. *n,* number of fibers. pCa_{50} and activation threshold (AT) are shown in negative log units. *Significantly different from pH 7.0 condition at same temperature, p<0.05. †Significantly different from comparable condition at 15℃, p<0.05 . ‡Significantly different from pH 6.2 condition at same temperature, p<0.05.

	15°C			30°C		
	pH 7.0	pH 6.2	pH 6.2, 30mM P_i	pH 7.0	pH 6.2	pH 6.2, 30mM P_i
n	*17*	*14*	*10*	*13*	*11*	*6*
pCa_{50}	6.16 ± 0.06	5.34 ± 0.03*	4.89 ± 0.09*‡	6.58 ± 0.03†	5.36 ± 0.02*	4.98 ± 0.11*‡
AT	6.70 ± 0.05	5.87 ± 0.06*	5.81 ± 0.10*	7.03 ± 0.04†	5.97 ± 0.06*	5.89 ± 0.15*
n_1	2.11 ± 0.35	2.75 ± 0.41	2.21 ± 0.31	2.17 ± 0.37	3.50 ± 0.60*	3.22 ± 0.83
n_2	4.43 ± 0.58	5.57 ± 0.82	2.59 ± 0.30*‡	5.02 ± 0.46	5.03 ± 0.97	2.46 ± 0.49*‡

Table 3.3: Type IIx fiber force characteristics

Values are means ± SEM, obtained from linearized Hill plots of the pCa-force curve. *n,* number of fibers. pCa_{50} and activation threshold (AT) are shown in negative log units. *Significantly different from pH 7.0 condition at same temperature, $p<0.05$. †Significantly different from comparable condition at 15℃, $p<0.05$. ‡Significantly different from pH 6.2 condition at same temperature, $p<0.05$.

At saturating Ca^{2+} (pCa 4.5), the depressive effects of pH 6.2 on force were less pronounced at 30℃ compared to 15℃ in al l fiber types such that peak force was significantly depressed in all fiber types at 15℃ but only in the fast type IIx fibers at 30℃. Under pH 6.2 + 30 mM P_i conditions, peak force was significantly depressed from control in all fiber types at both temperatures, with the greatest effects in type IIx fibers at both 15°C (61% force depression) and 30℃ (50% force depression) (Figure 3.3).

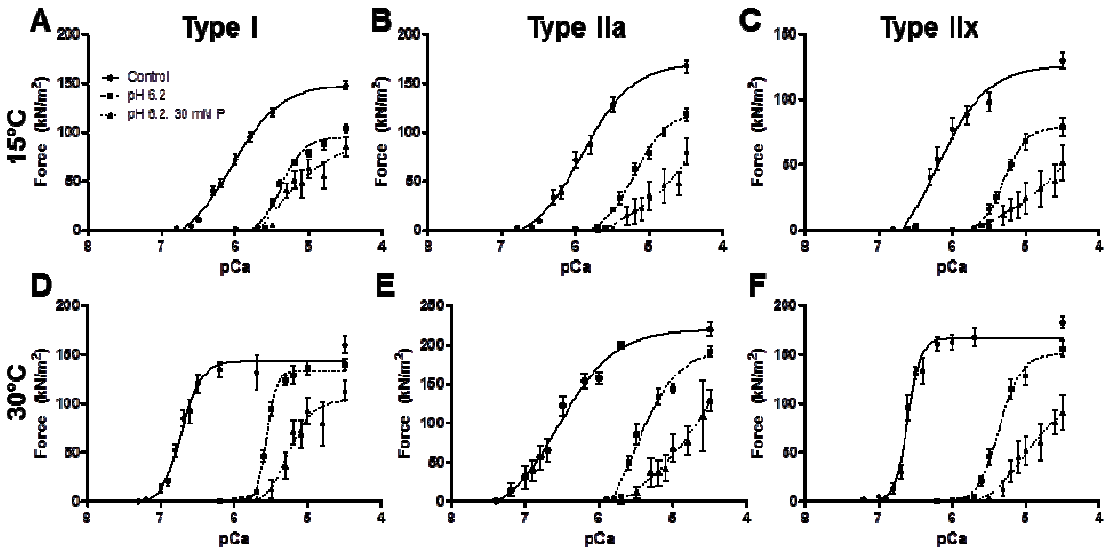

Figure 3.4: **Average pCa-force curves.**

(A) and (D) Type I, (B) and (E) Type IIa, (C) and (F) Type IIx at 15℃ (A -C) and 30℃ (D-F). Each data set represents force (means ± SEM) at each Ca^{2+} concentration (in negative log units) from all fibers included in the experiment.

At submaximal Ca^{2+}, pH 6.2 and pH 6.2, 30 mM P_i significantly reduced force in all fiber types at both temperatures. At 15℃ at a submaximal Ca^{2+} concentration of pCa 5.5 (5 µM), low cell pH depressed force by 74% in slow fibers (Figure 3.1A) and 86% in fast IIx fibers (Figure 3.2A), compared to control. At 30℃ and pCa 5.5, pH 6.2 depressed slow fiber force by 41% (Figures 3.1B and 3.6) and fast IIx fiber force by 73% (Figures 3.2B and 3.6). With pH 6.2 + 30 mM P_i conditions, no force was generated at pCa 6.0 at either temperature (Figures 3.1 and 3.2) while at pCa 5.5, force was reduced by 91, 95, and 98% in type I, IIa, and IIx fibers, respectively at 30℃, compared to control (Figure 3.6).

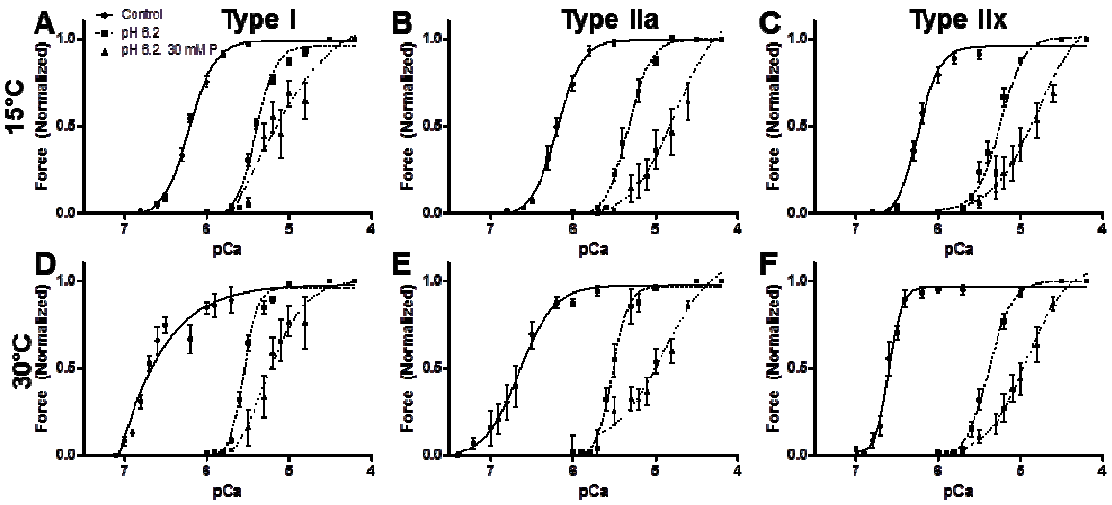

Figure 3.5: **Mean normalized pCa-force curves.**

(A) and (D) Type I, (B) and (E) Type IIa, (C) and (F) Type IIx at 15℃ (A -C) and 30℃ (D-F). Maximal isometric force (P_o) at each pCa normalized to the level obtained in pCa 4.5 at both temperatures in all conditions is plotted against pCa. Values are means ± SEM.

At pH 6.2, the pCa-force relationship in all fiber types was significantly shifted to higher free Ca^{2+} levels for a given percent of P_o, indicative of reduced myofibrillar Ca^{2+} sensitivity, with a greater shift at 30℃ (Figures 3.4 and 3.5). This resulted in lower pCa_{50} values; for example, in type I fibers, the low pH-induced change in pCa_{50} was 0.66 units at 15℃ and 1.21 units at 30℃ (Figure 3.7). At pH 6.2, 30 mM P_i, the pCa-force relationship showed an even greater reduction in myofibrillar Ca^{2+} sensitivity than with low pH alone at both temperatures, with larger effects at 30℃ (pCa_{50} change of 0.88 at 15℃ and 1.61 at 30℃ in type I fibers) (Figure 3.7). Under low cell pH conditions, the pCa_{50} in type IIx fibers was significantly lower than type I and IIa fibers at 30℃ (Tables 3.1-3.3).

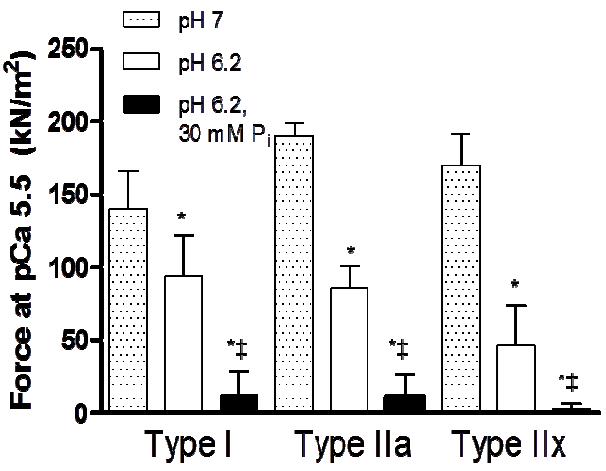

Figure 3.6: **Force at submaximal calcium.**

Force at pCa 5.5 (5 μM) for all fiber types in pH 7, pH 6.2, and pH 6.2 + 30 mM P_i conditions at 30℃. Values are means ± SEM. *Signi ficantly different from pH 7 condition, $p<0.05$. ‡Significantly different from pH 6.2 condition, $p<0.05$.

In both pH 7 and pH 6.2 conditions at 15℃, n_2 was significantly higher in type IIx fibers compared to type I fibers. Elevating both H^+ and P_i selectively reduced n_2 in type IIx fibers (Table 3.3) at both 15 and 30℃ such that fiber type differences seen at 15℃ in control and pH 6. 2 conditions were no longer apparent. Fibers generated force at lower Ca^{2+} concentrations (higher AT) in type I and IIa fibers vs. type IIx fibers at pH 7, and low pH increased the Ca^{2+} required to initiate force (AT) in all fiber types at both temperatures. The pH effect on AT was significantly exacerbated by the addition of 30 mM P_i in type I and IIa but not IIx fibers, which resulted in no fiber type differences in the AT at pH 6.2, 30 mM P_i conditions (Tables 3.1-3.3).

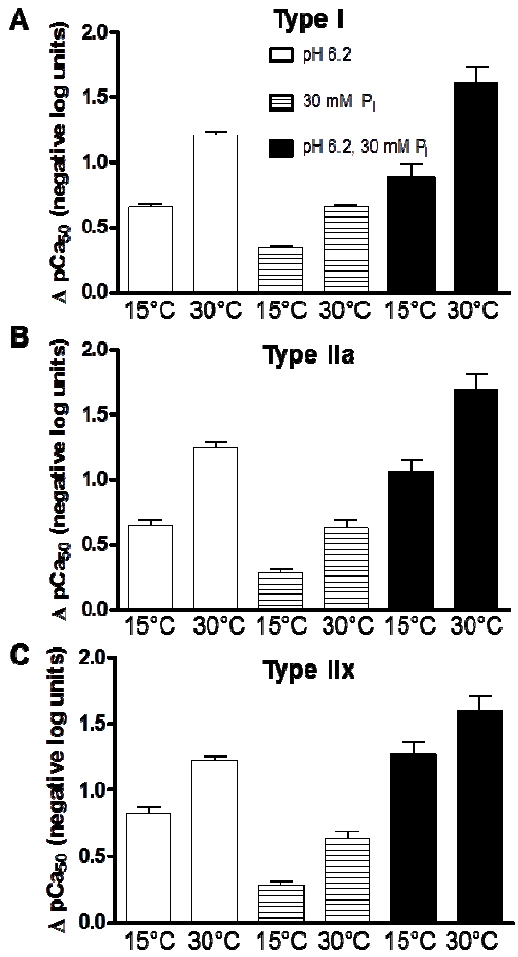

Figure 3.7: **Absolute change in pCa_{50}.**

Change in pCa_{50} from control induced by acidosis conditions (pH 6.2), elevated P_i (30mM), and pH 6.2 + 30 mM P_i at 15 and 30℃ for type I (A), type IIa (B), and ty pe IIx (C) fibers. Values (means ± SEM) are differences in mean pCa_{50} values in Tables 1-3. Data for the elevated P_i alone from Debold *et al.* (2006).

To better illustrate temperature effects, the pCa-force relationship was normalized to peak force for each condition (Figure 3.5). The low cell pH and low pH plus P_i-induced shift in the pCa-force curve is greater at 30℃ (Figure 3.5D -F) than 15℃ (Figure 3.5A -C) in all fiber types. The pH and pH+P_i effect on

reducing myofilament Ca^{2+} sensitivity was more pronounced at higher temperatures, as quantified by the greater decrease in pCa_{50} (Figure 3.7, white and black bars). The pH effect was significantly larger than the P_i effect (Figure 3.7, striped bars) (Debold *et al.* 2006) in all fiber types at both temperatures. The effects of pH 6.2 + 30 mM P_i on the change in pCa_{50} were additive in type IIx and IIa fibers at both temperatures but only at 30℃ fo r type I fibers (Figure 3.7, black bars).

Discussion

We have shown that low cell pH (6.2) reduces myofibrillar Ca^{2+} sensitivity in all fiber types, as indicated by a significantly depressed AT and pCa_{50}, and the effects are greater at near-physiological temperatures. Prior to this study, the effects of low cell pH on force at submaximal Ca^{2+} concentrations characteristic of fatigue at near-physiological temperatures (30℃) were unknown. At both 15 and 30℃, the combination of pH 6.2 and 30 mM inorg anic phosphate (P_i) further depresses AT in type I and IIa fibers and pCa_{50} and peak force in all fiber types greater than either ion alone. Low cell pH did not change n_2, suggesting that acidosis did not alter thick filament cooperativity; however, in combination with P_i, n_2 was depressed in fast IIx fibers at 15 and 30℃. These findings characterize the individual and collective roles of low cell pH and elevated P_i in force depression at near-physiological temperatures and implicate a critical role of both ions in mediating fatigue.

To maximize the stability of the preparation, skinned fiber experiments have predominantly been performed at lower, non-physiological (≤15℃) temperatures (Cooke *et al.* 1988; Metzger & Moss 1990a). Under these conditions, low cell pH significantly depressed force at submaximal and saturating Ca^{2+} concentrations (Fitzsimons *et al.* 2001; Knuth *et al.* 2006). When jump-plate technology emerged and fibers were set up at cold temperatures and studied at near-physiological temperatures (≥25℃), the depressive effects of low pH on peak force were reduced (Pate *et al.* 1995). This observation led to the hypothesis that the contribution of low pH or hydrogen ion to fatigue was minimal at physiological temperatures. However, Allen and Westerblad (2001) have shown that the amplitude of the Ca^{2+} transient declined with fatigue, reaching below one micromolar (pCa 6.0) levels. Thus, fatigue is more accurately mimicked in experiments carried out at submaximal Ca^{2+}. An important finding in this study was that low cell pH significantly contributed to force depression at submaximal Ca^{2+}, with a more pronounced effect at near-physiological temperatures (30℃).

Our results show that peak force increased in all fiber types with temperature. This is in agreement with Ranatunga and Wylie (1983) who reported peak force of the rat soleus and EDL muscles to increase by ~2 fold as temperature increased from 10 to 35℃. Davis and E pstein (2007) proposed that a local unfolding within the cross-bridge secondary/tertiary structure might cause a greater force generation with rising temperature. Ca^{2+} binding to troponin-C is enhanced at higher temperatures (Sweitzer & Moss 1990). Therefore, less Ca^{2+}

was required to develop force, as evidenced by a temperature-sensitive increase in the pCa for the AT and pCa_{50} in all fiber types. The temperature-induced shift in the pCa-force relationship toward lower free Ca^{2+} levels is consistent with previous findings in our lab (Debold *et al.* 2006) and others (Sweitzer & Moss 1990; Maughan *et al.* 1995) and results from a temperature induced increase in myofibrillar Ca^{2+} sensitivity. The forward rate constant of force generation (Figure 1.1, step 3) is greatly accelerated by increasing temperature (Zhao & Kawai 1994). Consequently, more high-force cross-bridges are formed at a given submaximal Ca^{2+} at high (30℃) compared to low (15℃) temperatures .

The myofibrillar Ca^{2+} sensitivity of force development is fiber type dependent with fast fibers activating at a higher free Ca^{2+} but with a greater degree of cooperative binding (Fitts 1994; 2008). Our results confirmed this, as AT values in slow type I fibers are higher (less calcium) than fast IIx fibers at both 15 and 30℃. Thick filament cooperativity, quantified by n_2, is temperature sensitive, with binding enhanced at higher temperatures (Sweitzer & Moss 1990; Swartz & Moss 1992; Debold *et al.* 2006). We observed the temperature sensitivity of n_2 to be true for slow type I and fast type IIa, but not fast IIx fibers. Debold *et al.* (2006) reported significant increases in n_2 with temperature in type I and II fibers but did not subdivide type II fibers into IIa and IIx. Because type IIx fibers have a high n_2 compared to type I or IIa fibers at 15℃, additional cooperative binding reserve may be less in IIx fibers, making any increase with temperature difficult to detect.

Consistent with the findings of others (Pate *et al.* 1995; Knuth *et al.* 2006), we found low cell pH (6.2) to depress peak force less at saturating Ca^{2+} concentrations (pCa 4.5) at higher compared to the lower temperatures, in that low pH had no significant effect on type I and IIa fiber peak force and only a modest effect on the peak force of type IIx fibers at 30℃. Our finding that low pH depresses P_o in fast type IIx fibers suggests that either the number of cross-bridges or the force per bridge remained depressed with increasing temperature (Metzger & Moss 1990a). Previously, Knuth *et al.* (2006) observed no pH effect on peak fast fiber force at 30℃ but fibers were not subdivided into IIa and IIx, and the lack of a low pH induced decline in force may have resulted from a high percentage of IIa fibers. It has been proposed that elevated H^+ inhibits the forward rate constant of force generation (Figure 1.1, step 3) (Fitts 2008). Since both acidosis and temperature affect this step, the effects should be additive, with temperature reducing the force-depressive effects of low pH. This was the case but to a lesser extent in type IIx fibers.

In muscle fatigue, decreasing cell pH is accompanied by an increase in inorganic phosphate (P_i) up to 30 mM, (Cady *et al.* 1989). Karatzaferi *et al*. (2008) found 30 mM P_i at 30℃ to depress peak force by ~25% in fast fibers, while Debold *et al.* (2004) observed a 19% and insignificant decline in type I and II fibers, respectively. The collective effects of low cell pH and elevated P_i on peak force on a given fiber type have been less studied. Potma *et al.* (1995) showed that at 15℃ and under pH 6.0, 30 mM P_i conditions, peak force was depressed by ~63 and ~86% in rabbit soleus and psoas fibers, respectively.

Karatzaferi *et al.* (2008) reported peak force reductions of 81 and 52% at 10 and 30℃, respectively, in rabbit psoas fibers (a muscle composed primarily of fast fibers) exposed to pH 6.2 + 30 mM P_i. Under the same conditions, we found a 44, 41, and 50% reduction in peak force in type I, IIa, and IIx fibers, respectively, at 30℃ with greater declines at 15℃. Elevated H^+ and P_i are hypothesized to depress peak force by different mechanisms, with H^+ depressing the forward rate constant and P_i accelerating the reverse rate constant of force generation (Figure 1.1, step 3); thus, it follows that the combined effects of low cell pH and elevated P_i on peak force would be additive (Metzger & Moss 1990b).

We demonstrate a greater right shift (i.e. increased Ca^{2+} for a given percent of P_o) in the pCa-force curve at 30℃ compared to 15℃ as a result of low cell pH, implicating low pH as a more critical mediator of fatigue than previously believed based on experiments carried out at maximal Ca^{2+} concentrations (Pate *et al.* 1995; Knuth *et al.* 2006). With low pH or low pH plus P_i, temperature did not affect pCa_{50}, an effect not observed in control conditions, where temperature elevates pCa_{50} in all fiber types. While elevating temperature can attenuate the effects of low pH and P_i on P_o at maximal Ca^{2+} concentrations, it does not have any effect on force at submaximal calcium concentrations. One possible explanation for this observation is that the inhibition of force resulting from the competitive inhibition by H^+ of Ca^{2+} binding to troponin-C effectively negates the increased myofibrillar Ca^{2+} sensitivity induced by increasing temperature (Sweitzer & Moss 1990; Wattanapermpool *et al.* 1995).

Early studies investigating the role of pH at submaximal Ca^{2+} concentrations in skinned fibers were conducted at room temperature (22-23℃) or lower (10-15℃) (Hermansen & Osnes 1972; Fabiato & Fabiato 1978; Metzger & Moss 1990) and a pH range of 6.2 to 7.4. Hermansen and Osnes (1972) showed no significant effect of pH in rabbit soleus fibers on the pCa-force curve at pH 6.5 vs. pH 7.0 conditions at room temperature, and at the same temperature, Fabiato and Fabiato (1978) reported pH 6.2 to shift the pCa_{50} approximately 0.35 units (~1 µM) compared to pH 7.0 in frog semitendinosus. Metzger and Moss (1990a) reported a similar 0.35 pCa unit (~1 µM) pCa_{50} shift from pH 7 to pH 6.2 at 15℃ in rat soleus fibers. Our data show a larger H^+-induced shift in pCa_{50} than previously reported, with pH 6.2 shifting the pCa_{50} of type I fibers 1.21 units at 30℃ and 0.66 units (~3 µM) at 15℃. An explanation for the differences between studies is not readily apparent but could relate to sample size which was considerably larger in our work and slight differences in temperature. At 15℃, even small differences in temperature would result in significant changes in the pCa_{50} (Sweitzer & Moss 1990; Davis & Epstein 2007). Finally, in mammalian fast muscle, Palmer and Kentish (1994) describe a 3.63 µM shift in pCa_{50} at pH 6.2 conditions at 25℃, a value comparable to the 4.11 µM shift we observed in the type IIx fibers at 30℃.

P_i alone (30 mM) reduced pCa_{50} more at 30℃ (0.66 units in type I fibers) than 15℃ (0.34 units) compared to control (Debold *et al.* 2006) (Figure 3.7). Our study has shown that at both 15 and 30℃, low cell pH has a greater depressive effect on myofibrillar Ca^{2+} sensitivity than P_i. A novel result of this study is that

the effects of low pH plus P_i on myofibrillar Ca^{2+} sensitivity are additive at both temperatures (Tables 3.1-3.3, Figure 3.7). The purpose of investigating the collective effects of low cell pH and elevated P_i was to more closely mimic *in vivo* fatigue in the skinned fiber preparation. We chose pH 6.2 and 30 mM P_i to represent the "worst case scenario" in fatigued muscle (Metzger & Fitts 1987; Cady *et al.* 1989). Moopanar and Allen (2006) showed that when mouse flexor digitorum brevis (FDB) fibers were fatigued using 400 ms, 100 Hz tetani at 37℃, the Ca^{2+} concentration required for 50% of peak force increased by 200nM. This is a considerably smaller shift than we show in skinned fibers with pH 6.2, 30 mM P_i conditions (~ 7 µM or 1.61 pCa units at 30℃ in ty pe I fibers). With isolated single living fibers contracting *in vitro,* the diffusion gradient (intracellular to extracellular) would have been high; thus, it seems unlikely that pH fell to 6.2 or that P_i reached 30 mM. This would in part explain the smaller differences in function than we show in the "worst case scenario" condition.

The rightward shift in the pCa-force curve to higher free Ca^{2+} levels as a result of low pH and low pH plus P_i increased at both temperatures and in a fiber type manner, with type IIx > type IIa > type I. With high intensity exercise, fast fibers depend more on glycolysis and thus produce more H^+ and P_i than slow fibers (Fitts 1994). This combined with the observation that fast fibers are more sensitive to the fatiguing effects of these ions (Tables 1-3), in part explains the increased fatigability of fast IIx vs. slow type I fibers.

Thick filament cooperativity assessed by n_2 is significantly depressed by 30 mM P_i at 15 but not 30℃ in fast fibers (Debold *et al.* 2006). The temperature

dependence was attributed to the P_i-induced decline in the number of high-force cross-bridges in fast fibers at 15 but not 30℃ (De bold *et al.* 2006). Interestingly, the pH 6.2 + 30 mM P_i condition depressed n_2 in type IIx fibers at both 15 and 30℃. A possible explanation for this is that the collective effects of low pH and elevated P_i countered the elevated temperature acceleration of the low-to high-force state (Figure 1.1, step 3) and shifts the distribution of cross-bridges more to a low-force or unbound state (Hibberd *et al.* 1985). Thus, the decline in n_2 in the low pH, high P_i condition may have resulted from fewer bound cross-bridges, which would not only reduce peak tension but also the ability for one bridge to influence the binding of another.

Acidosis significantly increased the amount of Ca^{2+} (lower pCa) required to initiate the development of force (AT) in all fiber types and both temperatures. Debold *et al.* (2006) observed a similar effect with 30 mM P_i except in type II fibers at 15℃, where AT was unaltered. The more p ronounced effect of low pH over high P_i on AT is likely due to the competitive inhibition of H^+ on Ca^{2+} binding to troponin-C (Wattanapermpool *et al.* 1995).

In this study, we determined that at Ca^{2+} levels characteristic of fatigue, low pH significantly depressed force at low (15℃) and near-physiological (30℃) temperatures and that in combination, low pH and elevated P_i significantly depressed myofibrillar Ca^{2+} sensitivity and P_o to a greater extent than either metabolite alone (Debold *et al.* 2006). In fast type IIx fibers, low pH plus P_i significantly depressed thick filament cooperativity, an effect primarily attributed to increased P_i, while low cell pH had a strong depressive effect on the Ca^{2+}

required for initial force development (AT) in all fiber types. Coupled to previous observations that maximal shortening velocity (V_o) and peak power are significantly depressed by low pH (Knuth *et al.* 2006), and peak power is significantly depressed by elevated P_i (Debold *et al.* 2004), it is clear that the fatigue-inducing effects of low cell pH and elevated P_i on cross-bridge function are substantial.

CHAPTER 4

PHOSPHATE AND ACIDOSIS ACT SYNERGISTICALLY TO DEPRESS PEAK POWER IN RAT MUSCLE FIBERS

Introduction

In chapter 3, it was shown that low pH (6.2) plus high P_i (30 mM) depressed P_o at 30℃ by 40-50% in type I and II fibers (Nelson & Fitts 2014), while Karatzaferi *et al.* (2008) reported a 50% decline in P_o in fast rabbit psoas fibers. They also observed a 20-40% drop in V_{max} with the effect dependent on the degree of myosin light chain two (MLC_2) phosphorylation. While characterizing the effects of low pH plus high P_i on V_{max} and P_o are important, work capacity is dependent on peak power, which is obtained at intermediate velocities and forces (Fitts 1994). The independent effects of low pH and high P_i at low (<25℃) and near-physiological temperatures (30℃) on peak power are well known (Debold *et al.* 2004; Knuth *et al.* 2006), but the effect of these ions acting together has only been studied in fast rabbit psoas fibers (Karatzaferi *et al.* 2008). Thus one goal of this chapter was to establish the effects of low pH plus high P_i on V_{max} and the force-power relationship in slow as well as fast fibers.

The sum of the forward and reverse rate constants (Figure 1.1, step 3) determines the rate of force redevelopment (k_{tr}) of a fully active fiber following a slack-unslack procedure (Brenner & Eisenberg 1986; Brenner 1988; Fitts 2008).

At saturating levels of Ca^{2+}, elevating P_i accelerates k_{tr}, and lowering pH does not change k_{tr} at 15℃ (Metzger & Moss 1990b; Tesi *et al.* 2000). Collective effects of low pH plus high P_i on k_{tr} at 15 or 30℃ are unknown and were therefore evaluated in this study.

Fiber stiffness is a reflection of the total number of cross-bridges (low- and high-force states). A reduced fiber stiffness would suggest fewer bridges, while an increase in low-force bridges but no change in the total number of bridges should leave stiffness unaltered. To our knowledge, the collective effects of elevated H^+ and P_i on fiber stiffness have not been studied. We hypothesized that low pH plus high P_i will not have a significant effect on fiber stiffness in that the ions decrease force by primarily increasing the number of low-force cross-bridges rather than a decline in force per bridge or a reduction in total number of cross-bridges. We tested this by determining fiber stiffness, the force-stiffness ratios, and by estimating the number of low-force cross-bridges in control (pH 7) and pH 6.2 + 30 mM P_i conditions.

Our results quantify the depression in velocity and power elicited by pH 6.2 + 30 mM P_i in both type I and II fibers and low (15℃), and n ear-physiological (30℃) temperatures and provide evidence that eleva tions in H^+ plus P_i strongly depress peak fiber power and may increase the number of low-force cross-bridges in slow and fast fibers.

Results

This work shows that two important kinetic measurements, velocity (V_o) and the rate constant of tension development (k_{tr}), following a slack-unslack perturbation, evaluated at both 15 and 30℃, are hi ghly temperature and fiber type dependent (Figure 3). k_{tr} significantly increased in a fiber type dependent fashion (I<IIa<IIx) at both temperatures (Table 4.1, Figure 4.1) and was significantly higher at 30℃ compared to 15℃ in al l fiber types.

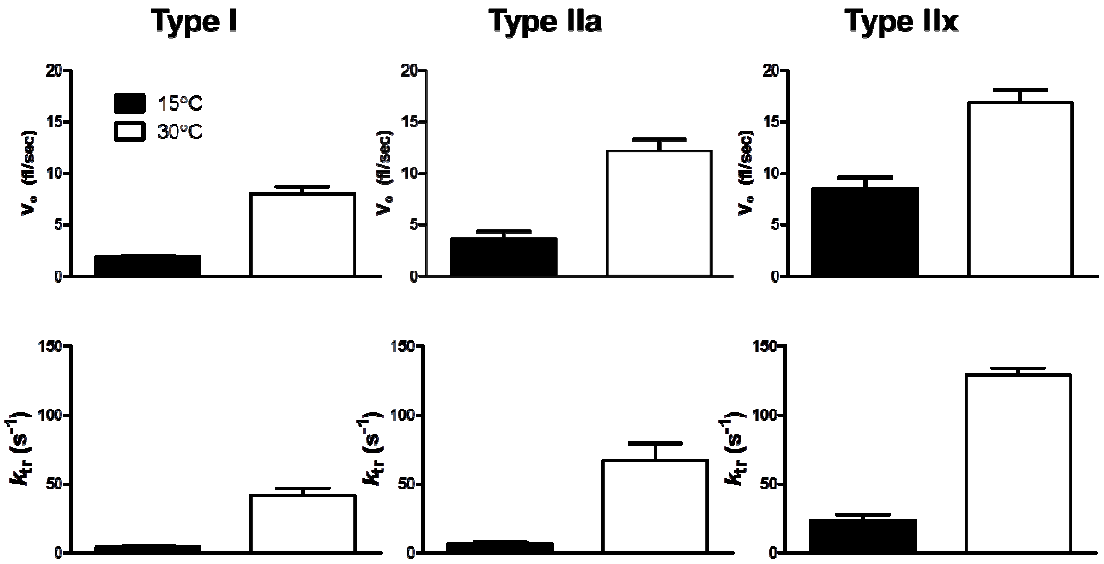

Figure 4.1: Temperature and fiber type dependence of V_o and k_{tr}

Vo (fl/sec) (A-C) and k_{tr} (s^{-1}) (D-F) at pH 7. All V_o and k_{tr} values were significantly higher at 30℃ compared to 15℃, and significantly increas ed with fiber type (I<IIa<IIx).

At 30℃ compared to 15℃, V_o increased by 4.2, 3.4, and 1.9 fold type I, IIa, and IIx fibers, respectively. As temperature was elevated, fiber k_{tr} increased by 11, 10, and 5.5 fold in type I, IIa, and IIx fibers, respectively. However, k_{tr} was unaffected by pH 6.2 + 30 mM P_i at 15 or 30℃ in type I or II fibers. A trend but insignificant decrease in k_{tr} (p=0.07) was observed in type I fibers at 30℃ (Table 4.1).

	15°C			30°C		
	n	pH 7	pH 6.2 + 30 mM Pi	*n*	pH 7	pH 6.2 + 30 mM Pi
Type I	11	3.8 ± 0.5	3.1 ± 0.4	10	41.2 ± 5.4	23.6 ± 7.6
Type IIa	11	6.2 ± 1.0*	5.8 ± 1.8	7	66.9 ± 12.3*	50.3 ± 13.2
Type IIx	11	23.1 ± 4.4*#	30.7 ± 10.1*#	6	128.4 ± 5.5*#	122.3 ± 16.0*#
Type II Combined	22	16.1 ± 3.2*	20.5 ± 6.5*	13	95.3 ± 11.2*	83.5 ± 14.2*

Table 4.1: The rate of force development (k_{tr}) is unchanged by pH 6.2 + 30 mM P_i.

Values are means ± SEM. Rate of force development (k_{tr}) is a rate constant, units s^{-1}. k_{tr}'s at 30℃ were all significantly higher than at 15℃ ($p<0.05$). There were no significant differences between pH 7 and pH 6.2 + 30 mM P_i conditions in any fiber type. * Significantly different from type I fibers, $p< 0.05$. # Significantly different from type IIa fibers, $p<0.05$.

The effects of the low cell pH (6.2) and elevated P_i (30 mM) condition on velocity (V_o and V_{max}) in slow and fast fibers are summarized in tables 4.2 and 4.3 and figure 4.2.

Condition	*n*	V_c (fl s^{-1})	Vmax (fl s^{-1})	a/P_o	V_{opt} (fl s^{-1})	P_{opt} (kN m^{-2})
15°C pH 7	14	1.89 ± 0.09	1.53 ± 0.09	0.07 ± 0.01	0.31 ± 0.02	23.5 ± 1.4
15°C pH 6.2 + 30 mM P_i	14	1.00 ± 0.18*	1.16 ± 0.09*	0.08 ± 0.03	0.23 ± 0.01*	11.4 ± 0.9*
% change		-47	-24	+13	-26	-51
30°C pH 7	12	8.00 ± 0.74	4.23 ± 0.12	0.27 ± 0.06	1.25 ± 0.07	41.4 ± 2.4
30°C pH 6.2 + 30 mM P_i	12	6.11 ± 0.79	3.58 ± 0.17*	0.20 ± 0.09	0.91 ± 0.09*	20.6 ± 1.1*
% change		-24	-15	-26	-27	-50

Table 4.2: Effect of pH 6.2 + 30 mM P_i on velocity and force parameters in type I fibers.

Values are means ± SEM. *n,* number of fibers studied. V_o, maximal shortening velocity determined from slack test. V_{max}, maximal unloaded shortening velocity determined from the Hill plot test. a/P_o, unitless parameter describing curvature of the force-velocity relationship. V_{opt} and P_{opt}, velocity and force at peak power *Significantly different from pH 7, $p<0.05$. At both pH 7 and pH 6.2, 30 mM P_i, all values at 30℃ were significantly higher than 15℃.

Condition	*n*	V_o (fl s^{-1})	Vmax (fl s^{-1})	a/P_o	V_{opt} (fl s^{-1})	P_{opt} (kN m^{-2})
15°C pH 7	20	5.97 ± 0.78	3.37 ± 0.30	0.21 ± 0.04	0.85 ± 0.15	27.0 ± 2.4
15°C pH 6.2 + 30 mM P_i	20	3.58 ± 0.50*	2.31 ± 0.40*	0.28 ± 0.07	0.83 ± 0.19	11.8 ± 1.5*
% change		-40	-31	+25	-2	-56
30°C pH 7	13	13.48 ± 1.00	6.24 ± 0.56	0.56 ± 0.08	2.38 ± 0.15	43.8 ± 3.5
30°C pH 6.2 + 30 mM P_i	13	8.76 ± 0.90*	4.55 ± 0.48*	0.59 ± 0.09	1.74 ± 0.15*	25.4 ± 2.5*
% change		-33	-31	+5	-27	-39

Table 4.3: Effect of pH 6.2 + 30 mM P_i on velocity and force parameters in type II fibers.

Values are means ± SEM. *n,* number of fibers studied. V_o, maximal shortening velocity determined from slack test. V_{max}, maximal unloaded shortening velocity determined from the Hill plot test. a/P_o, unitless parameter describing curvature of the force-velocity relationship. V_{opt} and P_{opt}, velocity and force at peak power *Significantly different from pH 7, $p<0.05$. At both pH 7 and pH 6.2, 30 mM P_i, all values at 30℃ were significantly higher than 15℃.

V_o is typically higher than V_{max}, especially at higher temperatures due to sarcomere non-uniformity that occurs with loaded contractions (Widrick *et al.* 1996). Temperature significantly increased velocity in type I and II fibers, while pH 6.2 + 30 mM P_i significantly depressed V_o in type I fibers at 15℃, type II fibers at both 15 and 30℃, and V_{max} in both fiber types at both temperatures. Raising the temperature from 15 to 30℃ blunted the pH+P_i induced depression in velocity in slow but not fast fibers such that V_{max} was depressed by 24 and 15% at 15 and 30℃, respectively, in type I fibers and depressed by 31% at both 15 and 30℃ in type II fibers (Tables 4.2 and 4.3). Composite force-velocity curves (Figure 4.2) illustrate that fast fibers exhibit less curvature as evidenced by the significantly higher a/P_o ratio (Tables 4.2 and 4.3) ($p=0.007$ at 15℃ and $p=0.009$ at 30℃). For both fiber types, the a/P_o ratio increased with an increase in temperature. Interestingly, pH 6.2 + 30 mM P_i had no effect on a/P_o in any condition, suggesting the FV relationship was uniformly decreased under these conditions.

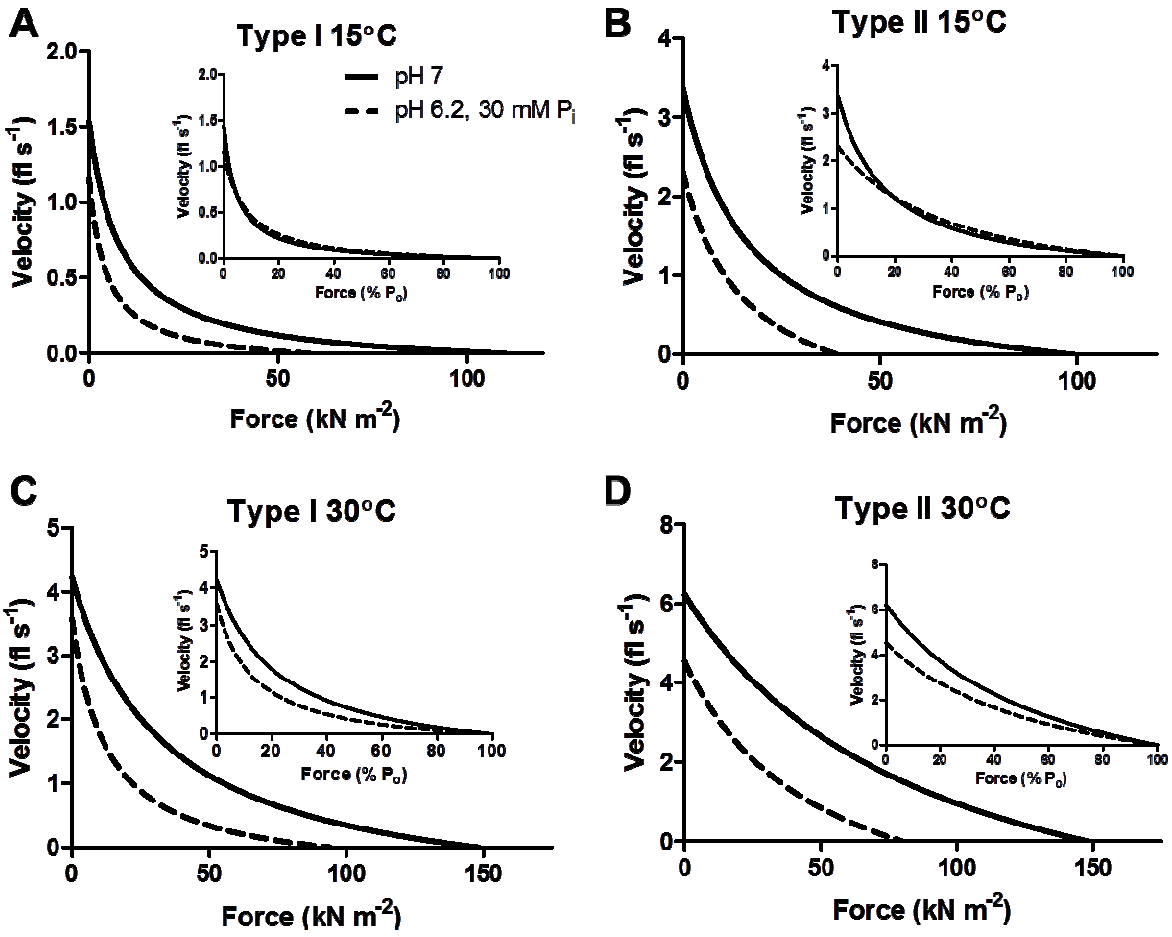

Figure 4.2: Average force-velocity curves in type I and II fibers at 15 and 30℃.

Shortening velocity is plotted as a function of force in kN/m^2 (main graphs) and as a function of percentage P_o (insets).

Temperature significantly increased peak power by 6-8 fold in type I and II fibers, while pH 6.2 + 30 mM P_i conditions depressed peak power in both fiber types by ~ 60% at low and high temperatures (Figure 4.3).

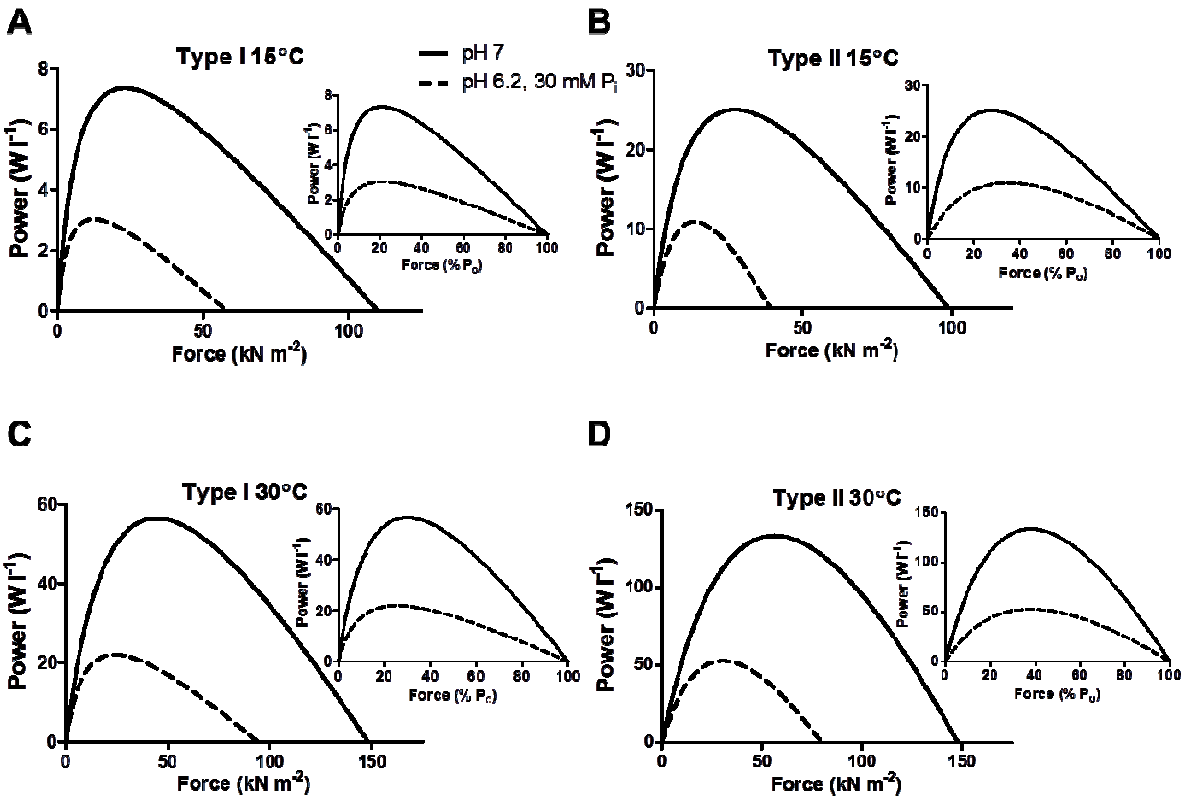

Figure 4.3: Average force-power curves in type I and II fibers at 15 and 30℃.

Power is plotted as a function of force in kN/m^2 (main graphs) and as a function of percentage P_o (insets).

Peak force (P_o), V_{max}, and peak power values from previous work in our lab (Debold *et al.* 2004; Knuth *et al.* 2006) in which the effects of pH 6.2 and 30 mM P_i were studied individually are compared to the current study in figures 4.4-4.6. The individual ions significantly depressed force from control at 15℃, with the order $P_i > H^+$, while with both ions together, the inhibition was not different from P_i alone. At 30℃, the high P_i and high P_i plus low pH conditions depressed type I force, while only the latter conditions inhibited type II fiber force (Figure 4.4). Low cell pH significantly slowed V_{max} in type I fibers at 30℃ and type II

fibers at both temperatures, while P_i had no significant effect on velocity (Figure 4.5). Except for the type I fibers at 15℃, the pH +Pi induced depression in V_{max} was not different than the depression of V_{max} by pH 6.2 alone (Figure 4.5). Individually, both pH 6.2 and 30 mM P_i significantly depressed peak power from control in type I and II fibers at both temperatures (Figure 4.6). At 30℃ the pH 6.2 + 30 mM P_i condition depressed peak power greater than either ion alone in both fiber types; however, at 15℃, the inhibition was not greater than that observed with higher P_i alone ($p=0.30$, $p=0.13$ in type I and II fibers, respectively) (Figure 4.6).

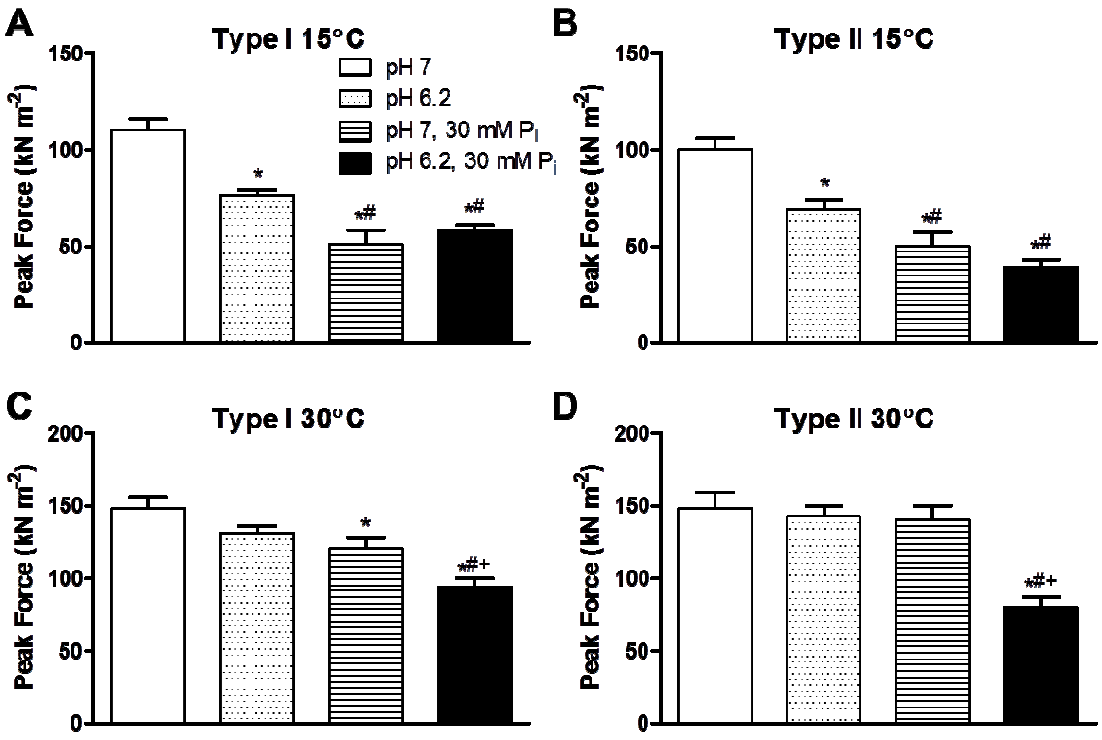

Figure 4.4: Peak force (P_o) elicited at pCa 4.5 in type I and II fibers at 15 and 30°C.

Values are means ± SEM. Data for pH 6.2 from Knuth *et al*. (2006) and data for pH 7, 30 mM P_i modified from Debold *et al*. (2004). *Significantly different from pH 7, $p<0.05$. $^{\#}$Significantly different from pH 6.2, $p<0.05$. $^{+}$Significantly different from pH 7, 30 mM P_i, $p<0.05$.

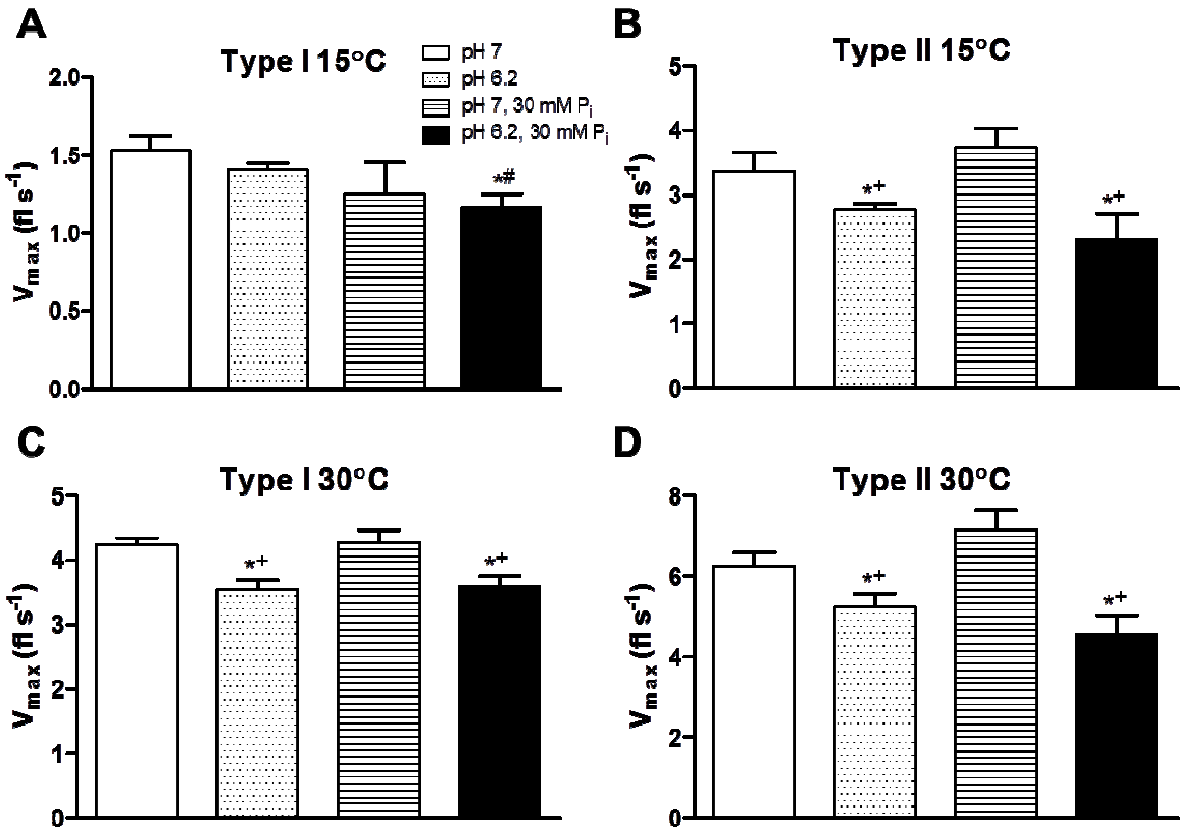

Figure 4.5: Maximal shortening velocity (V_{max}) in type I and II fibers at 15 and 30°C.

Values are means ± SEM, obtained from the Hill plot and compare individual and collective effects of pH and P_i. Data for pH 6.2 from Knuth *et al.* (2006) and data for pH 7, 30 mM P_i obtained from Debold *et al.* (2004). *Significantly different from pH 7, $p<0.05$. $^{\#}$Significantly different from pH 6.2, $p<0.05$. $^{+}$Significantly different from pH 7, 30 mM Pi, $p<0.05$.

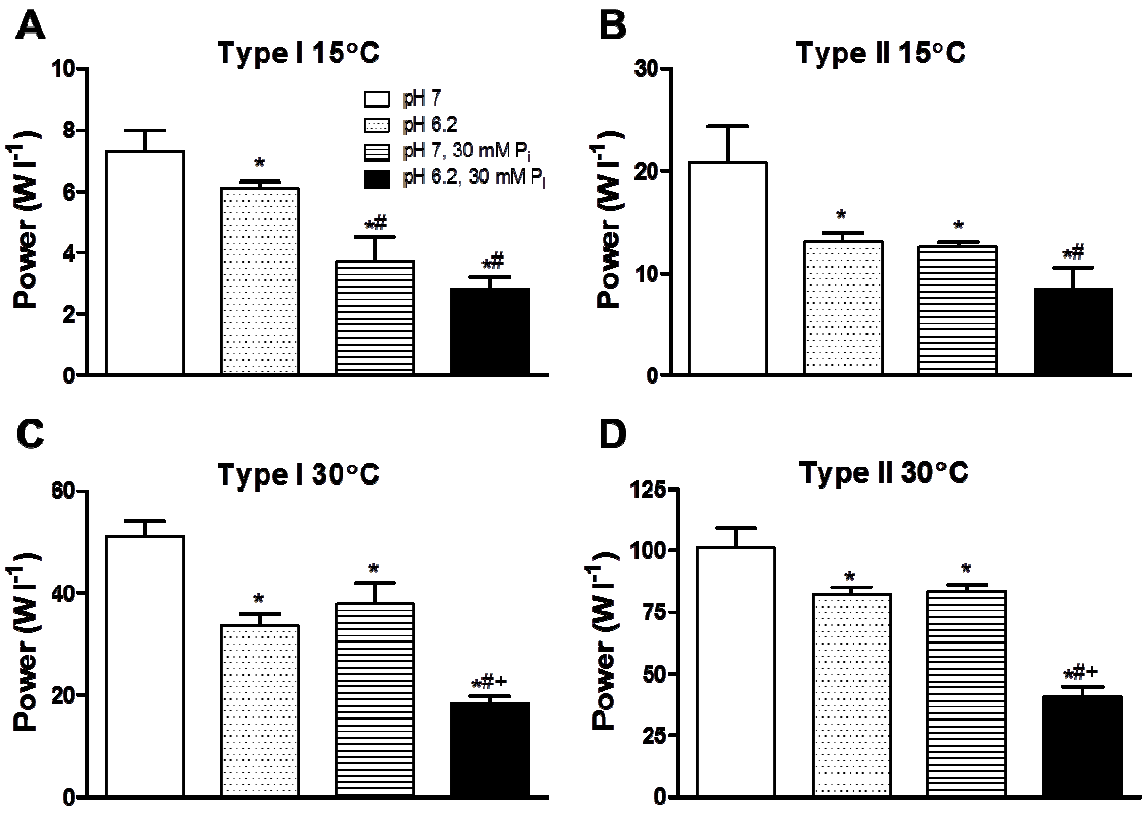

Figure 4.6: Peak normalized power in type I and II fibers at 15 and 30℃.

Values are means ± SEM. The relative power unit of watts/liter is equivalent of kN m^{-2} fl s^{-1}. Data for pH 6.2 from Knuth *et al*. (2006) and data for pH 7, 30 mM P_i obtained from Debold *et al*. (2004). *Significantly different from pH 7, $p<0.05$. #Significantly different from pH 6.2, $p<0.05$. +Significantly different from pH 7, 30 mM Pi, $p<0.05$.

Fiber stiffness, a reflection of the number of bound cross-bridges (both low and high-force states), was not different between fiber types or altered by the pH 6.2 + 30 mM P_i condition at either temperature (Figure 4.7). However, the force-stiffness ratio was significantly depressed across fiber types and temperatures in pH 6.2 + 30 mM P_i conditions, suggesting an increase in the number of low-force bridges and/or reduced force of the high force-state. Type II fibers had a higher

force-stiffness ratio than type I fibers in control but not pH 6.2 + 30 mM P_i conditions, implying that type II fibers either elicit more force or less stiffness per cross-bridge in the non-fatigued state (Figure 4.7).

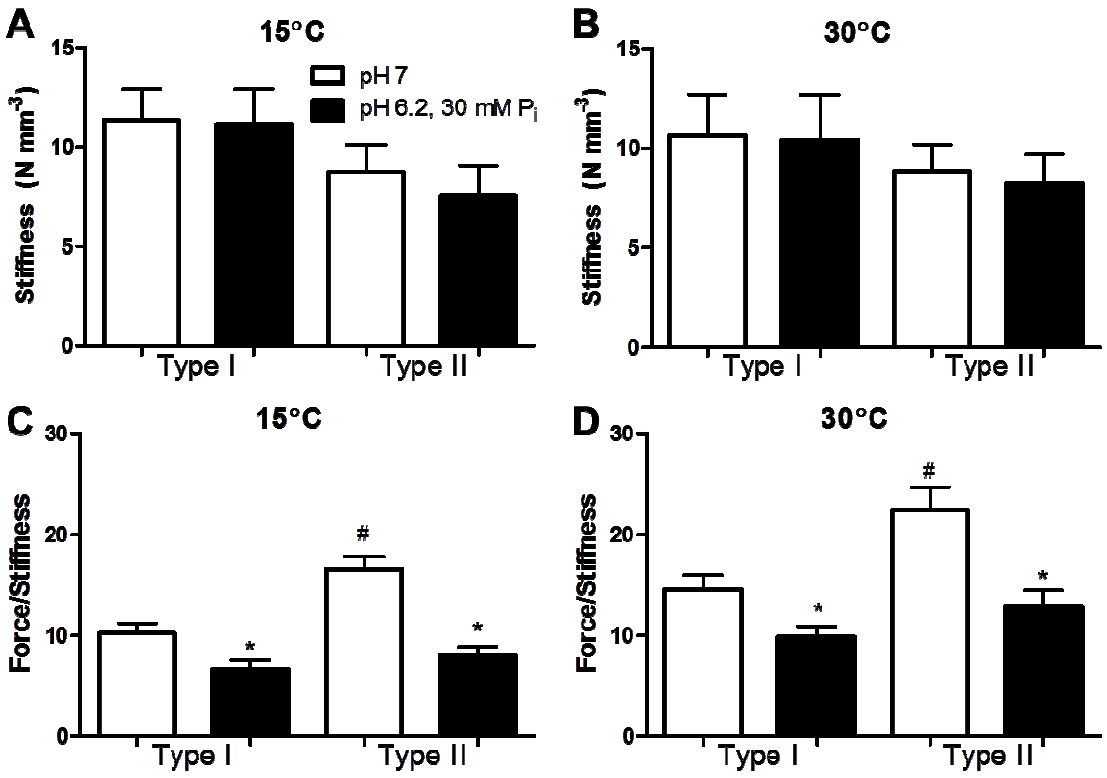

Figure 4.7: Stiffness and the force stiffness ratio in type I and II fibers at 15 and 30℃.

Data collected at pCa 4.5. (A) and (B) stiffness, (C) and (D) force stiffness ratio. Values are means ± SEM. *Significantly different from pH 7, $p<0.05$. #Significantly different than type I fibers, $p<0.05$. All values in (D) at 30℃ are significa ntly higher than the values in (C).

To further evaluate the effects of pH 6.2 + 30 mM P_i on the relative force-per-cross-bridge, we employed a technique of Colombini *et al.* (2010) described in *Methods*, in Figure 4.8. The y-intercept of these plots approximates the relative percentage of low-force cross-bridges. In type I and II fibers, pH 6.2 + 30 mM P_i conditions resulted in a plot with a higher y-intercept, implying a higher percentage of low-force cross-bridges. The difference in the pH 7 (<1%) vs. pH 6.2 + 30 mM P_i (7%) intercept was greater in type II fibers but the difference in the intercepts was not significantly different (p=0.19).

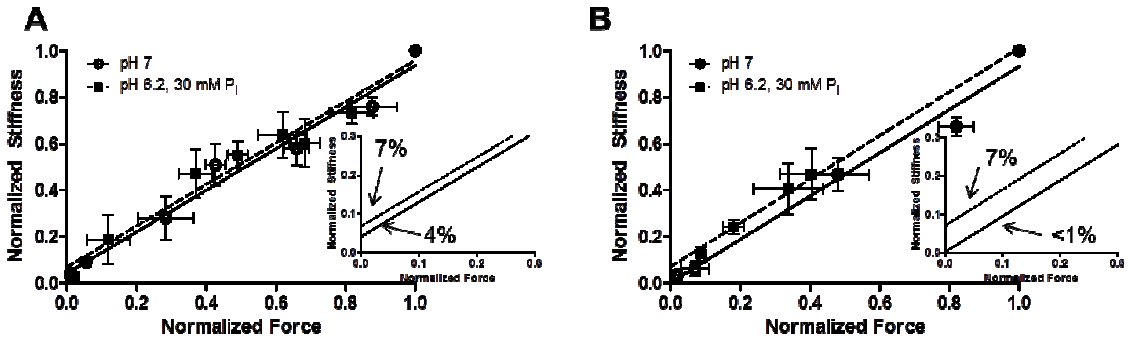

Figure 4.8: Low-force cross-bridge percentage determined by force vs. stiffness plot.

Force and stiffness elicited at a range of free Ca^{2+} concentrations were normalized to rigor force and stiffness in pH 7 and pH 6.2 + 30 mM P_i conditions at 15℃ in 6 type I (A) and 6 type II (B) fibers. The points from each fiber are means (±SEM) fit with a line and extrapolated to the ordinate, crossing a point that has stiffness but no force. Graphs show the complete range of points obtained. Insets show the best fit lines, zoomed in where the lines cross the x-axis.

Discussion

The objective of this study was to determine the combined effects of high H^+ and P_i on slow and fast fiber function and to provide a better understanding of how these ions alter the cross-bridge cycle. Additionally, to our knowledge, the results provide the first report of k_{tr} in the fast fiber sub-types IIa and IIx. Fiber k_{tr} is thought to reflect the sum of the forward and reverse rate constants of the weak to strong binding step (Figure 1, step 3) (Brenner 1988). Our finding of a 3.7-fold lower k_{tr} (at 15℃) in the type IIa vs. IIx fiber suggests t hat the weak to strong binding transition is considerably slower in the IIa fiber and in fact closer to the rate observed in the slow type I fiber (Figure 4.1). Interestingly, increasing temperature accelerated k_{tr} considerably more in the slow type I and fast type IIa fiber than in fast IIx fibers. Apparently, the forward rate constant of the weak to strong binding state is less temperature sensitive in the fast IIx fiber (Davis & Epstein 2007).

Regarding muscle fatigue, it is known to be in part caused by H^+ and P_i inhibition of force and power (Fitts 2008). The individual effects of these ions are well known, but the collective effects have been less studied (Debold *et al.* 2004; Karatzaferi *et al.* 2004; Debold *et al.* 2006; Knuth *et al.* 2006; Nelson & Fitts 2014). Our results demonstrate that the pH 6.2 + 30 mM P_i condition significantly inhibits peak fiber force, velocity and power in type I and II fibers at cold (15℃) and near-physiological (30℃) temperatures. Import antly, the inhibition of peak power is greater with pH 6.2 + 30 mM P_i than with either ion alone and is related

to a H^+ ion depression of velocity and P_i + H^+ inhibition of force. The latter occurred despite no change in fiber stiffness, suggesting that the total number of cross-bridges was unchanged.

At 30℃, the pH 6.2 + 30 mM P_i condition depressed V_{max} by ~30% in type II fibers, while for type I fibers, V_{max} declined by only 15%, demonstrating that under fatigue conditions, type II fibers are more susceptible to declines in velocity than type I fibers (p=0.011). With the exception of the type I fiber at 15℃, the depression in velocity observed in the pH 6.2 + 30 mM P_i condition was not greater than that observed in the pH 6.2 condition which implicates H^+ as the primary ion depressing velocity. The increased susceptibility of the fast type II fiber may be in part due to a higher myosin light chain kinase activity (Moore & Stull 1984) and higher myosin light chain 2 phosphorylation (MLC_2-P). In support of this possibility, Karatzaferi *et al*. (2008) showed MLC_2-P to exacerbate the decline in fast fiber velocity observed with elevating H^+ and P_i. Since MLC_2-P is thought to move the myosin head close to the actin binding site for myosin, this might, under fatigue conditions, result in more low-force cross-bridges which in turn would increase drag and slow velocity (Fitts 2008; Colson *et al.* 2010). Future studies are needed to test this hypothesis.

Low cell pH is thought to inhibit V_o by slowing ADP release from the myosin head, as evidence from *in vitro* motility and single molecule laser trap assays demonstrated a threefold increase in the duration of the ADP-bound state (Figure 1.1, state F) (Debold *et al.* 2008; Debold 2012). Recently, using the *in vitro* motility assay, Debold *et al*. (2008) observed pH 6.4 at 30℃ to decrease

actin filament velocity (V_{actin}), a measure analogous to unloaded shortening velocity, by over 65%. The decrease in V_{actin} is much larger than that observed in fibers, suggesting that the myofilament proteins and/or highly ordered architecture may attenuate some of the loss in unloaded shortening velocity with low cell pH (Debold 2012).

The depressive effects of pH 6.2 or 30 mM P_i on P_o are significantly attenuated at higher temperatures (Figure 4.4). We have shown that at submaximal Ca^{2+} concentrations characteristic of fatigue, both pH 6.2 alone, 30 mM P_i alone, and pH 6.2 + 30 mM P_i significantly depressed P_o at 15 and 30℃ (Debold *et al.* 2006; Nelson & Fitts 2014). Here, we emphasize that although the effects of pH 6.2 or 30 mM P_i on P_o at 30℃ and saturating Ca^{2+} (pCa 4.5) are minimal, when the metabolites are elevated simultaneously, a 36 and 46% depression in P_o in type I and II fibers, respectively, is apparent. Low cell pH and elevated P_i have been hypothesized to depress force at the same step of the cross-bridge cycle but by different mechanisms (Figure 1.1, step 3) (Fitts 2008). It is believed that H^+ slows the forward rate constant while P_i accelerates the reverse rate constant of this step. Our data on k_{tr} and stiffness support this hypothesis. We observed no effect of pH 6.2 + 30 mM P_i conditions on k_{tr} in either fiber type at 15 or 30℃. It is known that individually, P_i increases k_{tr} while low cell pH has no effect (Metzger & Moss 1990; Tesi *et al.* 2000). P_i is thought to increase k_{tr} by accelerating the reverse rate constant of step 3 (Figure 1.1), shifting the distribution of the cross-bridges toward the low-force state (Figure 1.1, state C) (Tesi *et al.* 2000). Metzger and Moss (1990b) showed pH 6.2 alone

to have no effect on k_{tr} at saturating Ca^{2+} (pCa 4.5) but depress k_{tr} at submaximal Ca^{2+}. They suggested that low cell pH depressed the forward rate constant of force generation (Figure 1.1, step 3) at submaximal but not maximal Ca^{2+} levels, with the former condition reducing the force of the strongly bound cross-bridges (Metzger & Moss 1990b). Our data show that low pH blunts the stimulatory effect of P_i on k_{tr}, suggesting either an inhibition of the forward rate constant and/or fewer bridges transitioning from the low-to high-force state.

Peak stiffness of slow and fast fibers was unchanged by the pH 6.2 + 30 mM P_i condition, and consistent with the findings of others, was independent of temperature (Galler & Hilber 1998). Because P_o was depressed by the pH 6.2 + 30 mM P_i condition, the force-stiffness ratio decreased in both fiber types at 15 and 30℃. This could be interpreted as an increase in the percentage of low-force bridges (Figure 1.1, state C) and/or less force per high-force cross-bridge (Figure 1.1, state D). Though not significant, we observed a trend toward an increased number of low-force bridges in type II fibers (Figure 4.8). The force vs. stiffness plot, obtained by activating with various levels of Ca^{2+}, extrapolated to the y-intercept, provides an estimate of the percentage of low-force cross-bridges. The intercept increased in the pH 6.2 + 30 mM P_i conditions compared to control conditions in type II fibers (p=0.19). Colombini *et al.* (2010) developed this technique using N-benzyl-p-toulene sulphonamide (BTS) to manipulate cross-bridge number, with total Ca^{2+} unchanged. One caution in interpreting our result where Ca^{2+} changed for each measurement is that Ca^{2+} may have effects independent of reducing force that might affect fiber stiffness or the slope of the

force-stiffness plot. Nonetheless, the data in type II fibers support the hypothesis that elevating H^+ and P_i shifts the distribution of cross-bridges to more low-force bridges, maintaining stiffness, while decreasing fiber force and peak power.

The depression in peak fiber power in pH 6.2 + 30 mM P_i conditions was not fiber type or temperature dependent, and at 30°C, was significantly more than the power depression by low pH or high P_i alone. Taken with the observation that peak stiffness and thus the total number of cross-bridges was unchanged suggests that the effects of pH 6.2 + 30 mM P_i are additive, supporting the hypothesis H^+ and P_i inhibit force (and thus power) by altering the forward and reverse rate constants of step 3 of the cross-bridge cycle (Figure 1.1), respectively (Fitts 2008). The observation that peak stiffness was unaltered by the fatigue conditions argues against a decline in the total number of bridges.

The curvature of the force-velocity relationship, defined by a unitless ratio, a/P_o, increased with temperature in both fiber types. Previously, we reported the ratio to change in a fiber-type dependent manner at 30℃ by pH 6.2 or 30 mM P_i. Knuth *et al.* (2006) found pH 6.2 to depress a/P_o in type I fibers and increase a/P_o in type II fibers, while Debold *et al*. (2004) observed 30 mM P_i to decrease a/P_o in both fiber types. Collectively the ions did not alter the a/P_o in either fiber type at 15 or 30℃. This is in agreement with Westerblad & Lannergren (1994), who studied intact single fibers from Xenopus, stimulated them with repeated tetani to achieve fatigue, and showed no change in a/P_o.

In summary, our results demonstrate that a highly significant depression in peak fiber power occurs by simultaneously elevating H^+ and P_i at near-

physiological temperatures. Since the important parameter for performance is peak power and not isometric force or maximal shortening velocity, these results estimate that up to 60% of power loss on the single fiber level could be due to the collective effects of low pH and elevated P_i. Furthermore, we suggest that the declines in P_o observed with fatigue may be in part due to the pH 6.2 + 30 mM P_i condition increasing the number of low-force cross-bridges. This, combined with the low cell pH prolongation of the time in the AM·ADP state of the cross-bridge cycle, thereby depressing velocity, implicates these ions as significant mediators of skeletal muscle fatigue.

CHAPTER 5

EFFECTS OF AGE AND FATIGUE ON SINGLE FIBER MECHANICAL PROPERTIES: A PILOT STUDY

Introduction

The ability of older adults to perform daily activities such as standing from a sitting position is compromised by the loss of muscle mass (sarcopenia) and reduced power, and the problem is exacerbated by fatigue (Kent-Braun *et al.* 2012; Frontera *et al.* 2012). The effects of age on skinned fiber force, velocity and power have been studied but at temperatures less than physiological (15-25℃) (Trappe *et al.* 2003; Krivickas *et al.* 2006; Miller *et al.* 2013). The effects of fatigue (elevating H^+ and P_i) on old versus young humans have been investigated in whole muscle but no data exists on the single fiber level (Kent-Braun *et al.* 2012).

There is controversy in the human single fiber literature as to whether there are declines in force, velocity, or power with age and if sex differences exist (Larsson *et al.* 1997; Krivickas *et al.* 2001; Trappe *et al.* 2003; Krivickas *et al.* 2006). Trappe *et al.* (2003) found that normalized muscle power (corrected for size of the fiber) did not differ among young and old men and women but did find that type IIa fibers from old women had significantly lower absolute force and power values (not corrected for size of the fiber) than all other groups. The authors suggest that the loss of muscle mass (and not changes in the contractile

elements) is the critical component that accounts for the decrease in whole muscle function with age (Trappe *et al.* 2003). Krivickas *et al.* (2006) found no significant sex differences in force, velocity, and power in fibers from old men versus women and concluded that sex differences in whole muscle function are not explained by differences in the contractile elements. The first part of the work presented here repeated experiments at pH 7 control conditions done by the aforementioned investigators and others but at 30℃. Though the rat data (Chapter 4) showed that power decrements with fatigue were similar at 15 and 30℃, it is nevertheless important to characterize age-related changes at the single fiber level in humans at the near-physiological temperature of 30℃.

The few mechanistic studies on the effects of age on human fibers at pH 7 have been limited to observations of k_{tr} and stiffness (Ochala *et al.* 2007; Miller *et al.* 2013). One study concluded that aging increased instantaneous stiffness per force unit in both type I and IIa fibers from men, suggestive of an increased number of low-force cross-bridges with age (Ochala *et al.* 2007). Miller and colleagues (2013) recently found stiffness to be elevated and k_{tr} depressed in old women (compared to young men, young women and old men) at 25℃. The authors concluded that slowed cross-bridge kinetics may be contributing to the reduced physical capacity associated with age, particularly in women.

The purpose of this chapter was to (1) characterize aging effects at pH 7, 30℃ and (2) begin the investigation of how fatigue -like conditions (pH 6.2 + 30 mM P_i) affect single fibers from old vs. young adults.

Results

The results section of this chapter focuses first on aging effects at pH 7 conditions (Figures 5.1-5.6) while the second half describes effects of elevating H^+ and P_i in the context of aging. Unless indicated, data on force, velocity, and power presented in this section are at the near-physiological temperature of 30℃. Mechanistic data (k_{tr}, stiffness, ATPase) are presented at 15, 23 or 30℃, as indicated with each figure.

						# fibers studied		
Sex	Age	Height (m)	Weight (kg)	BMI (kg/m^2)	Group	slow	fast	total
M	24	1.75	68.1	22.2	TR	6	8	14
M	26	1.91	81.0	20.2	TR	5	8	13
M	26	1.75	66.9	21.8	TR	1	1	2
F	27	1.58	50.0	20.2	TR	15	3	18
M	70	1.83	84.1	25.1	TR	13	2	15
M	71	1.91	109.4	30.1	SED	2	3	5
F	71	1.64	53.9	20.1	TR	14	0	14
F	72	1.46	64.0	30.0	SED	7	7	14
F	75	1.54	56.2	23.8	SED	12	0	12
M	78	1.80	76.5	23.5	TR	12	2	14
M	78	1.70	67.5	23.3	TR	10	2	12
F	81	1.63	53.2	20.1	TR	5	1	6

Table 5.1: Human subject characteristics.

Listed by age. BMI= body mass index. TR= trained, SED= sedentary. 139 total fibers studied, with 37/139 fast fibers (27%).

A list of the human subjects studied is in Table 5.1. 139 fibers were studied, 37 of which were fast type II (27%). In the young subjects studied, 20/47

(43%) were type II fibers while 17/92 (18%) of old subjects' fibers were type II's. The majority of the data presented here are on slow fibers.

Young men had fibers with significantly larger diameters than all other groups, while old women had significantly smaller fiber diameters than all other groups (Figure 5.1) Slow and fast fibers showed no difference in diameter and were thus combined in Figure 5.1.

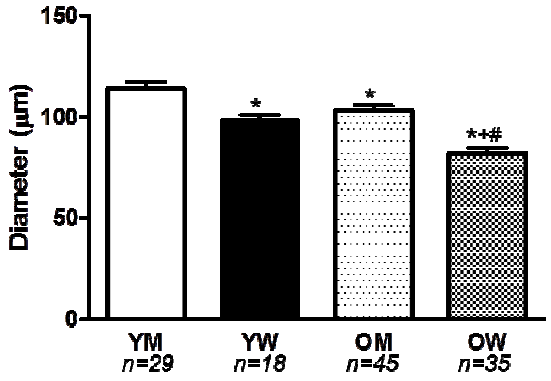

Figure 5.1: Human fiber diameters.

Values are means ± SEM. Young women (YW), old men (OM), and old women (OW) have significantly smaller fiber diameters than young men (YM). *Significantly different from young men, #significantly different from young women, +significantly different from old men, for all $p<0.05$.

Force can be expressed absolutely (mN) or per-cross sectional area (in kN/m^2), normalizing force to fiber size. A large fiber that produced a large amount of force may only produce an average force when corrected for cross-sectional area. In the context of muscular performance with advancing age, the more relevant measure is absolute force, shown in Figure 5.2A. Old women produced significantly less absolute force than all other groups. When

normalized for cross-sectional area, old women were still significantly less than young men but no different than young women or old men (Figure 5.2B). Fiber calcium sensitivity was not different between young and old adults, as they had similar pCa_{50}'s and activation thresholds (Figure 5.2C and D). Slow and fast fibers P_o's were not different and were therefore combined for the analysis in Figure 5.2A and B.

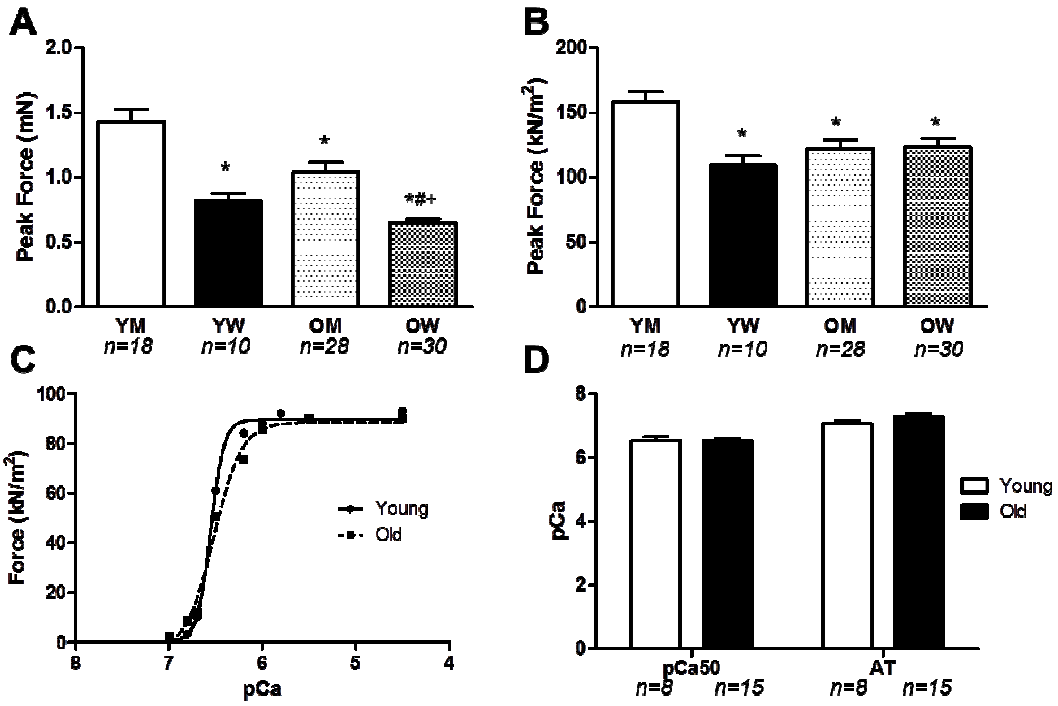

Figure 5.2: Peak force and pCa-force relationship.

All data collected at 30℃. For (A), (B), and (D), values are means ± SEM. (A) Absolute peak force expressed in mN combining slow and fast fibers. (B) Normalized peak force expressed in kN/m^2 combining slow and fast fibers. (C) Representative pCa-force curve for slow fibers from a young (solid line) and old (dashed line) female. (D) pCa_{50} and activation thresholds (AT) in young vs. old groups expressed in pCa units. *Significantly different from young men, #significantly different from young women, +significantly different from old men, for all $p<0.05$.

A sex, but not age difference, was apparent in maximal velocity and peak power in type I fibers. Young women had significantly slower V_{max}'s than young men while fibers from older women appeared to have slower V_{max}'s than fibers from old men, though this was not a significant difference (p=0.18) (Figure 5.3A). When the young and old values in a given sex were pooled (due to a lack of an age difference between sexes), men had significantly higher V_{max}'s than women (Figure 5.3B). Women, both young and old, had significantly lower peak power values than young men (Figure 5.3C and D). Pooled data in a given sex again showed men to have significantly higher peak power values than women (Figure 5.3D).

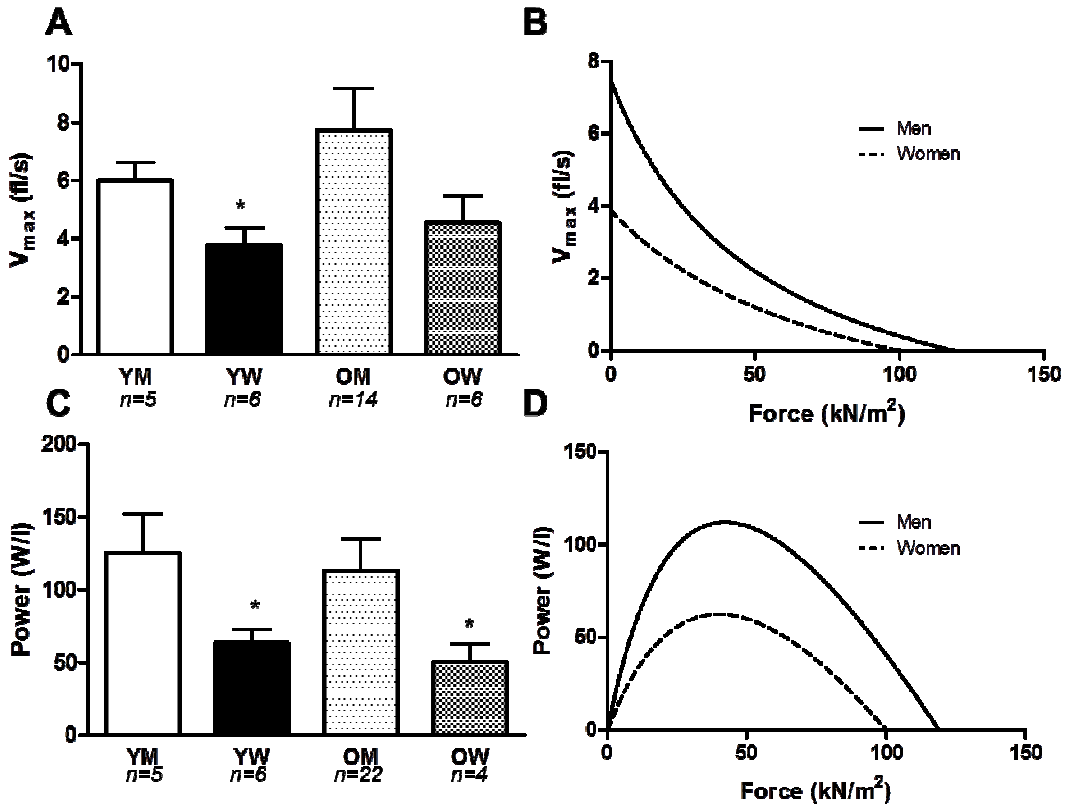

Figure 5.3: Peak velocity and power, force-velocity, and force-power relationship.

All data from slow fibers collected at 30℃. For (A) and (C), values are means ± SEM. (A) Maximal loaded shortening velocity (V_{max}) in fl/sec (B) Composite force-velocity curves, comparing fibers from old and young men (solid line) vs. old and young women (dashed line). (C) Normalized peak power in watts/liter. (D) Composite power curves comparing fibers from young and old men vs. young and old women. *Significantly different from young men, $p<0.05$.

The k_{tr} values presented in this chapter were performed at 15℃. Since the laser clamp technique was not employed with human fiber experiments, and optimal k_{tr} measurements at 30℃ require a laser clamp, k_{tr} data at 30℃ is not presented. Figure 5.4A shows stiffness-k_{tr} trace for representative slow fibers from a young male and old female overlaid. Note the time to redevelop tension is faster in the fiber from the young adult. Fibers from old women had significantly

lower k_{tr}'s than fibers from young women and old men but were not significantly different from young men (p=0.17) (Figure 5.4B).

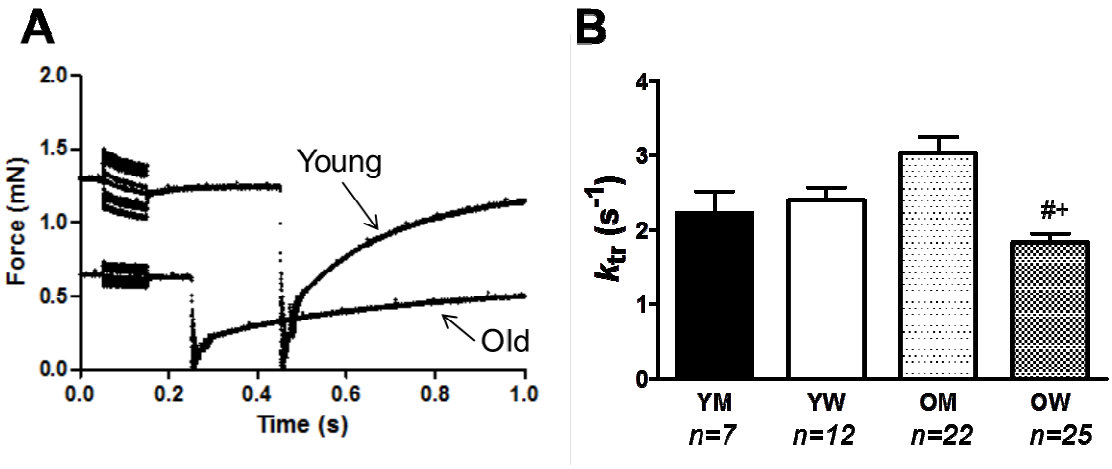

Figure 5.4: Rate of force development (k_{tr}) in slow fibers at 15℃.

(A) Representative stiffness-k_{tr} traces from a slow young male and slow old female fiber. (B) k_{tr}, a rate constant, expressed in s^{-1}. Values are means ± SEM. $^{\#}$Significantly different from young women, $^{+}$significantly different from old men, p<0.05.

Resting stiffness was not different between ages or sexes in slow fibers at 15℃ (Table 5.2). Peak stiffness was significantly higher in young men compared to old men while the force stiffness ratios did not different between groups (Table 5.2).

	Young Men	Young Women	Old Men	Old Women
n	*5*	*6*	*13*	*15*
Resting Stiffness (N/mm³)	0.15 ± 0.04	0.07 ± 0.04	0.09 ± 0.03	0.10 ± 0.02
Peak Stiffness (N/mm³)	8.4 ± 1.2	5.7 ± 1.2	5.8 ± 0.6*	6.0 ± 0.6
Force Stiffness ratio	14.3 ± 1.2	15.1 ± 1.2	13.8 ± 1.1	16.3 ± 1.0

Table 5.2: Resting and peak stiffness and force stiffness ratios.

Data from slow fibers at 15℃. Values are means ± S EM. *Significantly different from young men, $p<0.05$.

Amidst studying effects of age, sex, and fatigue on ATPase activity, we varied temperature while taking ATPase measurements and report ATPase activity to be highly temperature sensitive. To compare fiber type and temperature effects, fibers from all ages and sexes were combined in figure 5.5. In slow fibers, raising the temperature to 23℃ fro m 15℃ increased ATPase activity nearly 5-fold. At 30℃, ATPase activity increased 13-fold compared to 15℃ (Figure 5.5). Faster fibers had higher ATPase activity levels at 15 and 23℃ compared to slow fibers but there was no difference at 30℃; however, only 3 fast fibers were studied at 30°C (Figure 5.5). The majority of fiber ATPase experiments were conducted at room temperature (23℃) and are the da ta set presented in this chapter.

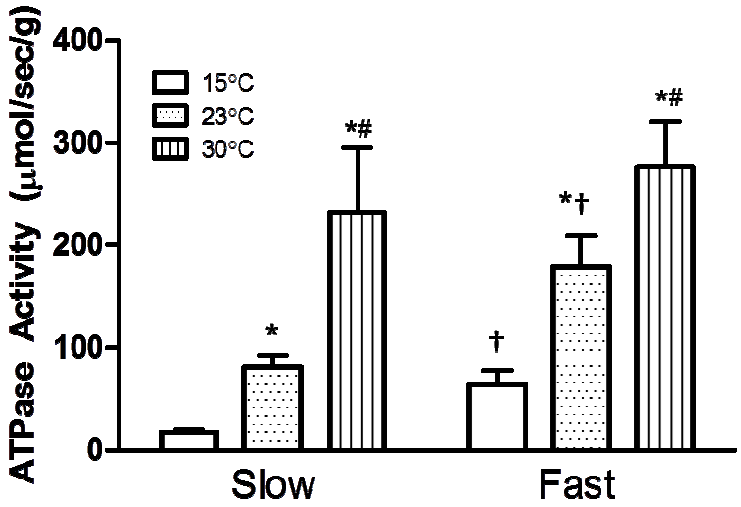

Figure 5.5: ATPase activity is temperature and fiber type dependent.

Data from slow and fast fibers (young and old, male and female) tested for ATPase activity in µmol/sec/g. Values are means ± SEM. For slow fibers, *n=6,22,6* and fast fibers, *n=6,14,3* at 15,23, and 30℃, respectively. *Significantly different from 15℃, #Significantly different from 23℃, †Significantly d ifferent from type I fiber at comparable temperature, for all $p<0.05$.

Economy, or the force produced per amount of ATPase activity, is shown in Figure 5.6B and was depressed in slow fibers from old women compared to young women and nearly depressed compared to old men ($p=0.058$). Old women trended ($p=0.06$) toward higher ATPase activity compared to old men (Figure 5.6A). No slow fiber data were available for young men because all fibers from young men that were tested for ATPase were fast.

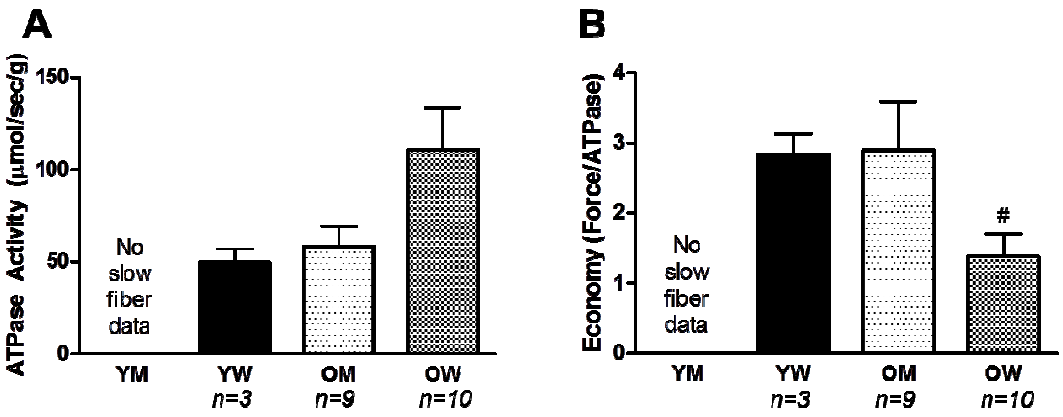

Figure 5.6: Economy (Force/ATPase) is depressed in older women.

Data from slow fibers at 23℃. Values are means ± SEM. (A) ATPase activity in µmol/sec/g. (B) Economy (P_o (kN/m^2) / ATPase activity). All fibers from young men tested for ATPase activity were fast. $^{\#}$Significantly different from young women, $p < 0.05$.

Similar to the rat data presented in chapters 3 and 4, pH 6.2 + 30 mM P_i conditions significantly depressed force and velocity at 30℃ in slow human fibers (Figure 5.7). This pH+P_i-induced decline in force and velocity was not different between young and old fibers. Because the decrements from pH 7 to pH 6.2 + 30 mM P_i were not different in fibers from young and old adults in a given sex, fibers in a given sex were combined for this analysis. Like rat fibers, pH 6.2 + 30 mM P_i significantly depressed calcium sensitivity in human fibers, but this depression was not different between young and old (data not shown). Decrements in peak power as a result of pH 6.2 + 30 mM P_i ranged from 47-57% amidst all groups (Table 5.3).

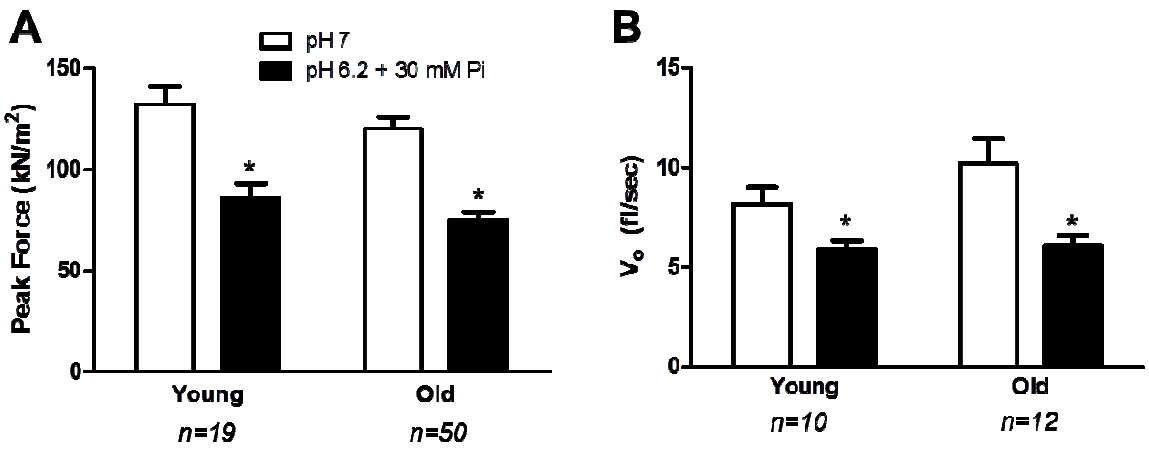

Figure 5.7: Effects of pH 6.2 + 30 mM P_i on force and velocity in young and old fibers.

Data from slow fibers at 30℃, male and female data pooled for each age group. Values are means ± SEM. (A) Peak force in kN/m^2. (B) Unloaded shortening velocity (V_o) in fl/sec. *Significantly different from pH 7 condition, $p < 0.05$.

	Young Men			Young Women		
	pH 7	pH 6.2 + 30 mM P_i	%Δ	pH 7	pH 6.2 + 30 mM P_i	%Δ
n		5			6	
Abs. Peak Power (μN fl s^{-1})	922 ± 139	397 ± 67*	↓57	497 ± 94	223 ± 49*	↓55
Norm. Peak Power (W/l)	125 ± 27	56 ± 15*	↓55	64 ± 9	29 ± 6*	↓55
a/P_o	0.58 ± 0.17	0.45 ± 0.15	↓22	0.98 ± 0.26	0.93 ± 0.27	↓6
V_{opt} (fl/sec)	2.20 ± 0.23	1.60 ± 0.22	↓27	1.54 ± 0.19	1.10 ± 0.17	↓29
P_{opt} (kN/m^2)	54.6 ± 7.2	33.1 ± 5.3*	↓39	41.1 ± 2.3	25.8 ± 2.4*	↓37
	Old Men			Old Women		
	pH 7	pH 6.2 + 30 mM P_i	%Δ	pH 7	pH 6.2 + 30 mM P_i	%Δ
n		10			5	
Abs. Peak Power (μN fl s^{-1})	961 ± 175	454 ± 113*	↓53	375 ± 84	194 ± 55	↓47
Norm. Peak Power (W/l)	113 ± 22	50 ± 12*	↓56	54 ± 10	27 ± 6*	↓50
a/P_o	0.58 ± 0.13	0.52 ± 0.05	↓10	0.53 ± 0.14	0.38 ± 0.10	↓30
V_{opt} (fl/sec)	2.78 ± 0.47	1.66 ± 0.28	↓40	1.95 ± 0.55	1.30 ± 0.22	↓33
P_{opt} (kN/m^2)	39.2 ± 4.7	26.7 ± 3.7	↓32	30.8 ± 3.8	20.2 ± 2.1*	↓34

Table 5.3: Power characteristics for human fibers at 30℃.

Values are means ± SEM. Data from slow fibers. *n,* number of fibers. Abs, absolute. Norm, normalized. a/P_o, unitless ratio describing the curvature of force-velocity plot. V_{opt} and P_{opt}, velocity and force at which peak power is obtained, respectively. Statistics were only run on pH 7 vs. pH 6.2 + 30 mM P_i in an individual group in this table. *Significantly different from pH 7 condition, $p < 0.05$.

There were no age or sex differences apparent in how elevated H^+ and/or P_i affected k_{tr}, so data presented in figure 5.8 combined all human fibers to assess how k_{tr} is altered by pH 6.2 alone, 30 mM P_i alone, or pH 6.2 + 30 mM P_i at 15℃. As observed with rat fibers, pH 6.2 + 30 mM P_i had no effect on k_{tr}, and in slow fibers, neither did elevating either ion alone (Figure 5.8A). In fast fibers, the pH 7 + 30 mM P_i condition yielded a significantly higher k_{tr} than any other experimental group (Figure 5.8B).

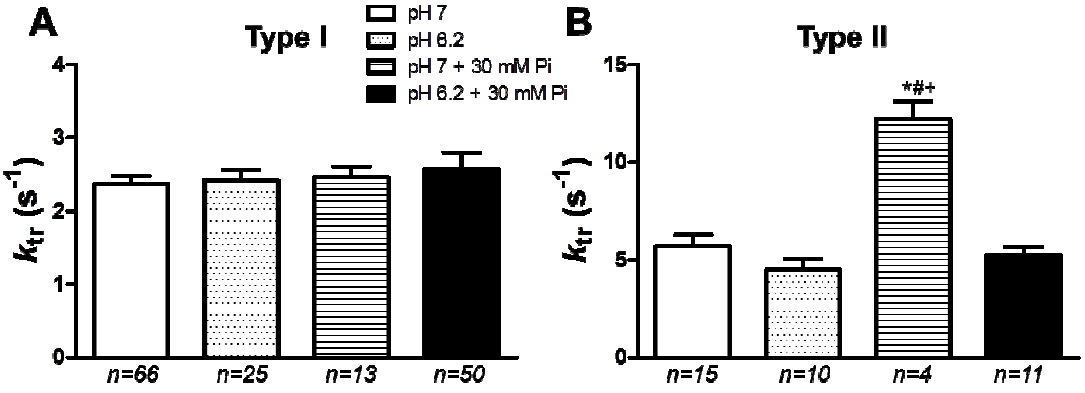

Figure 5.8: Effects of elevated H^+ and P_i on k_{tr} in slow and fast fibers.

Data collected at 15℃, all human fibers pooled to show effects of H^+ and P_i. Values are means ± SEM. k_{tr} in s^{-1} for (A) slow and (B) fast fibers. *Significantly different from pH 7 condition, $^{\#}$Significantly different from pH 6.2 condition, $^{+}$Significantly different from pH 6.2 + 30 mM P_i condition, $p < 0.05$.

Combining all human fibers due to no significant differences between ages and sexes, the pH 6.2 + 30 mM P_i condition significantly depressed peak stiffness and the force stiffness ratio to a similar degree in slow fibers at 15℃, while elevating P_i alone depressed peak stiffness and trended toward depressing

the force stiffness ratio (p=0.053) (Figure 5.9). Thus, it appears that the pH+P_i induced decrease in stiffness is primarily mediated by elevating P_i.

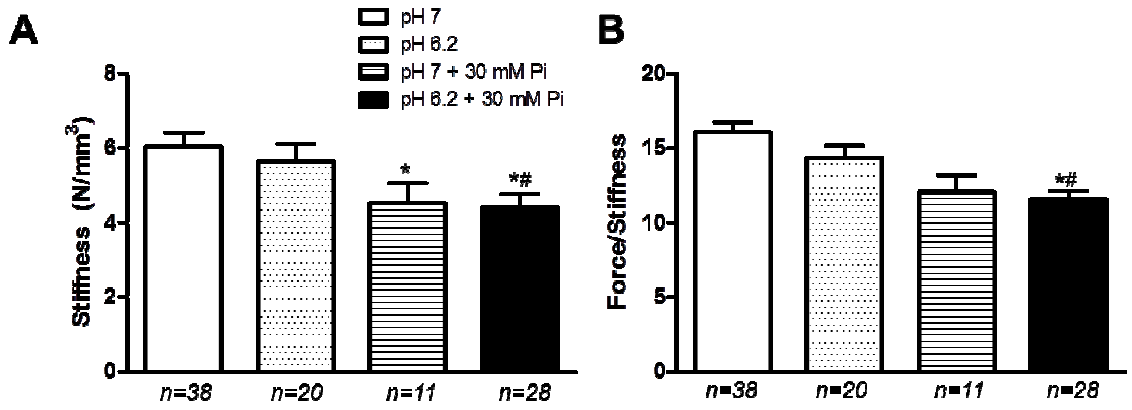

Figure 5.9: Effects of elevated H^+ and P_i on stiffness and the force stiffness ratio.

Data from slow fibers, collected at 15℃. All human fib ers pooled to show effects of H^+ and P_i. Values are means ± SEM. (A) Stiffness in N/mm^3. (B) Force stiffness ratio. *Significantly different from pH 7 condition, $^{\#}$Significantly different from pH 6.2 condition, $p < 0.05$.

To further evaluate the effects of age and/or pH 6.2 + 30 mM P_i on the relative force-per-cross-bridge, we employed a technique of Colombini *et al.* (2010), described in *Methods*, in Figure 5.10. The y-intercept of these plots approximates the relative percentage of low-force cross-bridges. While the intercept was higher for old vs. young fibers (11.6% vs. 6.8%), this difference was not significant. Similarly, in slow fibers, there was no significant difference between the y-intercept in pH 7 and pH 6.2 + 30 mM P_i conditions, regardless of age (data not shown). Combining all fibers from young and old adults to

compare effects of H^+ and P_i, a significant difference in the y-intercept or the percentage of low-force bridges was apparent in fast fibers in pH 7 vs. pH 6.2 + 30 mM P_i conditions (p=0.038) (Figure 5.10B).

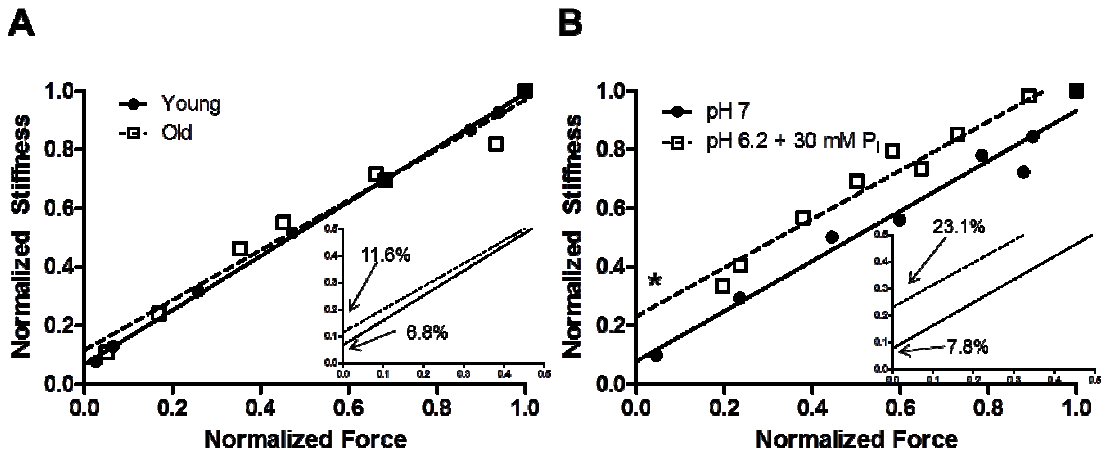

Figure 5.10: Low-force cross-bridge approximation plots.

Data collected at 15℃, points are means (n=6 -10 fibers) fitted with a linear regression and extrapolated to the x-axis. Insets zoom in at the point where the lines intersect the x-axis. % of low-force bridge approximation labeled on insets with each line. (A) Slow fibers only, all fibers from young adults (*n=11*) vs. fibers from old adults (*n=22*) at pH 7. (B) Fast fibers only, all human data pooled. pH 7 (*n= 9*) vs. pH 6.2 + 30 mM P_i (*n=5*). *in (B) indicates the intercepts are significantly different from one another, p<0.05.

Finally, the effects of elevating H^+ and P_i on myofibrillar ATPase and fiber economy were assessed. Figure 5.11 shows the effects of the ions individually and in combination in old women (5.11A,B) and old men (5.11C,D) in slow fibers at 23℃. The pH 6.2 + 30 mM P_i condition significantly depressed ATPase in old men and trended toward significantly decreasing ATPase in old women (p=0.064). No changes were observed in ATPase or economy with elevating

either ion alone, although the trend in older women was that increasing H^+ depressed ATPase but did not change economy, while increasing P_i maintained ATPase but depressed economy. In old men, the pH 6.2 + 30 mM P_i condition had no effect on economy but in old women, economy dropped 36%, though this was not a significant decrease (p=0.26).

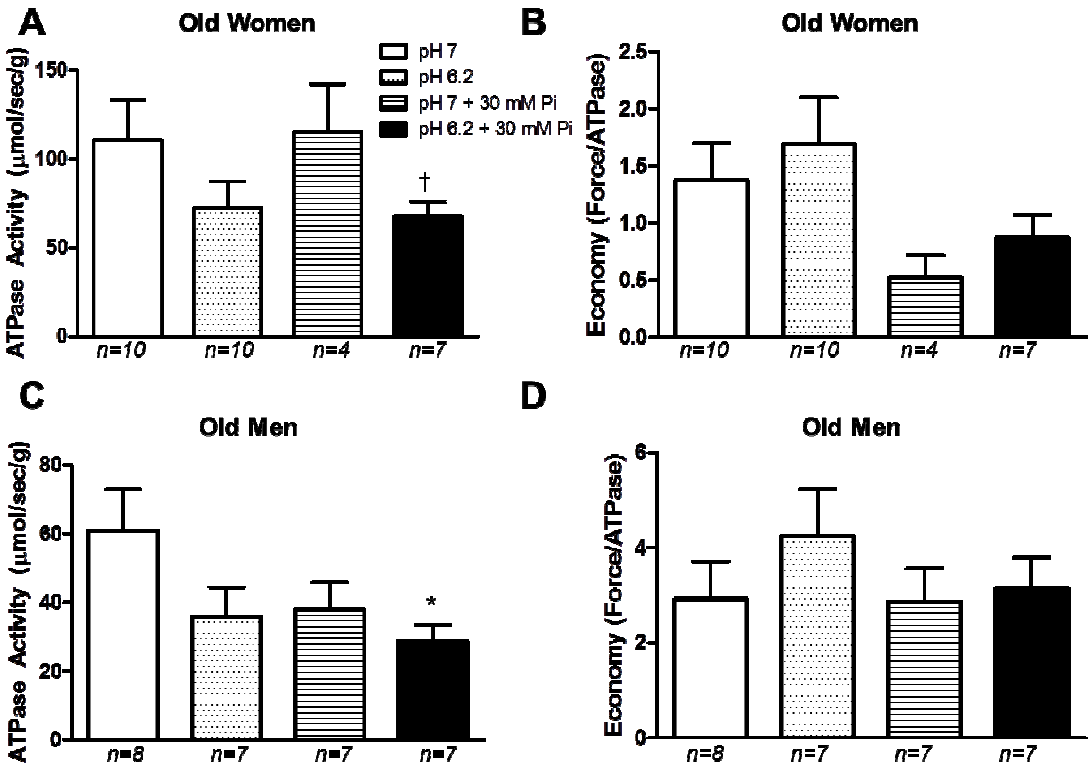

Figure 5.11: Effects of elevated H^+ and P_i on ATPase and economy.

Data from slow fibers collected at 23℃. Values are means ± SEM. (A) and (B) ATPase and economy, respectively, in old women (n=7 fibers). (C) and (D) ATPase and economy, respectively, in old men (n=7 fibers). *Significantly different from pH 7 condition, $p<0.05$. †Trending difference from pH 7 + 30 mM P_i condition (p=0.064).

Discussion

This chapter has explored the effects of age and fatigue on single fiber force, velocity and power, primarily in type I human fibers. We have also initiated studies to describe how k_{tr}, stiffness, and ATPase activity are altered with age and/or the fatigue condition of pH 6.2 + 30 mM P_i. This discussion will focus on some of the more interesting findings in this preliminary data and suggest where the current studies moving forward should be focused.

Age effects in control conditions

As described in table 5.1, the majority of the human subjects studied (9/12) were “life-long exercisers” or trained individuals. Since this data is preliminary, we combined all fibers from trained and sedentary individuals for this analysis. Moving forward, it will be important to separate data from fibers in trained vs. sedentary old and young adults as performance differences on the whole-body level are readily apparent in the literature (Kent-Braun *et al.* 2012; Hunter 2014).

We found absolute peak force to be depressed in fibers from old women compared to young men, young women, and old men (Figure 5.2A) and when normalized for fiber size, old women were still depressed compared to young men (Figure 5.2B). Our findings agree with some (D'Antona *et al.* 2003) and not others (Trappe *et al.* 2003), and show the complete opposite of Miller *et al*.

(2013), who found type I and IIa fibers from old women to have higher forces per cross-sectional area compared to the other 3 groups at 25℃. Our data are the first to show aging effects on single fiber force production at 30℃, but the 5℃ temperature change from 25 to 30℃ probably does no t explain our conflicting results with Miller *et al.* (2013). Rather, the discrepancy in the data could be related to average age and/or activity level between the young and old groups. Miller *et al.* (2013) matched their young and old subjects for activity level, whereas in this work, of the older women studied to date, two were trained and two were sedentary (Table 5.1). However, there was no difference in P_o at 30℃ in fibers from trained vs. sedentary subjects in this study (133 ± 11 kN/m^2, n=12 trained vs. 115 ± 11 kN/m^2, n=14 sedentary). The average age of the older women subjects was 75 (n=4) and 68 (n=7) in this and the Miller *et al.* (2013) study, respectively. Our finding that force per cross-sectional area is depressed in old women suggests a decreased concentration of actin and /or myosin in the muscle fibers, something that has been documented with both age and disuse (Fitts *et al.* 2001; D'Antona *et al.* 2003).

A sex but not age effect was apparent in V_{max} and peak power, in that type I fibers from young men and old men were faster and more powerful than those from young women and old women. We interpret these results with caution, as the n=6 fibers tested in the young women group were from one person. It may be that with additional young women subjects, this effect could be isolated to old women, which would agree with the findings of Krivickas *et al.* (2001), who found old women to have significantly lower V_o's than young men, young women, and

old men in type I and IIa fibers. The two human single fiber studies that have assessed aging effects on peak fiber power found no differences between ages or sexes (Trappe *et al.* 2003; Krivickas *et al.* 2006). Our data collected at 30℃ suggest that type I fibers from women, both young and old, generate less power than men. The lack of a decline in peak power in older men compared to young men is surprising in that peak force was significantly depressed between the two groups.

Our preliminary data show age-related depressions in force, velocity, and power specifically in type I fibers from old women at 30℃. Interestingly, we found old women to have slower k_{tr}'s than young women and old men (not significantly different from young men) (Figure 5.4), a finding that agrees with one published study (Miller *et al.* 2013). A lower k_{tr} is indicative of slowed cross-bridge kinetics, specifically at the low to high-force transition (Figure 1.1, step 3), and could partially account for the declines we observe in force and power in fibers from old women. We further observed fiber economy to be depressed in type I fibers from old women, in that for a given level of ATP hydrolysis, less force was produced (Figure 5.6). Additionally, old women trended toward higher ATPase activity levels in type I fibers, compared to young women and old men. Figure 5.12 illustrates an "unconventional branched path" of cross-bridge cycling originally proposed by Linari *et al.* (2010) to explain their findings that 25 mM P_i increased ATP splitting per cross-bridge two-fold in fast fibers (Kent-Braun *et al.* 2012).

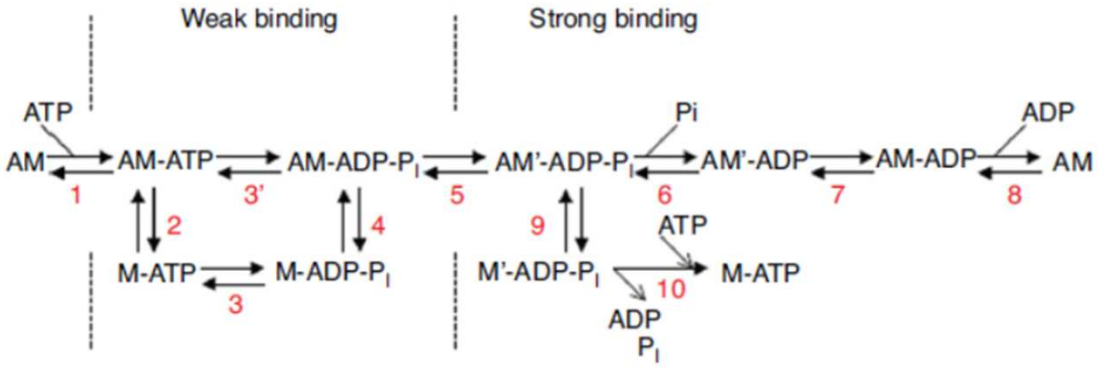

Figure 5.12: Schematic model of cross-bridge cycle with unconventional branched paths.

A, actin and M, myosin head. Scheme adapted from current models of ATP hydrolysis in the conventional path (steps 1-8) and the unconventional branched path (steps 9 and 10). Model modified from Linari *et al.* (2010) with permission from The Royal Society Proceedings B.

The scheme in Figure 5.12 proposes that P_i buildup allows the force generating state (AM'-ADP-P_i) to detach before the release of hydrolysis products (Figure 5.12, step 9). The state 9 product (M'-ADP-P_i) is structurally and kinetically different from the M-ADP-P_i state as the latter is in rapid equilibrium with the AM-ADP-P_i state (Figure 5.12, step 4) (Linari *et al.* 2010; Kent-Braun *et al.* 2012). The authors hypothesize that the M'-ADP-P_i state completes the normal structural change associated with the power stroke in the attached myosin head and the ATPase cycle by an irreversible release of P_i and ADP (Figure 5.12, step 10) (Linari *et al.* 2010). An increased flux through the branched path would allow maintenance of ATPase activity but reduced force, causing a decline in fiber economy, a phenomenon we observed in type I fibers

from old women. While this scheme was proposed to account for effects of elevating P_i, it also could represent a potential mechanism for depressed economy with age in type I fibers from old women.

Effects of age and elevated H^+, P_i and/or $H^+ + P_i$

The effects of both elevated H^+ and P_i on human single fiber function is unknown. While we would not anticipate results drastically different from animals, it was nevertheless novel and interesting to begin the investigation of how fatigue conditions affect human skinned fibers. Moreover, it was unknown how fibers from older men and women may respond to pH 6.2 + 30 mm P_i conditions compared to fibers from young adults.

Interestingly, in general, we found that pH 6.2 + 30 mM P_i depressed force, velocity, and power equally between ages and sexes. In our measures of stiffness, k_{tr}, and ATPase, we again found no significant differences in how fibers from older vs. younger adults responded to the pH 6.2 + 30 mM P_i fatigue condition. This would suggest that when faced with metabolic, fatigue-induced stress, aged fibers maintain function as well as young fibers.

We conducted experiments that assessed individual effects of H^+ (pH 6.2) and P_i (30 mM), as well as the collective pH+P_i effect, on human fibers. This data continues the discussions from chapters 3 and 4 in that it further characterizes the individual and collective effects of elevated H^+ and P_i on single fiber function. There were no major differences in how fibers from old versus

young adults responded to pH 6.2 + 30 mM P_i in our mechanistic measurements, so for the final discussion points, all human fiber data were combined to specifically assess effects of the metabolites.

Consistent with animal results, we found P_i to increase k_{tr} in type II fibers and decrease stiffness, as well as the force-stiffness ratio (p=0.053), in type I fibers (Tesi *et al.* 2000; Caremani *et al.* 2008) (Figures 5.8B and 5.9). In a recent study done on single molecules, Debold *et al*. (2013) showed that 30 mM P_i drastically reduced acto-myosin binding events and proposed that P_i induces premature detachment from a strongly bound state. This idea is consistent with our results that show P_i decreasing peak stiffness in human fibers (Figure 5.9). We also show that P_i depresses force more than ATPase, thereby reducing fiber economy (Figure 5.11), a finding in line with rabbit psoas data from Linari *et al.* (2010) and the model detailed in Figure 5.12. Though the ATPase and economy data did not reach statistical significance in the current sample size in Figure 5.11, the trend of P_i maintaining ATPase activity (compared to control) while depressing economy is apparent.

As discussed in Chapter 4, low cell pH (6.2), in single molecule laser-trap assays, has been shown to increase the duration of the ADP-bound state (Figure 1.1, state F) three-fold (Debold *et al.* 2008). It is by this mechanism that elevating H^+ may depress myofibrillar ATPase activity, a trend we observe in Figure 5.11A and C. By itself, elevating H^+ does not appear to alter economy, and this may be due to its propensity to prolong a population of cross-bridges in a force-producing, ADP-bound state. The hypothesis that low cell pH slows the

forward rate constant of force generation (Figure 1.1, step 3) is supported by the increased number of low-force bridges, at least in fast fibers, observed in Figure 5.10B, assuming this effect is primarily due to elevating H^+ and not P_i. This is purely an assumption, as one critical experiment missing from this work are low-force bridge approximation plots assessing the effects of elevating H^+ or P_i alone. Such plots would tease out if one or both of the ions are increasing the number of low-force bridges. The effects of H^+ on stiffness was only evaluated in a few fast fibers (n=2) and appeared to maintain peak stiffness while decreasing the force-stiffness ratio, reinforcing the findings in Figure 5.10B.

Of clinical interest is how a buildup of H^+ and P_i work together to depress muscle function. While elevating the metabolites simultaneously depressed ATPase activity in type I fibers from old men and women, there was no apparent effect on economy (Figure 5.11), suggesting that the inhibition of force and ATPase were similar. This differs from the findings of Potma *et al.* (1995) who observed no change in rat slow fiber ATPase but a 2-fold drop in economy. The authors also found a ~50% drop in ATPase activity and 4-fold decrease in fiber economy in fast rabbit fibers (Potma *et al.* 1995). Our data suggest that at least in humans, the H^+ induced decline in myofibrillar ATPase and inhibition of force by H^+ and P_i are balanced such that economy remains unchanged.

A simultaneous elevation of H^+ and P_i significantly decreased peak stiffness and the force-stiffness ratio, indicating that in type I human fibers, these metabolites decrease the number of total bridges (low and high force) and increased the number of low-force bridges. The latter would decrease force but

not stiffness. A second possibility for the decline in the force/stiffness ratio is that the metabolites reduced the force-per-bridge in pH 6.2 + 30mM P_i conditions. The effect for pH+Pi to depress peak stiffness appears to be primarily mediated by P_i, as P_i alone also significantly depressed stiffness (Figure 5.9A).

Summary and Future Directions

It is clear that studying effects of elevated H^+ and P_i individually can provide insights as to how they might work collectively to depress cross-bridge function. Future studies on human fibers should address the sex differences seen in velocity and power at pH 7, specifically obtaining data from additional young women to give insight as to whether fibers from females have a depressed peak power, a finding that would conflict with published data collected at 15℃ (Trappe *et al.* 2003). The specific cross-bridge changes observed in fibers from older women (decreased absolute force and force per cross-sectional area, slowed k_{tr}, and compromised economy) should be further investigated and all (k_{tr} and ATPase particularly) evaluated at 30℃. Finally, though we report no age differences in the response to fatiguing metabolites, strengthening this data is crucial, as it is novel and shows that fibers from older adults can handle elevations in H^+ and P_i as well as young.

CHAPTER 6

SUMMARY AND GENERAL DISCUSSION

Summary: H^+ and P_i

This goal of this dissertation was to elucidate the individual and collective effects of high H^+ and P_i on single skeletal muscle fiber function at the near-physiological temperature of 30℃. The primary fin dings (detailed in chapters 3 and 4) from animals are summarized in Table 6.1, with the novel findings in bold.

	Fiber type	pH 6.2	30 mM P_i	pH 6.2 + 30 mM P_i
Peak Force (P_o)	Type I	↓ 12%	↓ 19%	↓ **36%**
	Type II	ns	ns	↓ **46%**
Calcium Sensitivity (pCa_{50})	Type I	↓ **18%**	↓ 10%	↓ **24%**
	Type II	↓ **19%**	↓ 10%	↓ **24%**
Maximal Velocity (V_{max})	Type I	↓ 16%	ns	↓ **15%**
	Type II	↓ 16%	ns	↓ **31%**
Peak Power (W/l)	Type I	↓ 34%	↓ 26%	↓ **64%**
	Type II	↓ 18%	↓ 18%	↓ **59%**

Table 6.1: Summary of the effects of H^+ and P_i in type I and II fibers at 30℃.

Values are percent change from control conditions (pH 7, no added P_i), taken from Debold *et al.* 2004, Debold *et al.* 2006, Knuth *et al.* 2006, Nelson & Fitts 2014. ns= not significant. Bolded numbers are new data from this dissertation.

Interestingly, pH 6.2 or 30 mM P_i alone did not significantly affect P_o, while collectively, the ions depressed P_o by ~50% in type II fibers. A similar synergistic effect was apparent with peak power in type II fibers, which declined by 59% in the pH 6.2 + 30 mM P_i conditions compared to ~ 20% by either ion alone. $pH+P_i$ effects on velocity appeared to be primarily mediated by pH in type I fibers, as the collective effects were not different than the individual effects of pH 6.2. This suggests that the increased depression in peak power by both ions was more strongly driven by depressions in force.

In chapter 5, the effects of age and fatigue in human fibers were addressed. This work, in addition to the collective effects of low pH and high P_i observed in rat fibers in Chapter 4, utilized mechanistic measurements of k_{tr}, stiffness, and ATPase activity to tease out *how* H^+ and P_i may be mediating the decline in single fiber function observed in table 6.1. Figure 6.1 details the cross-bridge cycle similar to that presented in figures 1.1 and 5.12 but illustrates at which points in the cycle H^+ and P_i are compromising cross-bridge function.

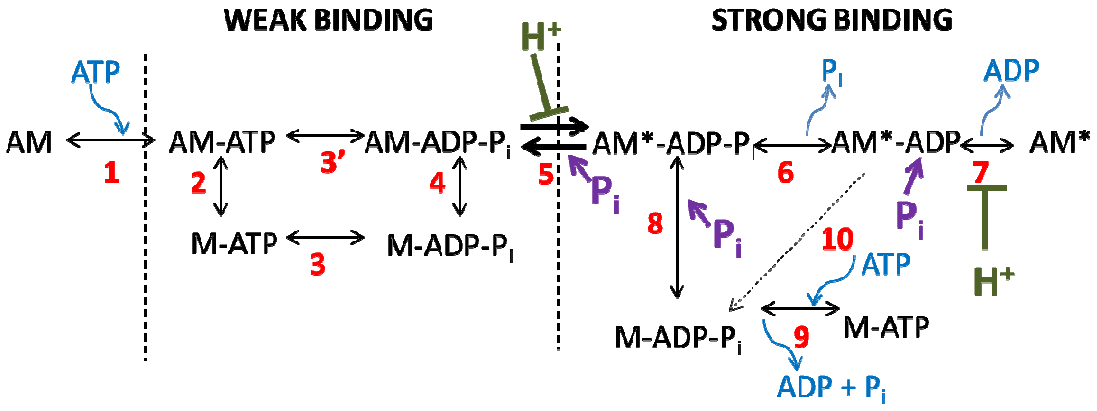

Figure 6.1: Model of the cross-bridge cycle. A, actin. M, myosin. Steps 8 and 9 represent an unconventional, branched pathway proposed by Linari *et al.* (2010) while step 10 represents a P_i-mediated detachment of the bridge proposed by Debold *et al.* (2013).

H^+ Effects

Utilizing data obtained from both human and rat type I fibers, we show slowed velocity, depressed force and myofibrillar ATPase, and maintained economy (force/ATPase ratio) in pH 6.2 alone conditions, all of which support the hypothesis that elevated H^+ slows the ADP release step, prolonging the time of attachment of the AM*-ADP state (Figure 6.1, step 7) (Debold 2012). In agreement with rat data from Metzger and Moss (1990b), we show no change in k_{tr} in type I or II human fibers at 15℃ with elevated H^+ alone, which may imply that H^+ is reducing the force of the high-force bridges rather than increasing the percentage of low-force bridges at maximal Ca^{2+} concentrations. However, at submaximal Ca^{2+} concentrations, pH 6.2 has a significant depressive effect on force, as indicated by drastic reductions in Ca^{2+} sensitivity (Chapter 3) (Nelson & Fitts 2014). Interestingly, at submaximal Ca^{2+}, Metzger and Moss (1990b) found

k_{tr} to be markedly depressed in all fiber types with low cell pH. It therefore appears the effects of H^+ to slow step 5 (Figure 6.1) are Ca^{2+} dependent, with stronger effects apparent at submaximal Ca^{2+} concentrations characteristic of fatigue (>pCa 5.0).

P_i Effects

Elevations in P_i have a smaller effect on Ca^{2+} sensitivity than elevations in H^+, and fatigue-levels of P_i do not alter velocity; however, P_i on its own depresses power (Table 6.1) (Debold *et al.* 2004; Nelson & Fitts 2014). The data presented in this dissertation on human fibers show an acceleratory effect of P_i on k_{tr} in type II fibers and a depressive effect of P_i on stiffness and the force stiffness ratio in type I fibers, supporting the hypothesis that P_i decreases the number of cross-bridges in both fiber types. Debold *et al*. (2013) suggested that P_i induces detachment from the strongly-bound post-power stroke state (Figure 6.1, step 10), a hypothesis that is supported by our findings that show a reduction in peak stiffness in 30 mM P_i. We also show a trend for 30 mM P_i to maintain myofibrillar ATPase while decreasing economy in type I human fibers, consistent with previous observations in animal work by Linari et al (2010) for which a model is depicted in figure 5.12 and steps 8 and 9 of Figure 6.1. Finally, P_i has been hypothesized to accelerate the reverse rate constant of step 5, a hypothesis supported by data that show an increased k_{tr} with elevated P_i (Tesi *et al.* 2002). All 3 actions of P_i depicted in Figure 6.1 ($+P_i$) support the hypothesis that P_i depresses force and ultimately power by decreasing the number of bound cross-

bridges. By accelerating the reverse of step 5, P_i may push more cross-bridges backwards through step 4 to the unbound M-ADP-P_i state.

Collective effects: H^+ + P_i

The novel studies conducted on the collective effects of low pH plus high P_i are most relevant clinically since H^+ and P_i rise concomitantly during a fatiguing event.

The effects of H^+ plus P_i on contractile function are fiber type specific with the type II fiber effects generally of greater magnitude (Debold *et al.* 2004; Knuth *et al.* 2006; Nelson & Fitts 2014). In chapter 4, we showed no change in k_{tr} in type I or II fibers at 15 or 30℃ in pH 6.2 + 30 mM P_i conditions. We also observed maintained stiffness and a depressed force-stiffness ratio (Figure 4.6), which provides strong evidence that the high H^+ plus P_i inhibition of force was caused by either less force per-bridge and/or an increase in the number of low-force bridges, and not by a decline in the total number of bridges. The force-stiffness plots in Figure 4.7 showed that in both slow and fast fibers, pH 6.2 + 30 mM P_i yielded ~7% of the cross-bridges in the low-force state. This is a negligible increase in low-force bridges from control conditions in slow fibers but a trending increase in fast fibers (~4% and 1% low-force bridges, respectively) ($p=0.19$ for fast fibers). Thus, these plots (Figure 4.7) support the hypothesis that elevating H^+ and P_i shifts the distribution of cross-bridges in fast fibers to more low-force bridges, maintaining stiffness, while decreasing fiber force. In slow fibers, the main effect may be a decline in the force per bridge.

Summary: Aging

Investigators studying age effects on muscle have inquired for decades if the decrements observed in whole body power production in older adults are due entirely to decreased muscle size (atrophy) or if there is a component in the muscle protein structure/function that is compromised with age. At this point in time, there is not a general consensus on this question. Trappe *et al.* (2003) suggested that differences in skeletal muscle function related to aging appear to be dependent on a decline in cell size/number, and that qualitatively, fibers from older adults function equivalently to that of younger adults when corrected for cell size. On the contrary, Miller *et al.* (2013) recently proposed that aging slows actomyosin cross-bridge kinetics in women.

It is apparent from the preliminary data in Chapter 5 that in agreement with Miller *et al.* (2013), skeletal muscle fibers from older adults, particularly older women, show compromised cross-bridge function. We observed absolute force, k_{tr}, and fiber economy to all be significantly depressed in older women compared to the other groups. A slower k_{tr} is suggestive of an age-related effect at the low-to high-force transition (Figure 6.1, step 5), an effect that would also depress force. One hypothesis to support this observation would be that older women have a greater percentage of low-force bridges. We tested this hypothesis with the low-force bridge plots (human fiber data shown in 5.10) and when fibers from older women were separated from the other groups (data not shown), we did not find a significant increase in the percentage of low-force bridges. However, our

sample size was low and this technique may need to be performed differently, as described in chapter 4. In skeletal muscle, decreased myosin light chain 2 phosphorylation (MLC_2-P) confines the myosin head near the thick filament backbone and reduces cross-bridge attachment rate (Stull *et al.* 2011). Miller *et al.* (2013) found a decreased MLC_2-P in the fast myosin isoform in fibers from older women and proposed this as a mechanism for the slowed cross-bridge kinetics they observed.

Perhaps the most intriguing observation from the human data was the decline in economy in type I fibers from old women. Moreover, there was a trend toward an increased myofibrillar ATPase activity in this same group of fibers. This data suggest that fibers from older women are cycling ATP unnecessarily, and we hypothesize that this may be in part, due to alterations in the myofilament proteins associated with the cross-bridge. Lowe *et al.* (2002) also found a decrease in economy in fibers from male, aged rats and proposed an age-related structural change in the ATPase catalytic domain of myosin as a potential explanation for their data. In an earlier paper, the same group of authors (Lowe *et al.* 2001) utilized electron paramagnetic resonance (EPR) to resolve and quantify the structural states of the myosin head, determining the fraction of heads in a strong-binding state during maximal isometric contraction. They found a significant decrease in the percentage of strongly-bound myosin heads in fibers from aged animals (Lowe *et al.* 2001).

Historically, most aging studies, including Lowe *et al.* (2001; 2002) have evaluated males, and as a consequence there is little physiological data on

women (Hunter 2014); thus, we can only speculate as to why the age-related changes we observed were isolated to fibers from older women. Hormonal factors may play a role in the differences we have observed. Estrogen has been shown to be associated with *in vivo* development of muscle size in female mice, while estrogen effects in human muscle are less understood (Enns & Tiidus 2010). Some human studies have shown that force is similar in men and premenopausal women but declines dramatically around the time of menopause, an effect diminished in women using hormone replacement therapy (Phillips *et al.* 1993; Doherty 2001). In ovariectomized rodents, reductions in contractility and isometric tetanic force have been observed and were reversed with estrogen replacement (Moran *et al.* 2007). These authors also observed that the fraction of strong-binding myosin was greater in estrogen-supplemented animals, suggesting that estrogen may influence muscle contractile properties through direct binding to myosin (Moran *et al.* 2007; Enns & Tiidus 2010). Thus declining estrogen concentrations associated with menopause may contribute to the susceptibility of muscle in women to weaken and/or change with age.

Significance

Skeletal muscle is not only the major tissue in the body from a volume point of view but also functions as a master regulator contributing to optimal organismal health (Manring *et al.* 2014). Musculoskeletal diseases have become the second greatest cause of disability, with more than 1.7 billion people affected

globally (Manring *et al.* 2014). The onset of fatigue can exacerbate any musculoskeletal disease or condition. The work presented in this dissertation has further identified the cellular mechanisms that contribute to skeletal muscle fatigue. While this dissertation focused specifically on fatigue at the cross-bridge level, there are many other sites of skeletal muscle fatigue, shown in Figure 6.2.

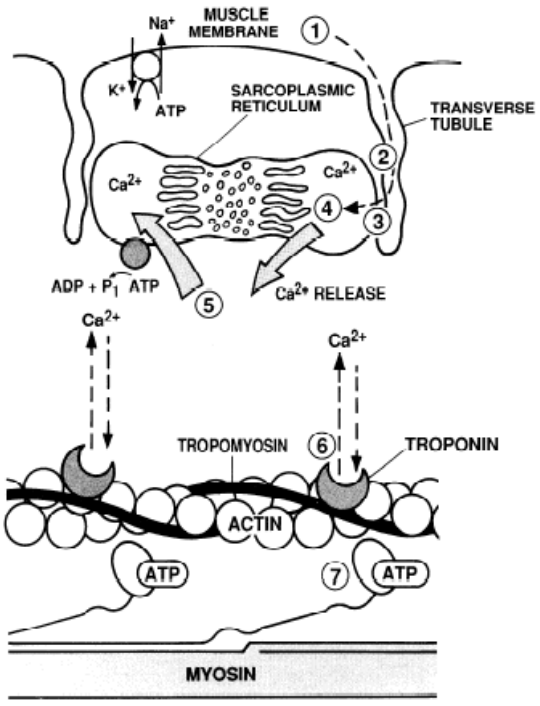

Figure 6.2: Diagrammatic representation of a muscle cell and possible sites of fatigue.

Figure replicated from ref. Fitts (1994). Numbers indicate the possible sites of fatigue, including the following 1) surface membrane 2) T-tubular charge movement, 3) mechanisms coupling T tubular charge movement with SR Ca^{2+} release, 4) SR Ca^{2+} release, 5) SR Ca^{2+} reuptake, 6) Ca^{2+} binding to troponin, 7) myosin binding to actin, ATP hydrolysis, and cross-bridge force development and cycle rate.

In addition to central fatigue (upstream of the neuromuscular junction), alterations in excitation-contraction coupling, Ca^{2+} regulation, metabolic alterations, and cross-bridge cycling all likely contribute to skeletal muscle fatigue.

Future studies should explore the independent effects of high H^+ and P_i on the percentage of low-force bridges. Studying the metabolites in isolation in this case is particularly important, as the data would implicate one or both of the ions as the primary mediator of the decreased force-stiffness ratio in both fiber types. It would also provide insight as to which is the primary ion driving the increased percentage of low force bridges in type II fibers observed in Chapter 4.

Chapter 5 of this thesis explored aging effects on single fiber function in humans and concluded that the most potent age-related changes at the level of the cross-bridge cycle were observed in fibers from older women. This, along with mechanistic studies of combined effects of pH plus P_i on rat fibers are novel and critical findings, but many important questions remain. Further studies are needed to elucidate any potential age-related changes at other sites in the muscle cell, such as the triad junction (t-tubule plus a pair of terminal cisternae from the SR), pictured in Figure 6.2 (#3). A recent review highlighted four triad proteins whose concentration and/or effectiveness has been shown to be reduced with aging, decreasing EC-coupling quality (Manring *et al.* 2014). It has also been proposed that fatigue is mediated more centrally in older versus younger adults (Kent-Braun *et al.* 2012). Multiple factors contribute to decreased

muscle size and function in old adults, i.e. sarcopenia, many of which warrant further investigation.

Estrogen replacement has been shown to improve whole body muscle strength in postmenopausal women (Enns & Tiidus 2010; Sipila *et al.* 2013). It would be interesting to see if older women engaging in some kind of estrogen supplementation had improved force, cross-bridge kinetics, and/or economy on the single fiber level. Such an improvement would suggest that estrogen can directly or indirectly modify muscle proteins involved in cross-bridge cycling.

Potential future experiments on the human fibers could also focus on molecular explanations for why there is a depressed k_{tr} and economy in fibers from older women. In an animal study, Prochniewicz *et al.* (2005) quantified cysteine content changes in actin and myosin and showed that that aging resulted in chemical changes in myosin, not actin, and those changes showed inhibitory effects on the actin-activated myosin ATPase. Though this study used male and female rats, it did not report any sex differences. It would be valuable to repeat this study on human fibers and assess if there are any differences in the myosin protein in fibers from older females versus older males or younger groups. Other animal studies found age-associated changes in the myosin molecule that could alter fiber economy (Prochniewicz *et al.* 2007). Except for the study by Miller *et al.* (2013), there is virtually nothing known about how sarcomeric proteins such as titin, myosin light chain 2, or myosin binding protein C change with age, particularly their phosphorylation states, which are thought to regulate actin-myosin binding kinetics (Colson *et al.* 2010; Scruggs & Solaro

2011). Alterations in any of these proteins could explain the depressed k_{tr} and reduced economy in older women.

The work presented in this dissertation further characterized cellular mechanisms of muscle fatigue at the cross-bridge by exploring individual and collective effects of elevating H^+ and P_i in single fibers from rats and young and old humans. It is the hope that future studies can expand upon the knowledge gained to further combat clinical muscle fatigue and sarcopenia.

APPENDIX I

THE TEMPERATURE DEPENDENCE OF FORCE, STIFFNESS, and KTR

A subset of experiments was conducted at control conditions only (pH 7, no added P_i) and the temperature dependence of force, stiffness, and k_{tr} was assessed. The rationale for conducting these experiments was two-fold. First, the single fiber microsystem (pictured in figure 2.1) had just been developed in the Fitts lab, and we wanted to be certain our temperature control system was sharp, yielding data that coincided with what was already known (Ranatunga & Wylie 1983; Galler & Hilber 1998; Davis & Epstein 2007; de Tombe & Stienen 2007). Second, we wanted to isolate the temperature effect on force, stiffness, and k_{tr} so if need be, we could separate it from the 'fatigue' effect.

Rat soleus and gastrocnemius fibers were subject to maximally activating solutions at 10, 15, 20 and 30℃. Force, stiffness , and k_{tr} were all assessed in one contraction, and an individual fiber was tested twice at each temperature. The order in which a given fiber was exposed to the four temperatures was randomized. Overall findings for these experiments are summarized in Figure A1.1.

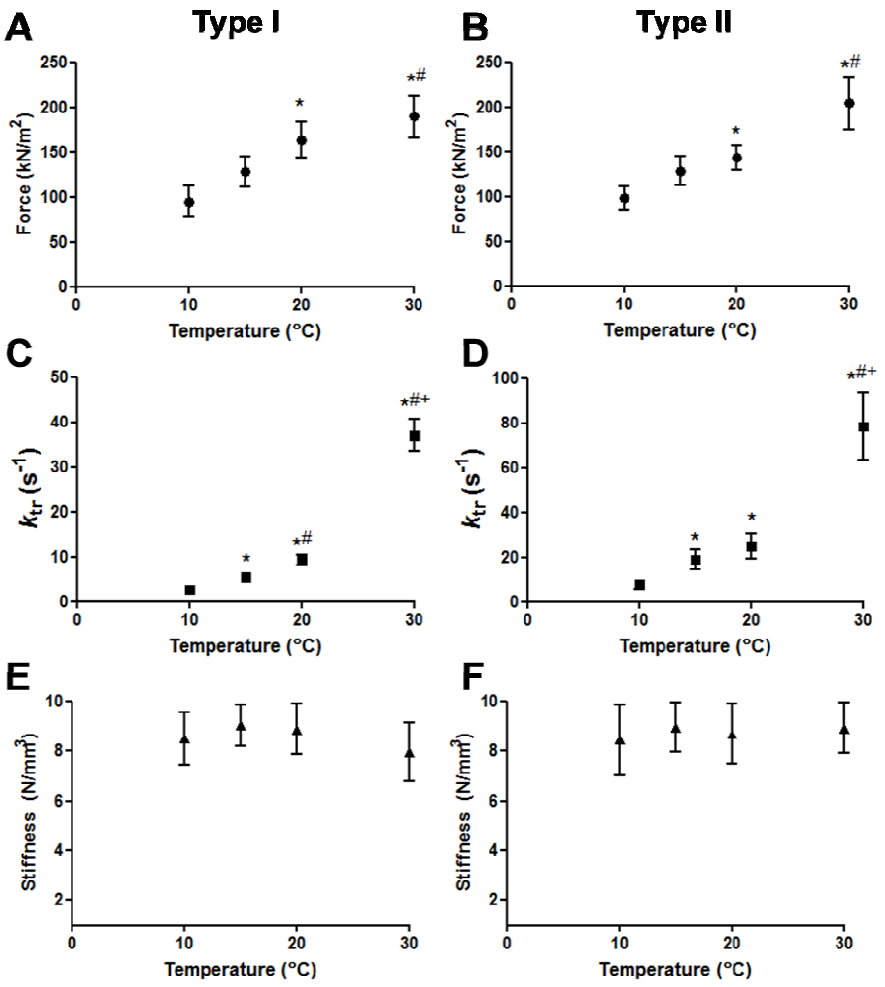

Figure A1.1: Temperature dependence of force, k_{tr}, and stiffness.

(A) and (B), force in kN/m^2. (C) and (D), k_{tr} in 1/s. (E) and (F) Stiffness in N/mm^3. All values are means ± SEM. (A), (C), and (E) type I fibers. (B), (D), and (F) type II fibers. * Significantly different from 10℃, $^{\#}$significantly different from 15℃, $^{+}$significantly different from 20℃, for all $p<0.05$.

Peak force increased with increasing temperature, as documented in chapters 3 and 4 of this dissertation as well as throughout the literature (Ranatunga & Wylie 1983; Pate *et al.* 1995; Galler & Hilber 1998; Ranatunga & Coupland 2010). The force produced at 20 versus 30℃ was not sig nificantly

different in either fiber type in the data presented here (Figure 1.1A and B). Most of the previous data on temperature vs. P_o describe a P_o plateau between 25 and 30℃ (Davis & Epstein 2007; Ranatunga & Coupland 2010).

k_{tr} is highly temperature sensitive, as shown in Figure A1.1 C and D. Here, the most drastic jump in k_{tr} came between 20 and 30℃, as both type I and II fiber k_{tr} increased nearly 4-fold in this temperature range. A few measurements were taken at 25℃ (n=3) and the values were generally intermediate between 20 and 30℃. For example, in one slow fiber, the k_{tr} values at 20, 25, and 30℃ were 12.0, 41.4, and 59.7 s^{-1}, respectively. In cardiac muscle, de Tombe & Stienen (2007) reported a more significant increase in k_{tr} between 20 and 25℃ than between 15 and 20℃. These data coincide with the model proposed by Davis & Epstein (2007) that shows a steep, linear relationship of the sum of the forward and reverse rate constants of force generation (k_{tr}) and temperature between 20 and 40℃.

Finally, stiffness was independent of temperature in the range tested here, in agreement with Galler and Hilber (1998) (Figure 1.2). Wang and Kawai (2001) show a steady increase in the force/stiffness ratio, primarily due to the increase in force (with primarily constant stiffness), over the temperature range 10-30℃, that plateaus in the 30-37℃ range. This and our findings would suggest that when force increases per an increase in temperature, it is a result of an increase in force per-cross-bridge instead of an increase in the number of bridges. Experiments conducted with isolated actin and myosins disagree with this

conclusion and argue that the number of cross-bridges increases as temperature does (Kawai *et al.* 2006).

APPENDIX II

EXPERIMENTALLY PHOSPHORYLATING SKINNED FIBERS AND THE ISOELECTRIC FOCUSING GEL

Karatzaferi *et al.* (2008) described a decrease in power in fast rabbit psoas fibers in fatigue conditions (pH 6.2 + 30 mM P_i) similar to that reported in chapter 4 of this document but interestingly, found that phosphorylation of the myosin regulatory light chain 2 (MLC_2-P) exacerbated this decrement in power (Figure 1.3). Two more interesting aspects about this finding were that (1) it was only the case at 30℃ and (2) it was attributed ent irely to decrements in velocity, and not force, in the pH 6.2 + 30 mM P_i condition. That is, at 30℃ in the pH 6.2 + 30 mM P_i condition, the authors reported an 18% and 40% decrease in V_{max} in non-phosphorylated and experimentally phosphorylated fibers, respectively (Karatzaferi *et al.* 2008). Depressions in power were not quantified in this paper but are shown in Figure 1.3 of the *Introduction* of this document.

It was the original intention of my dissertation to further explore this MLC_2-P-exacerbated decrease in power. While I began the process of exploring this effect, I did not investigate any physiological data in rat fibers and minimally explored phosphorylated vs. non-phosphorylated fibers in the human experiments. However, utilizing the methods in the paper described and others, I created a protocol for our lab to assess the MLC_2 phosphorylation status of single fibers (Franks-Skiba *et al.* 2007; Karatzaferi *et al.* 2008; Stewart *et al.* 2009).

This protocol involved experimentally phosphorylating the fibers, which was accomplished by exposing them to a skinning solution that contained phosphatase inhibitors, 20mM KH_2PO_4 and 20mM NaF, for 7-14 days. Stewart *et al.* (2010) reported that this incubation yielded >80% phosphorylated MLC_2's but did not detail how they arrived at this number. The authors also stated that the standard skinning solution without the phosphatase inhibitors left fibers with a 5-10% basal phosphorylation level of MLC_2. At this point, my goal was to make a gel that would show that our fibers were phosphorylated as Stewart *et al.* (2010) indicated.

One obstacle I encountered while creating this protocol was that the protein from one muscle fiber was not enough to show up with our silver-staining equipment in this type of gel. Stewart *et al.* (2010) used Pro-Q diamond staining on their gels, and we did not have those materials available at the time. Therefore, a successful isoelectric focusing (IEF) gel required protein from about 10 single fibers per lane. A successful gel is shown in Figure A2.1.

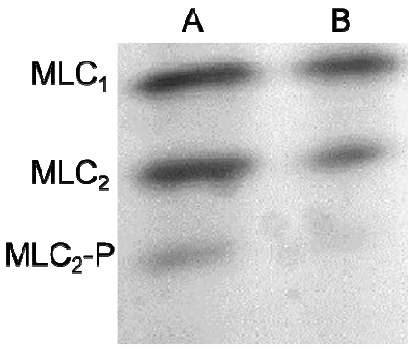

Figure A2.1: Isoelectric focusing gel showing the myosin light chain region.

Rat soleus fibers (n=10 in each lane) are shown here. Fully phosphorylated fibers are produced by incubation with 20mM KH_2PO_4 and 20mM NaF (Lane A) . Partially phosphorylated fibers incubated in standard skinning solution (50% Relaxing solution, 50% glycerol) (Lane B).

The full protocol (as written for future lab mates) is detailed below.

Protocol for Isoelectric Focusing Gels

(To Assess Myosin Light Chain-2 Phosphorylation)
Fitts Lab
Cassie Nelson
6-20-12

Stock Solutions for samples, gel making, gel running:
10% Triton X-100
8M Urea (Takes awhile to dissolve, heat up to 40℃ but no hotter to help dissolve)
IEF Sample Buffer
30% Bis-Acrylamide
20mM NaOH (Cathode Buffer) (Need about 1L per 2 gels)
20mM H_3PO_4 (Anode Buffer) (Need at least 3-4L per 2 gels)

Stock Solutions for staining:
20% TCA (trichloroacetic acid)
30% Methanol/10% Acetic Acid Solution
Solution A (From 12% silver staining protocol)
Solution B (From 12% silver staining protocol
90mM NaOH (Filtered)
Ammonium Hydroxide (from bottle, strong stuff)
Solution D (From 12% silver staining protocol)
Silver Nitrate (solid form, will need 1.16g)

Day 1 Procedure:

1. Pull fibers from bundles. Phosphorylated bundles have been exposed to a skinning solution with 20mM NaF and 20mM KH_2PO_4 for at least a week. Place about 10 fibers in 10-20ul of 8M urea.
2. Add IEF sample buffer in 1:1 ratio (i.e. if you added fibers to 20ul 8M urea, add 20ul more IEF buffer)
3. Sonicate samples for 60 sec each in Mynlieff lab.
4. Heat samples in boiling water for 90sec-2 minutes
5. Vortex samples to mix
6. Centrifuge samples at a reasonable speed (6,000rpm) for 20 seconds
7. Start preparing gel in sidearm flask. Ingredients are as follows:
   - 16.5 g urea
   - 6.00 ml 10% Triton X-100
   - 6.00 ml glass distilled water
   - 4.05 ml 30% Bis-Acrylamide
   - 1.50 ml Ampholytes (pH 4-6.5)

   Mix ingredients in this order on magnetic stirrer in sidearm flask with stirbar. Heat to 39℃ to help urea dissolve. This will take at least 10 minutes. While the ingredients dissolve, prepare gel cast plate.
8. Prepare gel cast plate(s) and check carefully for leaks with glass distilled water. If there are no leaks, be sure to completely remove water from gel loading region.
9. After the gel mixture has dissolved, degas for 5 minutes.
10. Add 100ul of 10% APS and 50ul of TEMED to gel mixture. Swirl to mix well.

11. Begin pouring gel(s). Add combs when you get toward the top.
12. Allow at least 1 hour for polymerization of gel (90 minutes may be better). Gel in between wells will disfigure a little bit but if you let it polymerize long enough, the lanes will be stable enough to use and be consistent.
13. Remove combs after polymerization and add 20mM NaOH to the top of the wells until they are full of the cathode buffer (20mM NaOH).
14. Carefully load samples. Large volumes are fine. 15-20 ul seems to work well.
15. Prepare gel for running.
16. Add enough anode buffer to the bottom and cathode buffer to the top for gel to run well.
17. Depending on how long you will be gone, run at 250-350 V overnight. (I.e. if running from 4pm-9am, 300V is good). Before you leave, check that the dye front is slightly descending on the gel.
18. There's no need for any temperature control of the IEF gel.

Day 2 Procedure:

1. Remove gel from plates- BE CAREFUL. These gels are VERY fragile and will rip extremely easily.
2. Fix the gel in 20% TCA solution for about 10 minutes. Don't need a large volume of TCA. The TCA solution turns the gel a milky white. Be careful touching the TCA. It's yucky stuff.
3. Rinse the gel in 30% methanol/10% acetic acid solution for about 5 minutes.
4. Place the gel in Solution A for 30 minutes minimum (60 might be best). The gel can also remain here for several days if you need a stopping point.
5. Place the gel in Solution B for 3 hours minimum.
6. Rinse the gel in deionized or glass distilled water for 15 minutes each at least 4 times after solution B exposure.
7. Proceed with silver staining procedure exactly as directed from the 12% SDS gel instructions.
8. Mount and dry the gel in Dr. Eddinger's lab. Needs at least overnight to dry—even longer in the humid summer months.

As mentioned, I did not study the physiology of this MLC_2-P effect in rat fibers but did do some experiments on phosphorylated human fibers. Unfortunately, my two attempts to run IEF gels on the human fibers were not successful. That is, I could not prove the human fibers were phosphorylated as I did the rat fibers in Figure A2.1. It is therefore hard to say if any of the human data comparing phosphorylated and non-phosphorylated fibers are legitimate. With that in mind, there was no effect of phosphorylation on the decrements seen in velocity or power at 30℃ in human type I fibers (fibers were combined across

sexes and ages for this analysis due to a small sample size). Combining sexes for this brief analysis could disguise effects seen in a given sex or age group, as Miller *et al.* (2013) reported decreased expression of the fast MLC_2-P isoform in fibers from old women.

It is worth restating that the effect Karazaferi *et al*. (2008) described was isolated to fast fibers, so it may be that slow fibers would not show the same effect. Fast fibers have been reported to have a higher myosin light chain kinase activity (Moore & Stull 1984) and higher myosin light chain 2 phosphorylation (MLC_2-P) (Fitts 1994). If there were more basal phosphorylation in the type II fibers, the effect Karatzaferi *et al.* (2008) described could be a fast fiber type-specific effect.

BIBLIOGRAPHY

Allen, DG & Westerblad, H (2001). Role of phosphate and calcium stores in muscle fatigue. *J Physiol* **536**, 657-665.

Allen, DG, Lamb, GD & Westerblad, H (2008). Impaired calcium release during fatigue. *J Appl Physiol* **104**, 296-305.

Allen, DG, Lamb, GD & Westerblad, H (2008). Skeletal Muscle Fatigue: Cellular Mechanisms. *Physiol Rev* **88**, 287-332.

Barany, M (1967). ATPase activity of myosin correlated with speed of muscle shortening. *J Gen Physiol* **50**, Suppl:197-218.

Bottinelli, R, Schiaffino, S & Reggiani, C (1991). Force-velocity relations and myosin heavy chain isoform compositions of skinned fibres from rat skeletal muscle. *J Physiol* **437**, 655-672.

Brenner, B (1988). Effect of Ca2+ on cross-bridge turnover kinetics in skinned single rabbit psoas fibers: implications for regulation of muscle contraction. *Proc Natl Acad Sci USA* **85**, 3265-3269.

Brenner, B (1987). Mechanical and structural approaches to correlation of cross-bridge action in muscle with actomyosin ATPase in solution. *Annu Rev Physiol* **49**, 655-672.

Brenner, B & Eisenberg, E (1986). Rate of force generation in muscle: correlation with actomyosin ATPase activity in solution. *Proc Natl Acad Sci USA* **83**, 3542-3546.

Brozovich, FV, Yates, LD & Gordon, AM (1988). Muscle force and stiffness during activation and relaxation. Implications for the actomyosin ATPase. *J Gen Physiol* **91**, 399-420.

Cady, EB, Jones, DA, Lynn, J & Newham, DJ (1989). Changes in force and intracellular metabolites during fatigue of human skeletal muscle. *J Physiol* **418**, 311-325.

Campbell, KS & Moss, RL (2003). SLControl: PC-based data acquisition and analysis for muscle mechanics. *Am J Physiol Heart Circ Physiol* **285**, H2857-64.

Caremani, M, Dantzig, J, Goldman, YE, Lombardi, V & Linari, M (2008). Effect of inorganic phosphate on the force and number of myosin cross-bridges during the isometric contraction of permeabilized muscle fibers from rabbit psoas. *Biophys J* **95**, 5798-5808.

Chase, PB & Kushmerick, MJ (1988). Effects of pH on contraction of rabbit fast and slow skeletal muscle fibers. *Biophys J* **53**, 935-946.

Colombini, B, Nocella, M, Bagni, MA, Griffiths, PJ & Cecchi, G (2010). Is the Cross-Bridge Stiffness Proportional to Tension during Muscle Fiber Activation?. *Biophys J* **98**, 2582-2590.

Colson, BA, Locher, MR, Bekyarova, T, Patel, JR, Fitzsimons, DP, Irving, TC & Moss, RL (2010). Differential roles of regulatory light chain and myosin binding protein-C phosphorylations in the modulation of cardiac force development. *J Physiol* **588**, 981-993.

Cooke, R, Franks, K, Luciani, GB & Pate, E (1988). The inhibition of rabbit skeletal muscle contraction by hydrogen ions and phosphate. *J Physiol* **395**, 77-97.

Coupland, ME, Puchert, E & Ranatunga, KW (2001). Temperature dependence of active tension in mammalian (rabbit psoas) muscle fibres: effect of inorganic phosphate. *J Physiol* **536**, 879-891.

D'Antona, G, Pellegrino, MA, Adami, R, Rossi, R, Carlizzi, CN, Canepari, M, Saltin, B & Bottinelli, R (2003). The effect of ageing and immobilization on structure and function of human skeletal muscle fibres. *J Physiol* **552**, 499-511.

Dantzig, JA, Goldman, YE, Millar, NC, Lacktis, J & Homsher, E (1992). Reversal of the cross-bridge force-generating transition by photogeneration of phosphate in rabbit psoas muscle fibres. *J Physiol* **451**, 247-278.

Davis, JS & Epstein, ND (2007). Mechanism of tension generation in muscle: an analysis of the forward and reverse rate constants. *Biophys J* **92**, 2865-2874.

de Tombe, PP & Stienen, GJ (2007). Impact of temperature on cross-bridge cycling kinetics in rat myocardium. *J Physiol* **584**, 591-600.

Debold, EP (2012). Recent insights into muscle fatigue at the cross-bridge level. *Front Physiol* **3**, 151.

Debold, EP, Beck, SE & Warshaw, DM (2008). Effect of low pH on single skeletal muscle myosin mechanics and kinetics. *Am J Physiol Cell Physiol* **295**, C173-9.

Debold, EP, Dave, H & Fitts, RH (2004). Fiber type and temperature dependence of inorganic phosphate: implications for fatigue. *Am J Physiol Cell Physiol* **287**, C673-81.

Debold, EP, Romatowski, J & Fitts, RH (2006). The depressive effect of Pi on the force-pCa relationship in skinned single muscle fibers is temperature dependent. *Am J Physiol Cell Physiol* **290**, C1041-50.

Debold, EP, Walcott, S, Woodward, M & Turner, MA (2013). Direct observation of phosphate inhibiting the force-generating capacity of a miniensemble of Myosin molecules. *Biophys J* **105**, 2374-2384.

Doherty, TJ (2001). The influence of aging and sex on skeletal muscle mass and strength. *Curr Opin Clin Nutr Metab Care* **4**, 503-508.

Edman, KA (1979). The velocity of unloaded shortening and its relation to sarcomere length and isometric force in vertebrate muscle fibres. *J Physiol* **291**, 143-159.

Enns, DL & Tiidus, PM (2010). The influence of estrogen on skeletal muscle: sex matters. *Sports Med* **40**, 41-58.

Fabiato, A & Fabiato, F (1979). Calculator programs for computing the composition of the solutions containing multiple metals and ligands used for experiments in skinned muscle cells. *J Physiol (Paris)* **75**, 463-505.

Fabiato, A & Fabiato, F (1978). Effects of pH on the myofilaments and the sarcoplasmic reticulum of skinned cells from cardiace and skeletal muscles. *J Physiol* **276**, 233-255.

Fabiato, A (1988). Computer programs for calculating total from specified free or free from specified total ionic concentrations in aqueous solutions containing multiple metals and ligands. In *Methods in Enzymology*, ed. Fleischer S & Fleischer B, pp. 378-417. Academic Press, Pasadena, CA.

Fitts, RH (2008). The cross-bridge cycle and skeletal muscle fatigue. *J Appl Physiol* **104**, 551-558.

Fitts, RH (1994). Cellular mechanisms of muscle fatigue. *Physiol Rev* **74**, 49-94.

Fitts, RH, Riley, DR & Widrick, JJ (2001). Functional and structural adaptations of skeletal muscle to microgravity. *J Exp Biol* **204**, 3201-3208.

Fitzsimons, DP, Patel, JR, Campbell, KS & Moss, RL (2001). Cooperative Mechanisms in the Activation Dependence of the Rate of Force Development in Rabbit Skinned Skeletal Muscle Fibers. *J Gen Physiol* **117**, 133-148.

Franks-Skiba, K, Lardelli, R, Goh, G & Cooke, R (2007). Myosin light chain phosphorylation inhibits muscle fiber shortening velocity in the presence of vanadate. *Am J Physiol Regul Integr Comp Physiol* **292**, R1603-12.

Frontera, WR, Suh, D, Krivickas, LS, Hughes, VA, Goldstein, R & Roubenoff, R (2000). Skeletal muscle fiber quality in older men and women. *Am J Physiol Cell Physiol* **279**, C611-8.

Frontera, WR, Zayas, AR & Rodriguez, N (2012). Aging of human muscle: understanding sarcopenia at the single muscle cell level. *Phys Med Rehabil Clin N Am* **23**, 201-7, xiii.

Galler, S & Hilber, K (1998). Tension/stiffness ratio of skinned rat skeletal muscle fibre types at various temperatures. *Acta Physiol Scand* **162**, 119-126.

Geeves, MA, Fedorov, R & Manstein, DJ (2005). Molecular mechanism of actomyosin-based motility. *Cell Mol Life Sci* **62**, 1462-1477.

Geeves, MA & Holmes, KC (1999). Structural mechanism of muscle contraction. *Annu Rev Biochem* **68**, 687-728.

Giulian, GG, Moss, RL & Greaser, M (1983). Improved methodology for analysis and quantitation of proteins on one-dimensional silver-stained slab gels. *Anal Biochem* **129**, 277-287.

Hermansen, L & Osnes, JB (1972). Blood and muscle pH after maximal exercise in man. *J Appl Physiol* **32**, 304-308.

Hibberd, MG, Dantzig, JA, Trentham, DR & Goldman, YE (1985). Phosphate release and force generation in skeletal muscle fibers. *Science* **228**, 1317-1319.

Hill, AV (1938). The Heat of Shortening and the Dynamic Constants of Muscle. *Proc R Soc B* **126**, pp. 136-195.

Holmes, KC & Geeves, MA (2000). The structural basis of muscle contraction. *Philos Trans R Soc Lond B Biol Sci* **355**, 419-431.

Hunter, SK (2014). Sex differences in human fatigability: mechanisms and insight to physiological responses. *Acta Physiol (Oxf)* **210**, 768-789.

Huxley, AF (1957). Muscle structure and theories of contraction. *Prog Biophys Biophys Chem* **7**, 255-318.

Huxley, HE (1969). The mechanism of muscular contraction. *Science* **164**, 1356-1365.

Janssen, I, Shepard, DS, Katzmarzyk, PT & Roubenoff, R (2004). The healthcare costs of sarcopenia in the United States. *J Am Geriatr Soc* **52**, 80-85.

Karatzaferi, C, Chinn, MK & Cooke, R (2004). The force exerted by a muscle cross-bridge depends directly on the strength of the actomyosin bond. *Biophys J* **87**, 2532-2544.

Karatzaferi, C, Franks-Skiba, K & Cooke, R (2008). Inhibition of shortening velocity of skinned skeletal muscle fibers in conditions that mimic fatigue. *Am J Physiol Regul Integr Comp Physiol* **294**, R948-55.

Kawai, M, Kido, T, Vogel, M, Fink, RH & Ishiwata, S (2006). Temperature change does not affect force between regulated actin filaments and heavy meromyosin in single-molecule experiments. *J Physiol* **574**, 877-887.

Kent-Braun, JA, Fitts, RH & Christie, A (2012). Skeletal Muscle Fatigue. In *Comprehensive Physiology*, ed. Terjung R, pp. 997. John Wiley & Sons, Inc., Columbia, MO.

Kim, AM, Tingen, CM & Woodruff, TK (2010). Sex bias in trials and treatment must end. *Nature* **465**, 688-689.

Knuth, ST, Dave, H, Peters, JR & Fitts, RH (2006). Low cell pH depresses peak power in rat skeletal muscle fibres at both 30 degrees C and 15 degrees C: implications for muscle fatigue. *J Physiol* **575**, 887-899.

Krivickas, LS, Fielding, RA, Murray, A, Callahan, D, Johansson, A, Dorer, DJ & Frontera, WR (2006). Sex differences in single muscle fiber power in older adults. *Med Sci Sports Exerc* **38**, 57-63.

Krivickas, LS, Suh, D, Wilkins, J, Hughes, VA, Roubenoff, R & Frontera, WR (2001). Age- and gender-related differences in maximum shortening velocity of skeletal muscle fibers. *Am J Phys Med Rehabil* **80**, 447-455; quiz 456-7.

Lanza, IR, Towse, TF, Caldwell, GE, Wigmore, DM & Kent-Braun, JA (2003). Effects of age on human muscle torque, velocity, and power in two muscle groups. *J Appl Physiol* **95**, 2361-2369.

Larsson, L, Li, X & Frontera, WR (1997). Effects of aging on shortening velocity and myosin isoform composition in single human skeletal muscle cells. *Am J Physiol* **272**, C638-49.

Linari, M, Caremani, M & Lombardi, V (2010). A kinetic model that explains the effect of inorganic phosphate on the mechanics and energetics of isometric contraction of fast skeletal muscle. *Proc Biol Sci* **277**, 19-27.

Lowe, DA, Surek, JT, Thomas, DD & Thompson, LV (2001). Electron paramagnetic resonance reveals age-related myosin structural changes in rat skeletal muscle fibers. *Am J Physiol Cell Physiol* **280**, C540-7.

Lowe, DA, Thomas, DD & Thompson, LV (2002). Force generation, but not myosin ATPase activity, declines with age in rat muscle fibers. *Am J Physiol Cell Physiol* **283**, C187-92.

Manring, H, Abreu, E, Brotto, L, Weisleder, N & Brotto, M (2014). Novel excitation-contraction coupling related genes reveal aspects of muscle weakness beyond atrophy-new hopes for treatment of musculoskeletal diseases. *Front Physiol* **5**, 37.

Martyn, DA & Gordon, AM (1992). Force and stiffness in glycerinated rabbit psoas fibers. Effects of calcium and elevated phosphate. *J Gen Physiol* **99**, 795-816.

Maughan, DW, Molloy, JE, Brotto, MA & Godt, RE (1995). Approximating the isometric force-calcium relation of intact frog muscle using skinned fibers. *Biophys J* **69**, 1484-1490.

Metzger, JM & Moss, RL (1990). pH modulation of the kinetics of a Ca2(+)-sensitive cross-bridge state transition in mammalian single skeletal muscle fibres. *J Physiol* **428**, 751-764.

Metzger, JM & Moss, RL (1987). Greater hydrogen ion-induced depression of tension and velocity in skinned single fibres of rat fast than slow muscles. *J Physiol* **393**, 727-742.

Metzger, JM & Fitts, RH (1987). Role of intracellular pH in muscle fatigue. *J Appl Physiol* **62**, 1392-1397.

Metzger, JM, Greaser, ML & Moss, RL (1989). Variations in cross-bridge attachment rate and tension with phosphorylation of myosin in mammalian skinned skeletal muscle fibers. Implications for twitch potentiation in intact muscle. *J Gen Physiol* **93**, 855-883.

Metzger, JM & Moss, RL (1990). Effects of tension and stiffness due to reduced pH in mammalian fast- and slow-twitch skinned skeletal muscle fibres. *J Physiol* **428**, 737-750.

Metzger, JM & Moss, RL (1987). Shortening velocity in skinned single muscle fibers. Influence of filament lattice spacing. *Biophys J* **52**, 127-131.

Metzger, J & Moss, R (1990). Calcium-sensitive cross-bridge transitions in mammalian fast and slow skeletal muscle fibers. *Science* **247**, 1088-1090.

Millar, NC & Homsher, E (1990). The effect of phosphate and calcium on force generation in glycerinated rabbit skeletal muscle fibers. A steady-state and transient kinetic study. *J Biol Chem* **265**, 20234-20240.

Miller, MS, Bedrin, NG, Callahan, DM, Previs, MJ, Jennings, ME,2nd, Ades, PA, Maughan, DW, Palmer, BM & Toth, MJ (2013). Age-related slowing of myosin actin cross-bridge kinetics is sex specific and predicts decrements in whole skeletal muscle performance in humans. *J Appl Physiol* **115**, 1004-1014.

Moopanar, TR & Allen, DG (2006). The activity-induced reduction of myofibrillar Ca2+ sensitivity in mouse skeletal muscle is reversed by dithiothreitol. *J Physiol* **571**, 191-200.

Moore, RL & Stull, JT (1984). Myosin light chain phosphorylation in fast and slow skeletal muscles in situ. *Am J Physiol* **247**, C462-71.

Moran, AL, Nelson, SA, Landisch, RM, Warren, GL & Lowe, DA (2007). Estradiol replacement reverses ovariectomy-induced muscle contractile and myosin dysfunction in mature female mice. *J Appl Physiol* **102**, 1387-1393.

Nelson, CR & Fitts, RH (2014). Effects of low cell pH and elevated inorganic phosphate on the pCa-force relationship in single muscle fibers at near-physiological temperatures. *Am J Physiol Cell Physiol* **306**, C670-8.

Nocella, M, Colombini, B, Benelli, G, Cecchi, G, Bagni, MA & Bruton, J (2011). Force decline during fatigue is due to both a decrease in the force per individual cross-bridge and the number of cross-bridges. *J Physiol* **589**, 3371-3381.

Ochala, J, Frontera, WR, Dorer, DJ, Van Hoecke, J & Krivickas, LS (2007). Single skeletal muscle fiber elastic and contractile characteristics in young and older men. *J Gerontol A Biol Sci Med Sci* **62**, 375-381.

Palmer, S & Kentish, JC (1994). The role of troponin C in modulating the Ca2+ sensitivity of mammalian skinned cardiac and skeletal muscle fibres. *J Physiol* **480**, 45-60.

Pate, E, Bhimani, M, Franks-Skiba, K & Cooke, R (1995). Reduced effect of pH on skinned rabbit psoas muscle mechanics at high temperatures: implications for fatigue. *J Physiol* **486**, 689-694.

Pate, E & Cooke, R (1989). Addition of phosphate to active muscle fibers probes actomyosin states within the powerstroke. *Pflugers Arch* **414**, 73-81.

Phillips, SK, Rook, KM, Siddle, NC, Bruce, SA & Woledge, RC (1993). Muscle weakness in women occurs at an earlier age than in men, but strength is preserved by hormone replacement therapy. *Clin Sci (Lond)* **84**, 95-98.

Potma, EJ, van Graas, IA & Stienen, GJ (1995). Influence of inorganic phosphate and pH on ATP utilization in fast and slow skeletal muscle fibers. *Biophys J* **69**, 2580-2589.

Prochniewicz, E, Thomas, DD & Thompson, LV (2005). Age-related decline in actomyosin function. *J Gerontol A Biol Sci Med Sci* **60**, 425-431.

Prochniewicz, E, Thompson, LV & Thomas, DD (2007). Age-related decline in actomyosin structure and function. *Exp Gerontol* **42**, 931-938.

Ranatunga, KW & Wylie, SR (1983). Temperature-dependent transitions in isometric contractions of rat muscle. *J Physiol* **339**, 87-95.

Ranatunga, KW & Coupland, ME (2010). Crossbridge mechanism(s) examined by temperature perturbation studies on muscle. *Adv Exp Med Biol* **682**, 247-266.

Schluter, JM & Fitts, RH (1994). Shortening velocity and ATPase activity of rat skeletal muscle fibers: effects of endurance exercise training. *Am J Physiol* **266**, C1699-73.

Scruggs, SB & Solaro, RJ (2011). The significance of regulatory light chain phosphorylation in cardiac physiology. *Arch Biochem Biophys* **510**, 129-134.

Silvestri, NJ & Wolfe, GI (2013). Asymptomatic/pauci-symptomatic creatine kinase elevations (hyperckemia). *Muscle Nerve* **47**, 805-815.

Sipila, S, Narici, M, Kjaer, M, Pollanen, E, Atkinson, RA, Hansen, M & Kovanen, V (2013). Sex hormones and skeletal muscle weakness. *Biogerontology* **14**, 231-245.

Stackhouse, SK, Reisman, DS & Binder-Macleod, SA (2001). Challenging the Role of pH in Skeletal Muscle Fatigue. *Phys Ther* **81**, 1897-1903.

Stephenson, DG & Williams, DA (1982). Effects of sarcomere length on the force-pCa relation in fast- and slow-twitch skinned muscle fibres from the rat. *J Physiol* **333**, 637-653.

Stewart, M, Franks-Skiba, K & Cooke, R (2009). Myosin regulatory light chain phosphorylation inhibits shortening velocities of skeletal muscle fibers in the presence of the myosin inhibitor blebbistatin. *J Muscle Res Cell Motil* **30**, 17-27.

Stewart, MA, Franks-Skiba, K, Chen, S & Cooke, R (2010). Myosin ATP turnover rate is a mechanism involved in thermogenesis in resting skeletal muscle fibers. *Proceedings of the National Academy of Sciences* **107**, 430-435.

Stull, JT, Kamm, KE & Vandenboom, R (2011). Myosin light chain kinase and the role of myosin light chain phosphorylation in skeletal muscle. *Arch Biochem Biophys* **510**, 120-128.

Swartz, DR & Moss, RL (1992). Influence of a strong-binding myosin analogue on calcium-sensitive mechanical properties of skinned skeletal muscle fibers. *J Biol Chem* **267**, 20497-20506.

Sweitzer, NK & Moss, RL (1990). The effect of altered temperature on Ca2(+)-sensitive force in permeabilized myocardium and skeletal muscle. Evidence for force dependence of thin filament activation. *J Gen Physiol* **96**, 1221-45.

Tesi, C, Colomo, F, Nencini, S, Piroddi, N & Poggesi, C (2000). The Effect of Inorganic Phosphate on Force Generation in Single Myofibrils from Rabbit Skeletal Muscle. *Biophys J* **78**, 3081-3092.

Tesi, C, Colomo, F, Piroddi, N & Poggesi, C (2002). Characterization of the cross-bridge force-generating step using inorganic phosphate and BDM in myofibrils from rabbit skeletal muscles. *The Journal of Physiology* **541**, 187-199.

Thompson, LV, Balog, EM & Fitts, RH (1992). Muscle fatigue in frog semitendinosus: role of intracellular pH. *Am J Physiol Cell Physiol* **262**, C1507-C1512.

Trappe, S, Gallagher, P, Harber, M, Carrithers, J, Fluckey, J & Trappe, T (2003). Single muscle fibre contractile properties in young and old men and women. *J Physiol* **552**, 47-58.

Wang, G & Kawai, M (2001). Effect of temperature on elementary steps of the cross-bridge cycle in rabbit soleus slow-twitch muscle fibres. *J Physiol* **531**, 219-234.

Wattanapermpool, J, Reiser, PJ & Solaro, RJ (1995). Troponin I isoforms and differential effects of acidic pH on soleus and cardiac myofilaments. *Am J Physiol Cell Physiol* **268**, C323-C330.

Westerblad, H & Allen, DG (1992). Myoplasmic free Mg2+ concentration during repetitive stimulation of single fibres from mouse skeletal muscle. *J Physiol* **453**, 413-434.

Westerblad, H & Allen, DG (1991). Changes of myoplasmic calcium concentration during fatigue in single mouse muscle fibers. *J Gen Physiol* **98**, 615-635.

Westerblad, H, Bruton, JD & Lännergren, J (1997). The effect of intracellular pH on contractile function of intact, single fibres of mouse muscle declines with increasing temperature. *J Physiol* **500**, 193-204.

Westerblad, H & Lannergren, J (1994). Changes of the force-velocity relation, isometric tension and relaxation rate during fatigue in intact, single fibres of Xenopus skeletal muscle. *J Muscle Res Cell Motil* **15**, 287-298.

Widrick, JJ, Norenberg, KM, Romatowski, JG, Blaser, CA, Karhanek, M, Sherwood, J, Trappe, SW, Trappe, TA, Costill, DL & Fitts, RH (1998). Force-velocity-power and force-pCa relationships of human soleus fibers after 17 days of bed rest. *J Appl Physiol* **85**, 1949-1956.

Widrick, JJ, Trappe, SW, Costill, DL & Fitts, RH (1996). Force-velocity and force-power properties of single muscle fibers from elite master runners and sedentary men. *Am J Physiol* **271**, C676-83.

Widrick, JJ (2002). Effect of Pi on unloaded shortening velocity of slow and fast mammalian muscle fibers. *Am J Physiol Cell Physiol* **282**, C647-C653.

Wilson, JR, McCully, KK, Mancini, DM, Boden, B & Chance, B (1988). Relationship of muscular fatigue to pH and diprotonated Pi in humans: a 31P-NMR study. *J Appl Physiol* **64**, 2333-2339.

Wood, DS, Zollman, J, Reuben, JP & Brandt, PW (1975). Human skeletal muscle: properties of the "chemically skinned" fiber. *Science* **187**, 1075-1076.

Zeng, W, Conibear, PB, Dickens, JL, Cowie, RA, Wakelin, S, Malnasi-Csizmadia, A & Bagshaw, CR (2004). Dynamics of actomyosin interactions in relation to the cross-bridge cycle*. Philos Trans R Soc Lond B Biol Sci* **359**, 1843-1855.

Zhao, Y & Kawai, M (1994). Kinetic and thermodynamic studies of the cross-bridge cycle in rabbit psoas muscle fibers*. Biophys J* **67**, 1655-1668.